USDA – Natural Resources Conservation Service

DRAFT Technical Note

Hydrologic Analyses of Post-Wildfire Conditions

June 2013

Cover photo: Nabours Mountain directly east of Glenwood NM.

Courtesy of: USDA Forest Service, Gila National Forest, Silver City NM

13

14 (This page intentionally blank)

Contents

List of Figures

List of Tables

Acknowledgements

Dan Moore, hydraulic engineer, Portland, Oregon (Case Study: Whitewater Creek; Gila Wilderness, New Mexico)

Nathaniel Todea, hydraulic engineer, Salt Lake City, Utah (Case Study: Post-fire Analysis for the 2012 Saratoga Fire)

Geoff, Cerrelli, retired (Case Study: The 2000 Montana Bitterroot Wildfires and the Development of the MT NRCS FIRE HYDRO method)

Steve Yochum, hydraulic engineer, Lakewood, Colorado (Case Study: Estimating Increased Flood Potential from the High Park Fire Area)

Introduction

America's forests have long experienced periodic wildfire. Climate, vegetation, steep terrain, and fire-inducing lightning strikes produce wildfire independently of human presence. Humans have become active in watershed management, often exacerbating wildfire risks. We have refined our attempts to manage the landscape, observing the effectiveness and long-term ramifications of various practices, and understanding the extent to which healthy forests need wildfire. Concurrently, societal and economic pressure to settle forestlands has increased, placing at risk more lives, property, and infrastructure.

Whether caused by humans or by nature, wildfire's effects on the landscape cause problems. Communities downstream of burn areas often experience larger than normal flood events, along with extraordinary amounts of sediment and woody debris. Bridges and culverts clog and wash out. Streambanks erode and buildings thought to be invulnerable experience inundation or undercutting. Human lives are sometimes lost.

The Natural Resources Conservation Service (NRCS) plays an important role in helping downstream communities prepare for post-wildfire impacts. The Agency is a leader in applied hydrologic analyses, and today plays an important role in the dissemination of spatially distributed geographic data. Geographic Information Systems (GIS) help hydrologists quickly analyze the landscape factors that affect runoff and erosion. As wildfire creates a relatively sudden disturbance in these geographic factors, the resulting hydrologic effects can also be surprising and sudden.

This technical note clarifies the services NRCS provides to help landowners and communities prepare for harmful post-wildfire hydrologic effects. Since various Federal agencies play different roles in response to wildfire, a handy reference list delineates agencies and their mandates. The role of the NRCS Emergency Watershed Protection (EWP) program is explained. The physical phenomena of rainfall-runoff and erosion in fire-affected watersheds are described, along with analysis techniques that enable hydrologists and hydraulic engineers to evaluate hydrologic effects. Finally, several case studies are presented that describe the services NRCS provided for communities in fire-ravaged watersheds.

The Role of Federal Agencies

NRCS helps people apply good stewardship to their land. As individual landowners seek to take advantage of the benefits of conservation, they rely on NRCS technical expertise in agronomy, rangeland management, nutrient and pesticide management, and hydrology, among other disciplines. Good management of the land helps mitigate the effects of wildfire. After a watershed has burned, NRCS can provide rapid assessments of expected increased flood peaks and sediment flow in streams. As post-fire spatial data becomes available, NRCS can provide downstream communities with scientifically derived technical assessments of ongoing streamflow and sedimentation potential.

While NRCS technical experts in field, area, and state offices, as well as national technical centers, can provide hydrologic analyses at no cost to the landowner, NRCS also provides congressionally funded financial assistance. The Emergency Watershed Protection Program (EWP) can contribute to mitigating the detrimental effects in post-wildfire watersheds. EWP provides funding for mitigation measures such as upland mulching, debris and sediment basins, streambank protection, and flood damage repair.

NRCS hydrology and GIS experts also perform analyses to determine best locations for data collection stations. In addition to the existing SNOTEL and SCAN network of stations, these analyses can help site small temporary data collection stations, which help provide flash flood warnings for burned watersheds. However, many other Federal agencies have significant roles concerning wildfire (Table 1).

Table 1. Federal agencies and their roles concerning wildfire events.

agency	roles
USDA Forest Service	
pre-event	forest management, information dissemination, training, fire tower lookout staffing and status monitoring
during-event	infrastructure protection
post-event	damage assessment, Emergency Watershed Protection (EWP), Burned Area Emergency Response (BAER Teams)
National Interagency Fire Center*	
pre-event	information dissemination, training, agency coordination
during-event	fire-fight coordination
US National Weather Service	
during-event	forecasting fire conditions
post-event	flash flood warnings
US Geological Survey	
pre-event	data collection through gage network
post-event	short-term gage installation and data collection, research on hazards caused by wildfire
Federal Emergency Management Agency	
pre-event	disaster preparedness, information dissemination
post-event	financial assistance
US Bureau of Land Management	
pre-event	federal rangeland management

*Sponsoring Federal agencies include USDA Forest Service, Bureau of Land Management, NOAA National Weather Service, National Park Service, Bureau of Indian Affairs, US Fish and Wildlife Service, and US Fire Administration—FEMA.

NRCS and the Emergency Watershed Protection (EWP) Program

The NRCS administers this financial assistance program. A national emergency declaration is not required to qualify for assistance. The program encourages implementation of emergency measures after a natural disaster, which helps protect against imminent hazards to life and property. Even though a recently burned watershed may be experiencing clear weather, the nature of wildfire impacts is an immediate elevation of hazard potential on downstream resource concerns until the watershed landscape has largely recovered. Depending on the severity and timing of the wildfire event, the hazards may persist long afterward.

The EWP program provides financial and technical assistance to design and fund such measures as upland mulching and other storm runoff control practices, removal of debris or excess sediment from streambeds, establishment of cover on critically eroding lands or streambanks, repair of conservation practices, and purchase of floodplain easements.

Congressional authorization for the program comes from Public Law 81-516, Section 216; Public Law 95-334, Sections 403-405; and 7 CFR. The NRCS cost-share is as high as 75 percent of the construction of emergency measures, except in limited resource areas where NRCS funding may rise as high as 90 percent. NRCS determines whether a site qualifies as a limited resource area using the most recent US Census data and the following criteria. The county must have:

1) Housing values less than 75 percent of the State housing value average;
2) Per capita income less than or equal to 75 percent of the national per capita average income; and
3) Unemployment (based on annual unemployment figures) at least twice the US national average over the past three years.

EWP recovery assistance is available to eligible sponsors, which must be a legal entity of a State government, State agency, or any Native American tribe or tribal organization. An individual may only receive assistance through sponsorship by a project sponsor. The sponsor must be able to provide the remaining 25 percent of the financial assistance above that covered by NRCS. The sponsor's portion may be in the form of cash, in-kind services, or a combination of both. The project sponsor must submit an application for the EWP program to the NRCS Field Office, or NRCS State Office. Sponsors have 60 days after the disaster to request assistance from NRCS.

The public law defines an exigency situation as one that demands "immediate attention to avoid potential loss of life or property, including situations where a second event may occur, shortly thereafter, that could compound the impairment, cause new damages, or the potential loss of life if action to remedy the situation is not taken immediately." (7CFR)

Overview of Physical Processes

As the only known water planet, Earth experiences a most profound yet conceptually simple natural process: the hydrologic cycle. Liquid water can only exist in a relatively small range of temperatures, and Earth has the precise set of circumstances that allow the cycling of water from vapor in the atmosphere, to snow and ice at high land elevations, to melt and liquid runoff downstream to the oceans, and evaporation back into the atmosphere.

Figure 1. The hydrologic cycle (NASA 2012).

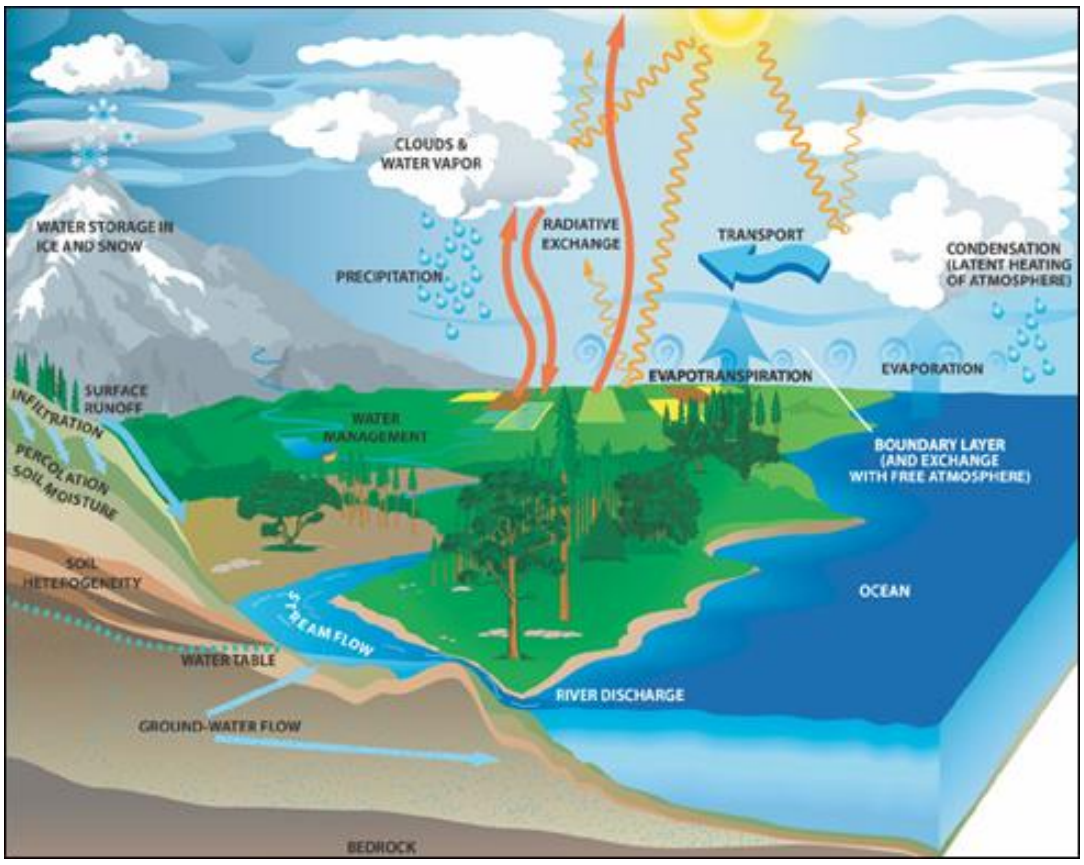

The hydrologic cycle depends on Earth's moderate air temperatures that allow water to pass through all three of these phases, liquid, gas, and solid. No other known planet gives water this flexibility. If the range of planetary surface temperatures in our solar system were placed at each end of a foot-long ruler, the average annual variation in a typical mountain watershed in the United States would fall on that scale between about 3.6 to 4.4 inches.

Figure 2. Planetary surface temperature variation in degrees Celsius

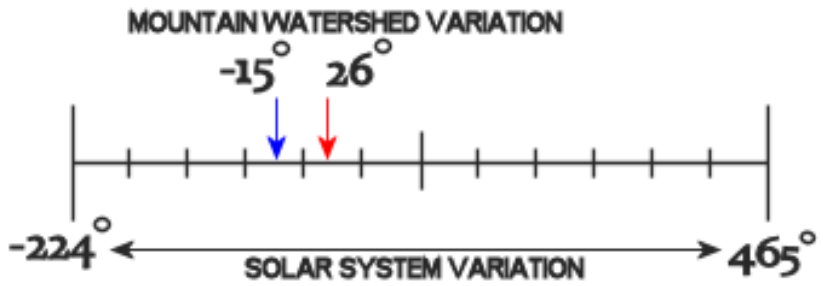

As Figure 1 illustrates, liquid water returns to vapor by more pathways than evaporation from the ocean surface. Inland lakes and streams experience evaporation. Soil itself experiences evaporation. Plants draw water from the soil and lose some of it from their leaves in the process called transpiration. Even snow can return moisture to the air by sublimation, a phase change from solid directly to gas, skipping the liquid phase.

Vegetation is a key component that affects the timing of the hydrologic cycle. As precipitation falls, it may be intercepted by leaves, which helps some of it evaporate, but also helps delay runoff and protect the soil from the erosive impact of direct rainfall. Liquid water beneath vegetation is then shielded from the sun's direct exposure and highest evaporative power. As liquid water flows across the ground, vegetation and organic litter slow the runoff, providing more opportunity for infiltration. Vegetation, through its network of roots, provides an additional avenue for infiltration. Secondly, vegetation helps the soil resist the erosive forces of flowing water both within overland pathways as well as within stream corridors. The wildfire destruction of vegetation and forest litter eliminates this hydrologic buffer, resulting in enhanced runoff and increased flooding. This increased flood risk will remain until vegetation and soil cover is reestablished.

Hence, wildfires cause hydrologic shifts for a number of years. Substantially increased runoff and sediment production results from the loss of vegetation, soil cover, and fire-induced water repellency, all of which tend to shift the rainfall response from infiltration-dominated to surface runoff-dominated processes. One study found that 10-year rainfall events on a wildfire-impacted landscape resulted in 100-year or 200-year (pre-fire recurrence) floods (Conedera et al. 2003).

Such shifts in runoff lead to the potential for loss of life and property, and impacts to infrastructure. Scale effects further complicate predictions, with greater runoff enhancement in smaller catchments and overestimation tendencies in larger catchments (Stoof et al. 2011).

Mountain Soils and Vegetation

Mountain watersheds have several characteristics that significantly differentiate runoff response from that of lower elevation watersheds. Steeper slopes promote faster flow, but also mountain soils tend to be unconsolidated and shallow. Forest litter may create a duff layer that retains moisture and increases flow resistance. However, underneath the mountain soils often contain meager organic matter. They can have higher sand and gravel content, shallow depth to bedrock, and less ability to hold moisture. As wildfire often removes vegetation and duff, these conditions provide less hillslope storage and enhance runoff.

The character of vegetation in mountain watersheds can vary significantly, depending on geographic region. The Olympic Range in Washington State and the west slopes of the Cascades from British Columbia to Northern California grow dense forests with significant understory. A short distance east of the Cascade crest the tree species change, with much lower density and less understory.

Figure 3 illustrates part of a vegetation map compiled by LandFire, a Federal interagency mapping initiative (LandFire 2010). Also known as "Landscape Fire and Resource Management Planning Tools" this program was formed by the US Department of Interior and the USDA Forest Service, with the goal of providing "a comprehensive, consistent, scientifically credible suite of spatial data layers for the entire United States," including vegetation types, forest canopy, canopy heights, fire regime classes, and more. Subdivided by geographic region, these high-resolution maps can be downloaded from the LandFire website at: http://www.landfire.gov/index.php.

Figure 3. Oregon Vegetation Types, as mapped by LandFire (2010).

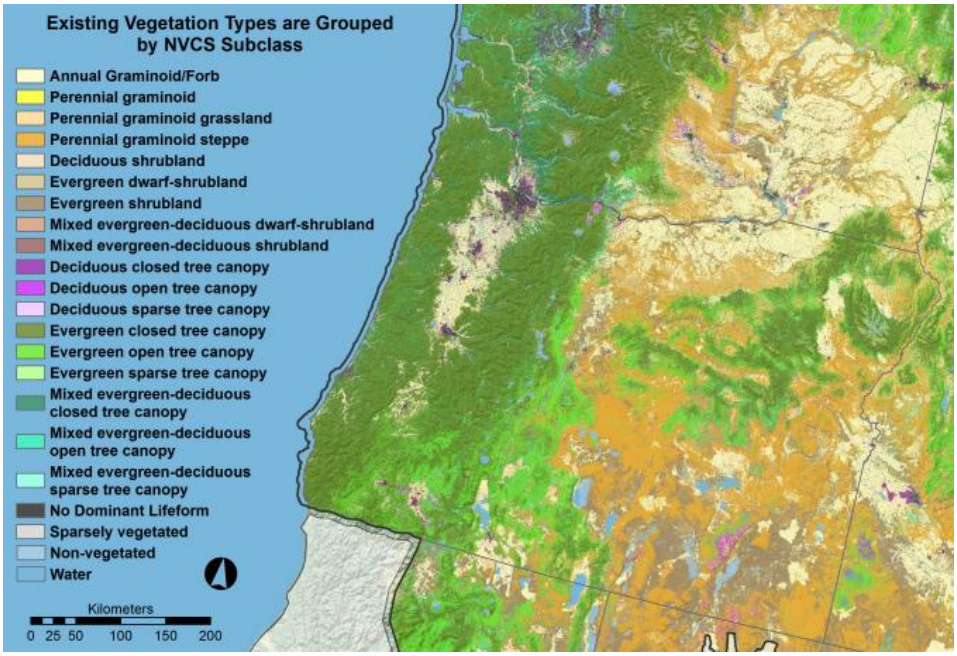

Forest cover also plays a role in the ability of a mountain watershed to store water in snowpack and thus delay its runoff. Concerning solar radiation, the forest canopy provides a much lower albedo than either bare earth or snow. While this factor raises thermal radiation, the offset provided by the forest canopy comes in the form of raised humidity, shade of shortwave radiation, and reduction of wind convection currents. The landscape retaining the greatest snowpack potential may be forests of less density with interspersed meadows. Greater snow accumulations occur, with the forest still providing some of the positive affects mentioned above.

The general slope and aspect of a mountainous watershed impacts the density of its vegetation, largely due to available water needed for plants to grow. North facing slopes tend to have more dense vegetal cover than south facing slopes because less solar radiation results in less evaporation, leaving more moisture available for plant growth.

Effect of Wildfire on Soils and Vegetation

Although wildfire events vary in intensity and burn-severity, the general affect is to reduce vegetation and ground cover, resulting in increased runoff and erosion. Fire can also cause the soil to become "hydrophobic" which greatly reduces infiltration and further increases runoff. For many past wildfire events, researchers attempting to quantify post-fire hydrologic effects have studied the particular combination of vegetation type and fire burn-severity. Because wildfire affects a watershed in more aspects than hydrology, sometimes terminology can be confusing. The ecosystem response, for example, may include soil erosion, vegetation regeneration, restoration of microbial community structure, faunal recolonization, and introduction of invasive species (Keeley 2009). The National Wildfire Coordinating Group (NWCG 2006) has produced a glossary of wildland fire terminology, which can be accessed on the web at: http://www.nwcg.gov/pms/pubs/glossary/index.htm. Similar clarifications of wildfire terminology are found in Parsons, et al. (2010).

As specifically related to hydrologic response, the following terms and definitions are generally accepted:

Burned Area Emergency Response (BAER):

BAER is a rapid assessment process undertaken by the Federal land management agencies (Table 1) in the event of fires exceeding defined thresholds for size, severity, and/or soil resource damage (Safford, et al. 2008). The intent of the BAER program is to determine whether wildfire-caused changes in soil hydrologic function have resulted in hazardous conditions that threaten life, health, property, or critical cultural and natural resources due to flooding, erosion, and debris flows. The BAER process is typically organized by the USDA Forest Service, but other federal, state, and local agencies can participate. See the section Soil Burn Severity Mapping for more details on interpretation of the BAER determined classifications. See also the USDA Forest Service BAER web page: http://www.fs.fed.us/biology/watershed/burnareas/index.html.

burned area reflectance classification (BARC)

The BARC process is a spatial data analysis technique for creating GIS layers of soil burn severity by comparing the reflectance difference in certain wavelengths between pre- and a post-fire aerial images (Safford, et al. 2008). BARC informs BAER decisions about locations requiring field visits. The imagery processing is also called "Landsat differenced Normalized Burn Ratio" or dNBR, which is defined below. Comparison with field-collected data has indicated that BARC products can be more indicative of post-fire vegetative condition than soil condition, especially in low to moderately burned areas (Hudak et al. 2004).

burn severity

Burn severity, a qualitative assessment of the heat pulse directed toward the ground during a fire, relates to soil heating, large fuel and duff consumption, consumption of the litter and organic layer beneath trees and isolated shrubs, and mortality of buried plant parts (NWCG 2006). Burn severity is subdivided into two indices, one for soil and one for vegetation. A comparison with the term fire intensity is illustrated in Figure 4.

On-the-ground evaluations of soil burn severity are based on observations of the following changes in soil characteristics (Parsons et al. 2010):

- loss of effective ground cover due to consumption of litter and duff
- surface color change due to char, ash cover, or soil oxidation
- loss of soil structure due to consumption of soil organic matter
- consumption of fine roots in the surface soil horizon
- formation of water repellent layers that reduce infiltration

fire intensity

Fire intensity, a description of the physical combustion process of energy release from organic matter, represents the energy released during various phases of a wildfire (Keeley 2009). The concept can apply to various aspects of a currently ongoing wildfire event, such as fireline intensity, which is the rate of heat transfer per unit length of the fireline. By contrast, burn severity is a post-fire condition. (See Figure 4.)

Figure 4. Differentiating between fire intensity and burn severity (from Parsons, et al. 2010).

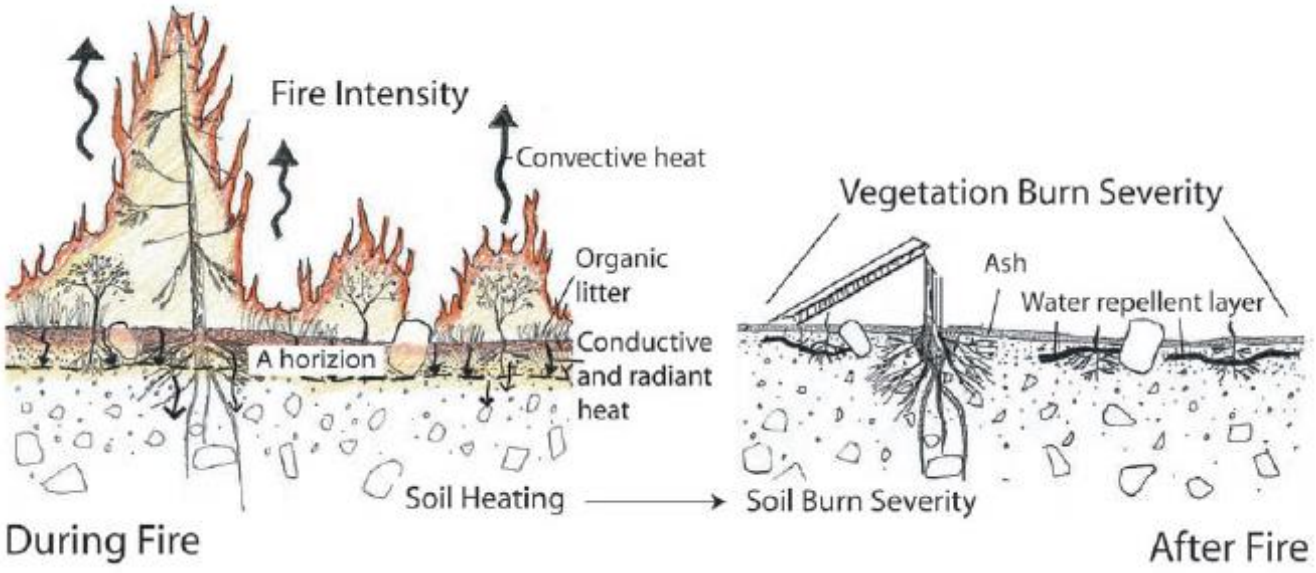

fire severity

Sometimes overly general in usage, the term fire severity has most commonly been employed in empirical studies to refer to the immediate impact on soil and vegetation of heat pulses above and below ground, particularly by indexing the degree of organic matter consumed (Keeley 2009). In this usage, the term is very similar to burn severity, the latter term preferred by BAER specialists.

Landsat differenced Normalized Burn Ratio (dNBR)

By comparing pre-fire and post-fire Landsat imagery, particularly the reflectance of bands 4 and 7, the dNBR analysis enables classification of burn severity. The BARC classification for soil burn severity uses this process. To properly assign vegetation burn severity, a modification of the process called RdNBR – where R stands for relative - is used. Comparing the absolute difference in images using dNBR tends to assign too much weight to pre-burn vegetation conditions. The relative version, RdNBR, removes this bias (Safford, et al. 2008; Miller and Thode 2007). See the section Soil Burn Severity Mapping for more details on interpretation of the BAER determined classifications.

hydrophobicity or water repellency (of soil)

A characteristic of soil generally related to organic matter, soil hydrophobicity is the tendency of the soil to resist wetting or infiltration of moisture. A relatively thin hydrophobic layer can occur in a non-burned forest, due to the leaching of organic matter from the duff into the soil. During wildfire, however, the hydrophobic layer can shift downward in the soil and increase in thickness. The intense heat of the wildfire produces a marked temperature gradient in the upper soil layer due to the fact that dry soil is a poor heat conductor (DeBano 1981). However, that temperature gradient tends to transport vaporized organic matter downward and then, upon reaching a cooler depth, condense and coat soil particles with water repellent organic compounds. Refer to Figure 5 for a schematic between unburned and burned condition and also to the section on Wildfire Induced Soil Hydrophobicity, for a more detailed discussion.

Figure 5. Soil-water repellency (hydrophobicity) as altered by wildfire (from DeBano 1981).

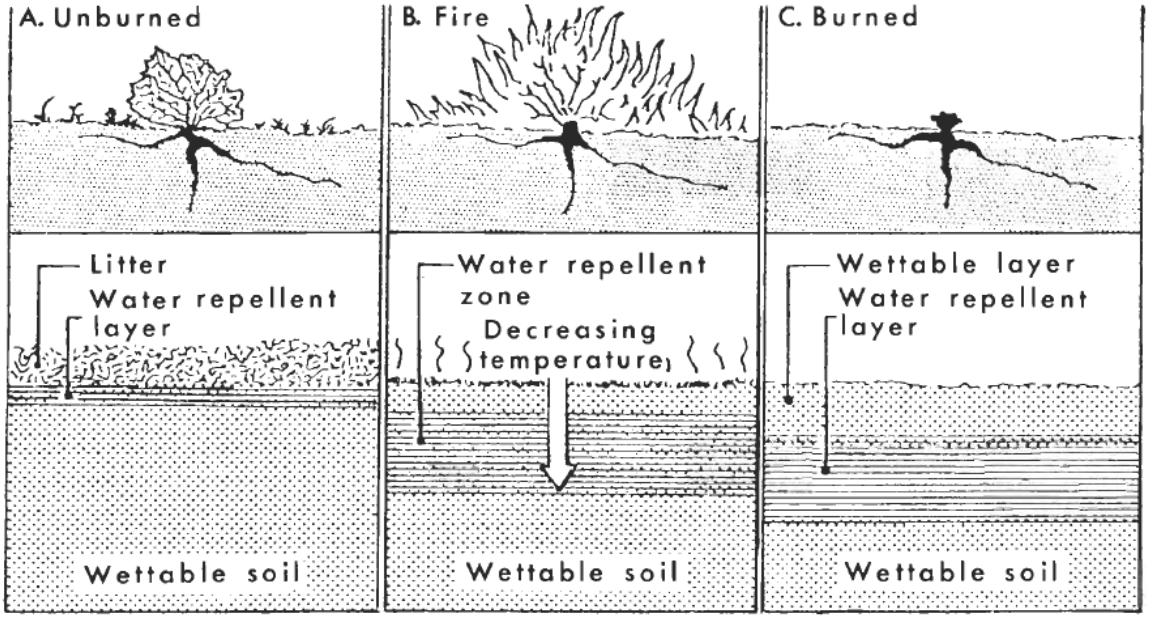

rapid assessments of vegetation condition after wildfire (RAVG)

A process used by USDA Forest Service specialists to prepare spatial mapping of wildfire effects on vegetation, RAVG uses Landsat Thematic Map images and accounts for before and after wildfire conditions. In particular, the reduction of vegetation due to wildfire is indexed by basal area loss, where basal area is a forest management term referring to the sum of cross-sectional

areas of trees and stems at breast-height for a given section of land. Although the BAER teams generally focus on rapid assessment of soil burn severity using BARC, the RAVG project creates maps of wildfire on vegetation, usually within thirty days of fire containment. Further historical information on vegetation effects is produced by the cooperative project Monitoring Trends in Burn Severity (MTBS) through the website http://www.mtbs.gov/.

Soil Burn Severity Mapping

The USDA Forest Service BAER teams assess soil burn severity and produce high-resolution GIS-based maps. The process uses remote sensing (BARC) with field verification (Parsons et al. 2010). The GIS soil burn severity layers generally use three categories that are defined as follows (Parsons et al. 2010):

low soil burn severity

Surface organic layers are not completely consumed and roots are generally unchanged, due to minimal heat penetration of the soil. While exposed mineral soil may appear lightly charred, the canopy and understory vegetation generally appears unchanged.

moderate soil burn severity

Up to eighty percent of the pre-fire ground cover may be consumed. Roots may be scorched but generally not completely consumed, and soil structure is unchanged.

high soil burn severity

All or nearly all of the pre-fire ground cover is generally consumed, along with roots up to 0.1 inches (0.25 cm) in diameter. Charring may be visible on larger roots. Significant bare or ash-covered soil is exposed and soil structure is less stable due to loss of root mass.

Wildfire Induced Soil Hydrophobicity

The development of soil hydrophobicity is multi-factored and does not necessarily correlate with soil burn severity (Parsons et al. 2010). The depth and thickness of wildfire-induced soil hydrophobicity is dependent upon vegetation type, amount of soil organic matter, soil texture, fire residence time, and burn temperature (DeBano 1981, Huffman, et al. 2001). An important

pre-condition is that organic matter must exist for the wildfire to vaporize, leading to condensation of the hydrophobic compounds within the soil profile (DeBano et al. 1967).

Greater water repellency has been generally associated with coarse-grained soil texture. Given a limited supply of condensing hydrophobic substances, the smaller surface areas of coarse-grained soils are more completely covered than the greater surface area of silts and clays (Doerr et al. 2000).

In addition, the susceptibility of soil texture to hydrophobicity has been related to hydrologic soil group classification. This soil characteristic is a standard parameter of the USDA Natural Resources Conservation Service (NRCS) Soil Survey. Of the four hydrologic soil groups, coarse-grained soils tend to be classified as hydrologic soil groups A or B (greater tendency toward hydrophobicity), while silt and clay tend toward hydrologic soil groups C or D (less hydrophobic tendency).

A field procedure to detect soil hydrophobicity is as follows. Scrape away any ash layer and test the upper mineral soil layer by placing several individual drops of water on the air-dried surface. If the drops remain after one minute, the layer is considered to be hydrophobic. (See Figure 6.)

Figure 6. Water droplets resisting infiltration into soil due to extreme hydrophobicity (Doerr et al. 2000). Hypodermic needle provides scale.

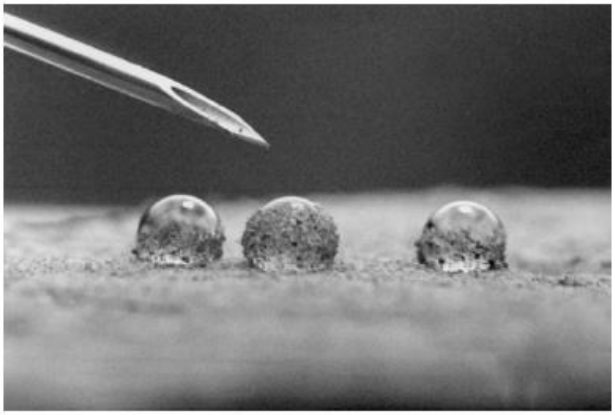

Less severe burning often causes hydrophobicity of the soil surface. In locations that have experienced greater burn severity, the top of the hydrophobic layer may be at some depth, say 0.5 to 3 inches. Recognizing this possibility, the lower layers should be tested if it is found that the top layer is not water repellent. Scrape away 0.5 to 1 inch of soil depth and repeat the water drop test. By continuing this procedure, both the depth of the top and bottom of the hydrophobic layer may be determined for that location. This field procedure can be repeated over time to investigate hydrophobicity persistence. Considerable spatial variability in hydrophobicity can be expected.

More extensive field procedures have been developed to quantify the degree of hydrophobicity, such as measuring the water drop penetration time (WDPT). For more severe hydrophobicity, ethanol drops are sometimes used in a critical surface tension (CST) test. These and other more extensive procedures are discussed in the literature (Huffman et al. 2001, Scott 2000, Doerr 1998, Robichaud et al. 2008).

The persistence of hydrophobicity is dependent upon several factors, including wetting-drying cycles, and both physical and biological action (Huffman, et al. 2001 and DeBano, 1981).

Contact by moisture is a factor in the breakdown of hydrophobicity. Although first contact with moisture is repelled, a soil moisture threshold may be exceeded, at which point the layer will allow some infiltration. Upon drying the layer may again become hydrophobic. However, this wetting and drying process, along with other physical and biological factors, removes hydrophobicity over time. Among the factors that help break down hydrophobicity are impact of wildlife trodding, impact of falling vegetation, such as branches, root penetration of the water repellent layer, and the freeze-thaw process. The hydrophobicity may be minimized in as short a time as a few months (Huffman et al. 2001), but more extensive hydrophobic layers can persist for up to six years (Dyrness 1976).

Hydrologic Modeling

Rainfall-runoff process modeling has a long history and numerous computer programs have been developed for the task. These models vary in complexity. In general, the pertinent aspects of the landscape are accounted for. These include land cover, soils, elevation, slope, sub-basin shape, vegetation character, and flow time of concentration Meteorological factors are characterized, either using actual storm hyetographs of one or more precipitation gages, or theoretical less-frequent event storms, such as the 100-year 24-hour storm. Precipitation is distributed over time using pre-determined synthetic storm distribution curves that define rainfall intensity throughout the storm. The shape of the runoff hydrograph is often estimated using one of several possible unit-hydrograph estimation methods. Finally, for larger watersheds flow routing is needed to transform and attenuate flow through stream systems.

Continuous simulation models, such as AGNPS (USDA-ARS, 2013a) and SWAT (USDA-ARS, 2013b.) help analyze runoff, sedimentation, and water quality issues over longer time periods, such as decades. For assessment of rainfall-runoff after wildfire the hydrologic model of choice is usually singular storm-event-based, and predictive in nature. Commonly used models are HEC-HMS from the US Army Corps of Engineers Hydrologic Engineering Center (USACE-HEC, 2013), and either WinTR-20 or WinTR-55, from the NRCS (USDA-NRCS, 2013). BAER teams often implement WILDCAT (Hawkins and Greenberg 1990). KINEROS2 (Smith et al. 2005, Canfield and Goodrich 2005) has also been implemented for wildfire area runoff simulation, through the AGWA GIS-based tool for watershed assessments.

Accounting for changes in runoff hydrology due to wildfire is generally a matter of determining the extent to which runoff has been accelerated due to the loss of vegetation or the lack of infiltration due to soil hydrophobicity. With the NRCS models, WinTR-20 and WinTR-55, runoff is computed using the SCS Curve Number (CN) method. The SCS CN method lends itself to adjustment for the effects of wildfire through selection of CN itself (accounting for burned areas) and by an adjustment in time of concentration (accounting for accelerated post-fire runoff). A brief summary of the CN method is provided, followed by a discussion of wildfire-induced adjustment of the modeling parameters. Limitations of the method in forested, wildfire-impacted landscapes are also discussed.

Other infiltration methods, available in models such as HEC-HMS, do not employ runoff curve numbers. Adjusting these methods to account for wildfire effects is discussed in its own section.

Overview of the CN method

The CN method is most commonly used to predict runoff from wildfire-impacted landscapes. As documented in USDA-NRCS (2004b), the NRCS method for estimating direct runoff from individual storm rainfall events is of the following form:

$$Q = \frac{(P-I_a)^2}{(P-I_a)+S} \quad \text{if} \quad P > I_a \qquad\qquad Q = 0 \quad \text{if} \quad P \leq I_a \qquad \text{(eq. 1)}$$

where Q is the depth of runoff (inches), P is the depth of rainfall (inches), I_a is the initial abstraction (inches), and S is the maximum potential retention (inches). The equation derivation, while not physically based, does respect conservation of mass (USDA-NRCS 2004b). The Curve Number (CN) is defined as:

$$CN = \frac{1000}{10+S} \qquad \text{(eq. 2)}$$

The initial abstraction was initially described and has traditionally been used as shown in equation 3a. More recent research (Hawkins, et al. 2002) has suggested equation 3b.

$$I_a = 0.2\,S \qquad \text{(eq. 3a)}$$

$$I_a = 0.05\,S \qquad \text{(eq. 3b)}$$

The CN is a simple catchment-scale method that gives simplified results at a watershed outlet. More accurate results are expected for larger, higher-intensity rain events. The method is documented is in the NRCS National Engineering Handbook, Part 630, Hydrology, Chapters 9 and 10 (USDA-NRCS 2004a, USDA-NRCS 2004b), in Rallison (1980), and Rallison and Miller (1982), as well as in numerous other publications. However, little quantitative information has been published of the database on which it was developed (Maidment 1992). In general, the method was developed for rural watersheds in various parts of the United States, within 24

states, was developed for single storms, not continuous or partial storm simulation; and was not intended to recreate a specific response from an actual storm (Rallison, 1980).

Adjusting Time of Concentration for Wildfire Effects

Watershed time of concentration is defined as the time required for drainage from the most hydraulically remote point in the watershed to its outlet. Time of concentration, and the related parameter, lag time, are shown on the dimensionless unity hydrograph schematic, Figure 7. This definition and methods for computing the parameter are discussed in USDA-NRCS (2010).

Figure 7. The relation between time of concentration (Tc), lag (L), and the dimensionless unit hydrograph (USDA-NRCS 2010).

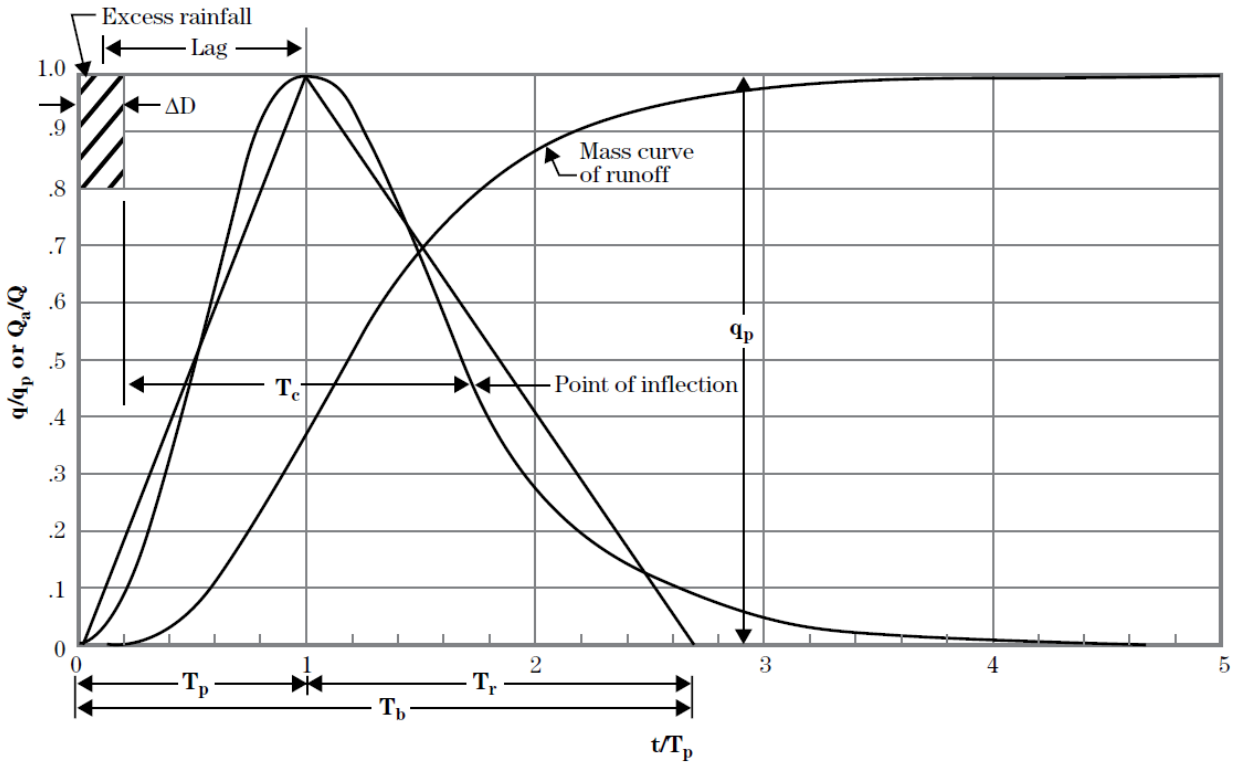

where:

Lag = Lag (hr)

T_c = time of concentration (hr)

T_p = time to peak (hr)

T_r = time of recession (hr)

712 T_b = time base of triangular approximation (hr)
713 ΔD = duration of excess rainfall (hr)
714 t/Tp = ratio between time interval and time to peak (dimensionless)
715 q = discharge rate at time t (ft^3/sec)
716 q_p = peak discharge rate at time T_p, (ft^3/sec)
717 Q_a = runoff volume up to t (in)
718 Q = total runoff volume (in)
719
720 The runoff models WinTR-20 and WinTR-55 use time of concentration to estimate the shape of
721 the unit hydrograph that is used to determine a flood runoff hydrograph. The reference provides
722 two methods for computing time of concentration, termed the Watershed Lag Method and the
723 Velocity Method.
724
725 ***Watershed Lag Method***
726 The Watershed Lag Method employs the following equation, in which the only wildfire-affected
727 variable is curve number.

728 $$T_c = \frac{L^{0.8}(\frac{1000}{CN} - 9)^{0.07}}{1140Y^{0.5}} \quad \text{(eq. 4)}$$

729 where:
730 T_c = time of concentration (hr)
731 L = flow length (ft)
732 CN = curve number (dimensionless)
733 Y = average land slope (percent)
734
735 Note that Y is the land slope, not the flow profile slope. Both the average land slope and the flow
736 length can be easily determined from GIS. USDA-NRCS (2010) gives several ways to estimate
737 Y. The reference also suggests that the development of this lag method equation precludes its
738 use for watersheds larger than 19 square miles.
739
740
741

Velocity Method

The second approach proposed by USDA-NRCS (2010) is called the Velocity Method, which sums the estimated flow times of three types of flow from the most hydraulically distant point in the watershed, namely, sheet flow, shallow concentrated flow, and channel flow. The reference suggests that sheet flow occurs for no more than 100 feet before transitioning to shallow concentrated flow. This second type of flow is considered to not yet have entered a well-defined channel, but to have converged in swales, small rills, and gullies. A rule of thumb is that shallow concentrated flow should not be assumed to extend longer than 1,000 feet, although this length can vary substantially. For example, the distance from drainage divides to channel heads has been found to vary from 400 to 4,200 feet (mean of 1,400 feet) in the Front Range of Colorado (Henkle et al. 2011). Runoff from post-fire conditions may cause the channel head to migrate upstream, shortening the distance of shallow concentrated flow.

An equation for the travel time of the overland flow segment, provided in USDA-NRCS (2010), was developed from the kinematic wave equation:

$$T_{overland} = \frac{0.007(nL)^{0.08}}{P^{0.5}S^{0.4}} \quad \text{(eq. 5)}$$

where:

$T_{overland}$ = travel time (hr)

n = Manning's roughness coefficient for overland flow, obtained from Table 2

L = sheet flow length (ft < 100)

P = 2-year, 24-hour rainfall (in)

S = land slope (ft/ft)

765 **Table 2. Manning's roughness coefficients for sheet flow (depth generally ≤ 0.1 ft)**

Surface description	n [1/]
Smooth surface (concrete, asphalt, gravel, or bare soil)	0.011
Fallow (no residue)	0.05
Cultivated soils:	
Residue cover ≤ 20%	0.06
Residue cover > 20%	0.17
Grass:	
Short-grass prairie	0.15
Dense grasses [2/]	0.24
Bermudagrass	0.41
Range (natural)	0.13
Woods: [3/]	
Light underbrush	0.40
Dense underbrush	0.80

1 The Manning's n values are a composite of information compiled by Engman (1986).
2 Includes species such as weeping lovegrass, bluegrass, buffalo grass, blue grama grass, and native grass mixtures.
3 When selecting n, consider cover to a height of about 0.1 ft. This is the only part of the plant cover that will obstruct sheet flow.

766

767

768 For the shallow, concentrated flow segment, NRCS (2010) suggests the following equation:

769 $$T_{shallow} = \frac{L}{3600V} \quad \text{(eq. 6)}$$

770 where:

771 $T_{shallow}$ = travel time (hr)

772 L = flow length (ft < 1000)

773 V = flow velocity (ft/sec, from Table 3)

774

775 **Table 3. Shallow-concentrated flow velocity equations, where s=flow slope in ft/ft**

Table 3 Shallow-concentrated flow velocity equations, where s = flow slope in ft/ft

Flow type	Manning's *n*	Velocity equation (ft/sec)
Pavement and small upland gullies	0.025	$V = 20.328(s)^{0.5}$
Grassed waterways	0.050	$V = 16.135(s)^{0.5}$
Nearly bare and untilled (overland flow); and alluvial fans in western mountain regions	0.051	$V = 9.965(s)^{0.5}$
Cultivated straight row crops	0.058	$V = 8.762(s)^{0.5}$
Short-grass pasture	0.073	$V = 6.962(s)^{0.5}$
Minimum tillage cultivation, contour or strip-cropped, and woodlands	0.101	$V = 5.032(s)^{0.5}$
Forest with heavy ground litter and hay meadows	0.202	$V = 2.516(s)^{0.5}$

776

777

778 For the channel flow segment, NRCS (2010) suggests using the velocity form of Manning's
779 equation:

780 $$V_{channel} = \frac{1.486 R^{2/3} S^{1/2}}{n} \quad \text{(eq. 7)}$$

781 where:

782 V_{channel} = flow velocity (ft/sec)

783 R = hydraulic radius (ft)

784 S = flow slope (ft/ft)

785 n = Manning's roughness coefficient for channel flow

786

787 Note that hydraulic radius is equivalent to the flow cross-sectional area divided by the wetted
788 perimeter. The equation has the disadvantage that, although flow slope and Manning's
789 roughness coefficient can be reasonably estimated, the hydraulic radius cannot. One way to
790 handle this unknown is to transform the equation so that flow area becomes the unknown
791 variable. Then it is possible to obtain the flow area from regional hydraulic geometry relations
792 that relate flow area to watershed drainage area. Typically, these regional relationships use
793 bankfull flow, although not all regions have been studied. Even given the availability of an
794 equation relating cross-sectional area to drainage area, an estimate must be made of the
795 relationship between flow depth and width for, say, a trapezoidal channel (Figure 8).

796

Figure 8. Trapezoidal channel dimensions.

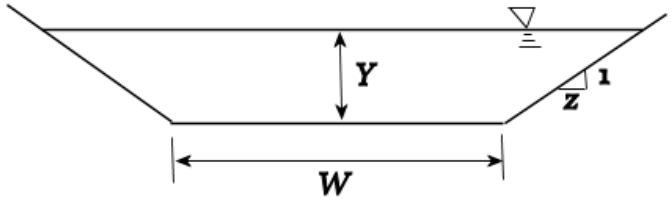

From Figure 8, cross-sectional flow area is defined as:

$$A = YW + zY^2 \quad \text{(eq. 8)}$$

For simplification, group the Manning's equation terms already estimated:

$$\emptyset = \frac{1.486S^{0.5}}{n} \quad \text{(eq. 9)}$$

Since hydraulic radius equals flow area divided by wetted perimeter, for a trapezoidal channel shape the equation becomes:

$$V_{channel} = \emptyset A^{2/3}\left(W + 2Y\sqrt{1+z^2}\right)^{-2/3} \quad \text{(eq. 10)}$$

If we can assume that W is some multiple of Y then equation 10 is reduced to:

$$V_{channel} = \emptyset \mu A^{1/3} \quad \text{(eq. 11)}$$

where:

$V_{channel}$ = flow velocity (ft/sec)

A = cross-sectional flow area (ft^2)

$\emptyset$ = result of equation 9

μ = value from table 4

Table 4. Channel flow parameters for estimating velocity.

z	W	μ
2	2Y	0.4571
2	3Y	0.4474
2	4Y	0.4372
3	2Y	0.4163
3	3Y	0.4102
3	4Y	0.4034
3	5Y	0.3966
4	2Y	0.3852
4	3Y	0.3811
4	4Y	0.3764
4	5Y	0.3716

Having obtained bankfull flow area from a regional hydraulic geometry equation, an estimate of channel velocity is available, and travel time for the channel segment becomes:

$$T_{channel} = \frac{L}{3600 V_{channel}} \quad \text{(eq. 12)}$$

where:

$T_{channel}$ = travel time (hr)

L = flow length

V = flow velocity (ft/sec, from equation 10)

Note that the Velocity Method lends itself well to computation using GIS. For example, given a digital elevation model of 10 meter by 10-meter grids, a flow accumulation layer is developed. For travel time computations, flow in a given grid cell would be considered overland if the flow accumulation value is 3 or less. Assuming shallow concentrated flow extends for 1,000 feet, a grid cell would be considered to contain shallow concentrated flow if the flow accumulation value is between 3 and 30. Any grid cell with a flow accumulation value above 30 would be

considered to contain channel flow. The drainage area to that channel flow grid cell would be obtained by a conversion from the flow accumulation value. In this manner, the travel time from any location to the outlet can be computed.

Adjusting Curve Number for Wildfire Effects

The NRCS Curve Number method was empirically derived using data from about twenty-four agricultural watersheds across the country (Rallison 1980). While generally thought of as an index of infiltration, it should be noted that the method incorporates assumptions about interception and depression storage. As its derivation was a curve-fitting exercise, tables of curve numbers for different land surfaces resulted. While field determination of curve number for a watershed could be computed from measured rainfall and streamflow (with baseflow assumptions) this is rarely attempted. One study of ten Appalachian forested watersheds found that measured curve numbers varied significantly from published suggested values (Tedela, et al. 2012). However, the study also found very wide confidence limits for the measured values. One watershed, with a measured mean curve number of 57, had 95% confidence interval of 32 to 83.

Application of the SCS Curve Number method for Western and more arid watersheds has been dependent on subsequent estimations of applicable curve numbers, such as found in Table 5 (USDA-SCS, 1991.)

Table 5. Runoff curve numbers for arid and semiarid rangelands

cover type	hydrologic condition	A	B	C	D
Herbaceous-mixture of grass, weeds, and low-growing brush, with brush the minor element	poor		80	87	93
	fair		71	81	89
	good		62	74	85
Oak-aspen-mountain brush mixture of oak brush, aspen, mountain mahogany, bitter brush, maple, and other brush	poor		66	74	79
	fair		48	57	63
	good		30	41	48
Pinyon-juniper-pinyon, juniper, or both; grass understory	poor		75	85	89
	fair		58	73	80
	good		41	61	71
Sagebrush with grass understory	poor		67	80	86
	fair		51	63	70
	good		35	47	55
Desert shrub-major plants include saltbush greasewood, creosotebush, blackbrush, bursage, palo verde, mesquite, and cactus	poor	63	77	85	88
	fair	55	72	81	86
	good	49	68	79	84

note: average runoff conditions. (group A only developed for desert shrub)

Hydrologic condition defined as follows:

poor: < 30% ground cover (litter, grass, and brush overstory)

fair: 30 to 70% ground cover

good: >70% ground cover

Existing methods for adjusting runoff curve numbers to account for wildfire effects are, for the most part, based heavily upon the hydrologic judgment of practitioners who have studied burned watersheds. A number of publications, including Foltz, et al. (2009) have documented these methods. For a synopsis of the state of the art, research issues related to post-wildfire runoff and erosion processes, and suggested areas needing further work, see Moody, et al. (2013).

One of the first efforts to establish some methodology for adjustment of runoff curve numbers for the effects of wildfire was Cerrelli (2005). Studying Montana wildfire events in 2000 and 2001, Cerrelli created an Excel spreadsheet that computes watershed curve numbers for four conditions: 1) pre-fire, 2) early post-fire with possible hydrophobicity, 3) medium term post-fire with hydrophobicity no longer in effect, but little re-emergent vegetation, and 4) later post fire, after one growing season. For high burn severity areas, the investigation included a table of

wildfire affected curve numbers. See Table 6. The Fire Hydrology spreadsheet and user notes can be downloaded from ftp://ftp.wcc.nrcs.usda.gov/wntsc/H&H/wildfire/.

Table 6. Suggested fire-effected runoff curve numbers from Cerrelli (2005).

hydrologic soil group	high burn severity CN
A	64
B	78
C	85
D	88

In addition, the guidance for moderate burn severity was to use the published curve number tables, but with cover type in "fair" condition, and for low burn severity, to pay attention to the aspect of the fire-burned slopes. For low burn severity, with north and east facing slopes, the guidance was to use cover type "good" condition, and for south and west facing slopes to use a curve number between cover type "fair" and "good" condition.

Cerrelli's investigation, method development, and use on the Montana Bitterroot wildfires of 2000, are documented in the case study section of this technical note.

The USDA Forest Service has provided web-based guidance for determination of wildfire affected runoff curve numbers, which includes Cerrelli's work. (See: http://forest.moscowfsl.wsu.edu/BAERTOOLS/ROADTRT/Peakflow/CN/.) Additionally, the experiences of forest hydrologists is documented, for example, post-fire runoff curve numbers for Forest Service Region 1 as suggested by two different investigators as shown in Table 7 and Table 8. (See Figure 9 for a map of the USDA Forest Service Regions.)

894 **Table 7. Forest Region 1 curve numbers**

post-fire condition	CN range
high burn severity, with hydrophobic soils	93-98
high burn severity, without hydrophobic soils	90-95

895

896 **Table 8. Forest Region 1 curve numbers**

post-fire condition	CN range
moderate burn severity	80
low burn severity	70-72
unburned	60-64
moderate burn severity, with BAER treatments	75
moderate burn severity, with hydrophobic soils	66

897

898 **Figure 9. USDA Forest Service Regions**

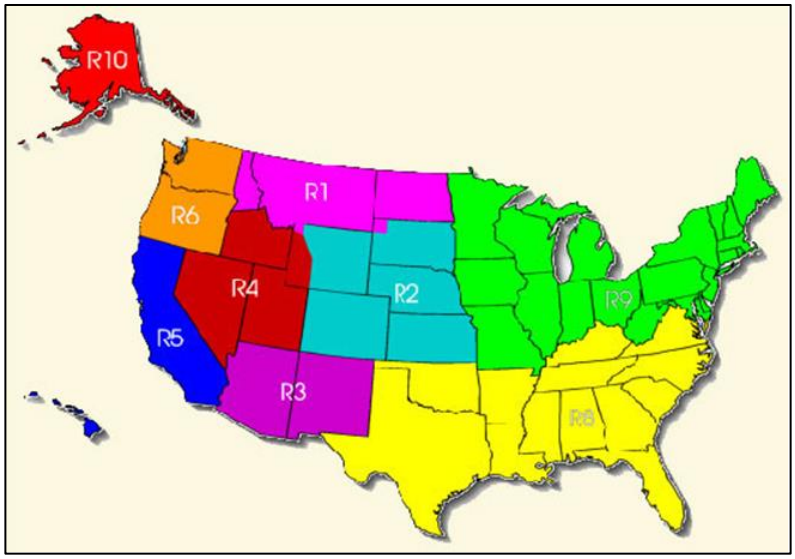

899

900

901 Other forest service hydrologists suggest runoff curve numbers for Forest Service Region 3

902 (Arizona and New Mexico) as shown in Table 9 and Table 10.

Table 9. Forest Region 3 curve numbers

post-fire condition	CN range
high burn severity, with hydrophobic soils	95
high burn severity, without hydrophobic soils	92
moderate burn severity, with hydrophobic soils	89
moderate burn severity, without hydrophobic soils	87
low burn severity	80-83
unburned	55-75

Table 10. Forest Region 3 curve numbers

post-fire condition	CN range
high burn severity, with hydrophobic soils	95
high burn severity, without hydrophobic soils	90-91
moderate burn severity, with hydrophobic soils	90
moderate burn severity, without hydrophobic soils	85
low burn severity	$CN_{pre\text{-}fire} + 5$
straw mulch with good coverage	60
seeding with log erosion barriers, 1-year post-fire	75
log erosion barriers without hydrophobic soils	85

Table 9 was published in Livingston (2005). Another investigation by the Forest Service produced a table comparing pre-fire to post-fire runoff curve numbers for the 2003 Aspen Fire in Arizona. (See Table 11.)

Table 11. Forest Region 3 pre-fire and post-fire curve numbers

hydrologic soil group	$CN_{pre\text{-}fire}$	$CN_{post\text{-}fire}$		
		low burn severity	moderate burn severity	high burn severity
B	56	65	--	--
C	67	70-75	80	90
D	77	80-85	90	95

CN methodology limitations in forested watersheds

Post fire runoff prediction using the CN technique is hampered by the very little available field data available to reliably select CN values from measured rainfall and runoff in burned catchments. Estimates are provided above, but additional research would be beneficial for o appropriately define CNs for post fire and treatment conditions.

More fundamentally, the reliability of the CN method for predicting peak flow from forested, mountainous watersheds is questionable. Forested watersheds in unburned conditions may be dominated by saturation-excess overland flow, where runoff is produced from relatively small and variable portions of a catchment when rainfall depths exceed the soil capacity to retain water. Newly burned catchments, on the other hand, may be dominated by infiltration-excess (Hortonian) overland flow, where surface runoff is generated when rainfall intensity is greater than soil infiltration capacity, and flow runs down the hillslope surface. For example, rainfall-runoff modeling performed in the San Dimas Experimental Forest (Chen et al. 2013) found that pre-fire runoff predictions were more accurate using the CN method, while KINEROS2 performed better for post-fire conditions. These results suggest fundamental shifts in runoff mechanisms between pre- and post-fire conditions, complicating modeling strategies.

In general, saturation-excess overland flow may likely be the dominant source of streamflow for storms of lower intensity while infiltration-excessive overland flow may be dominant during high-intensity storms. The CN method does not assume either overland flow mechanism, but merely tries to predict the runoff portion of catchment-scale storm-generated streamflow, while ignoring the underlying processes (Garen and Moore 2005). Hence, the CN method ignores

shifts in domain streamflow generating mechanisms in forested catchments, as surface conditions change due to such disturbances as wildfire, and as rainfall magnitude ranges between 2-year and 100-year storm events. Thus, the CN method is vulnerable to such behavior as CN decreasing with increasing rainfall. Inability to achieve a stable CN value was found by Hawkins (1993) and Springer and Hawkins (2005), while Tedela et al. (2012) found poor predictive capabilities of single tabulated CN values for predicting peak flows in forested watersheds.

These studies underscore the value of calibrating storm runoff models using measured precipitation and streamflow data, whether pre- or post-wildfire. Where these data exist, modeling attempts shortly after a wildfire event will suffer from a very short data record. However, landscape conditions after a wildfire may also be expected to evolve relatively rapidly, as vegetation begins to regrow and hydrophobic effects wane. See the Whitewater-Baldy case study for an example of model calibration using data of less than one-year record-length after a wildfire.

Post-Wildfire Infiltration Modeling by Other Methods than CN

The limitations of the CN method discussed above are not necessarily overcome by other process-based infiltration models. As argued by Bevin (1989 and 2001) physically based models suffer from a number of practical limitations, including problems of scale and parameter dimensionality. As to scale, these models often use equations of physical processes at a point on the landscape, with input parameters applicable at that point, to represent considerably large watershed areas where those parameters may vary significantly. As to dimensionality, the equation input parameters may be numerous and without possibility of calibration. The more input parameters borne by a model the greater the uncertainty of the true impact of any one of them on the outcome being predicted.

Nevertheless, the fact that high-resolution soils data, for example, is becoming more and more readily available, along with digital elevation grids, vegetation and burn severity mapping, the process-based infiltration models may be expected to perform as well or better than the CN method. For example, the Green and Ampt (GA) method is a simplification of Richard's equation for infiltration that has a limited number of parameters that can be reasonably estimated

using soils data. As discussed in the HEC-HMS User Manual (USCOE-HEC, 2013) GA infiltration is estimated using equation 13, with parameters correlated with soil texture (Table 12).

$$f_t = K\left[\frac{1+(\emptyset-\theta_i)S_f}{F_t}\right] \quad \text{(eq. 13)}$$

where:

f_t = loss during time period, t

K = saturated hydraulic conductivity

ϕ = soil porosity (volume air/volume soil)

θ_i = initial soil water content (volume water/volume soil)

S_f = wetting front suction

F_t = cumulative loss at time t

Table 12. Green and Ampt parameters for soil texture classes and soil horizons (Rawls, et al. 1983, and Saxton, et al. 1986)

texture	horizon	$\varphi_{effective}$ (cm^3/cm^3)	K_{sat} (cm/hr)	S_f (cm)	$\theta_{fieldCap}$ (cm^3/cm^3)	$\theta_{wiltingPt}$ (cm^3/cm^3)
sand	combined	0.417	23.56	4.95	0.13	0.06
	A	0.431	--	5.34	--	--
	B	0.421	--	6.38	--	--
	C	0.408	--	2.07	--	--
loamy sand	combined	0.401	5.98	6.13	0.15	0.07
	A	0.424	--	6.01	--	--
	B	0.412	--	4.21	--	--
	C	0.385	--	5.16	--	--
sandy loam	combined	0.412	2.18	11.01	0.20	0.09
	A	0.469	--	15.24	--	--
	B	0.428	--	8.89	--	--
	C	0.389	--	6.79	--	--
loam	combined	0.434	0.68	8.89	0.26	0.12
	A	0.476	--	10.01	--	--
	B	0.489	--	6.40	--	--
	C	0.382	--	9.27	--	--
silt loam	combined	0.486	1.30	16.68	0.29	0.11
	A	0.514	--	10.91	--	--
	B	0.515	--	7.21	--	--
	C	0.460	--	12.62	--	--
sandy clay loam	combined	0.330	0.30	21.85	0.26	0.16
	B	0.330	--	26.10	--	--
	C	0.332	--	23.90	--	--
clay loam	combined	0.309	0.20	20.88	0.33	0.19
	A	0.430	--	27.00	--	--
	B	0.397	--	18.52	--	--
	C	0.400	--	15.21	--	--
silty clay loam	combined	0.432	0.20	27.30	0.37	0.19
	A	0.477	--	13.97	--	--
	B	0.441	--	18.56	--	--
	C	0.451	--	21.54	--	--
sandy clay	combined	0.321	0.12	23.90	0.35	0.25
	B	0.335	--	36.74	--	--
silty clay	combined	0.423	0.10	29.22	0.42	0.26
	B	0.424	--	30.66	--	--
	C	0.416	--	45.65	--	--
clay	combined	0.385	0.06	31.63	0.48	0.35
	B	0.412	--	27.72	--	--
	C	0.419	--	54.65	--	--

The remaining parameter from equation 13 is initial soil moisture content, which must be between zero (a completely dry soil) and the effective porosity. The user may estimate this value using an antecedent soil moisture index and values from Table 12 for field capacity and wilting point. Note that field capacity is considered to be the soil moisture content at which further downward drainage by gravity is negligible. A soil is considered to reach field capacity two to three days after saturation. Wilting point is considered the soil moisture content below which vegetation cannot be sustained.

Figure 10 shows the HEC-HMS input interface for the Green and Ampt loss equation. To account for post-wildfire hydrophobicity with the Green and Ampt, one can raise the percent imperviousness and/or reduce hydraulic conductivity. The use of this loss method is demonstrated in the Whitewater Creek case study.

Figure 10. HEC-HMS Green and Ampt input interface (USCOE-HEC 2013)

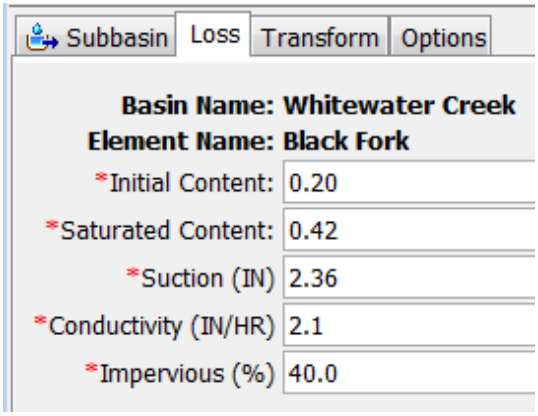

Canfield, et al. (2005) included in their field studies of post-wildfire conditions some examination of the effect on saturated hydraulic conductivity. The increase over time of K_{sat} (Figure 11) may be an indication of the breakdown of hydrophobicity.

Figure 11. Optimal hillslope hydraulic conductivity, Cerro Grande NM fire (Canfield, et al. 2005)

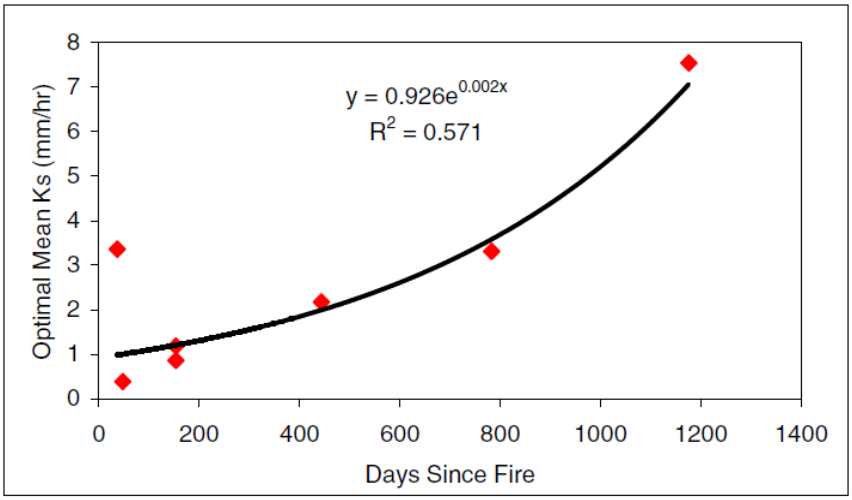

Adjusting Unit Hydrograph Parameters for Post-Wildfire Effects

Synthetic Unit Hydrograph Peak Rate Factor

The SCS curve number method employs a triangular unit hydrograph estimate. The shape of a unit hydrograph is affected by time of concentration and a shape coefficient, called the peak rate factor, varying from about 300 to 600. The peak rate factor is generally considered to be dependent on the overall sub-basin storage effects on flow routing. A flat swampy watershed will generally result in a peak rate factor closer to 300, whereas steep mountainous terrain might be near 600. Referring to Figure 7, the CN method dimensionless unit hydrograph is approximated by a triangle, which was developed by assuming that, for an "average" watershed, time of recession would be about 1.67 times the time to peak (USDA-NRCS 2007).

From Figure 7, the area under the triangle represents the direct runoff from a watershed (Q). Using the variables shown in Figure 7, direct runoff is computed as shown in equation 14a. Reordering to solve for peak discharge results in equation 14b.

$$Q = \frac{q_p(T_P+T_r)}{2} \quad \text{(eq. 14a)}$$

$$q_p = \frac{2Q}{(T_p+T_r)} \quad \text{(eq. 14b)}$$

Equation 14b is then expressed as equation 15 (McCuen and Bondelid, 1983) in "terms ordinarily used" (USDA-NRCS 2007) by assuming the dimensionless unit hydrograph pertains to the direct runoff of one inch in one hour from one square mile of drainage area.

$$q_p = \frac{D_f A Q}{t_p} \quad \text{(eq. 15)}$$

where:

A = drainage area (mi^2)

Q = direct runoff (in)

D_f = peak rate factor

t_p = time to peak (hr)

The peak rate factor (equation 16) relates to the proportion of the time to peak to the total runoff time and includes a conversion factor (between cfs, square miles, inches, and hours).

$$D_f = \frac{1290.67\, T_p}{(T_p + T_r)} \quad \text{(eq. 16)}$$

For the "average" watershed (USDA-NRCS 2007), T_p = 1 and T_r = 1.667, so the peak rate factor resolves to 484. The NRCS hydrology model WinTR-20 contains this default peak rate factor. Most users do not bother to check whether their particular watershed is "average," with time of recession 1.667 times the time to peak. To use a different peak rate factor the user must develop their own dimensionless unit hydrograph and enter it into the program.

Swampy watersheds are known to result in much lower peak rate factors, and Dendy (1987) found one Southwest Florida watershed to range between 188 and 257 and another to range between 302 and 390. Fang (2005) studied the impact of changing peak rate factors for a given watershed. Figure 12 shows the synthetic unit hydrograph for a 4.6 square mile watershed and a time of concentration of 2.3 hours. The standard peak rate factor produces a peak of about 1460 cfs. Changing only the peak rate factor (to 600) raised the peak to 1800 cfs. Changing the peak rate factor to 370 lowered the peak to about 1100 cfs.

Figure 12. Effect of peak rate factor on unit hydrograph shape Fang (2005)

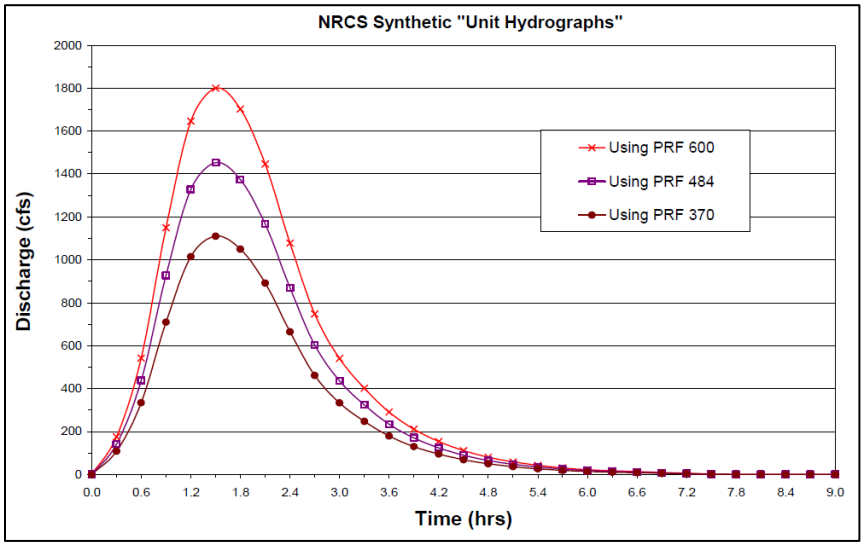

NRCS has provided guidance for computing peak rate factors other than the default 484 USDA-NRCS (2007) but the procedures require adequate streamflow and precipitation records. The document provides dimensionless unit hydrographs, computed at intervals of 50, between 100 and 600 (Appendix 16B) which can then be used as direct input to WinTR-20.

One difficulty in applying the NRCS dimensionless unit hydrographs of WinTR-20 to Western mountainous watersheds is that the default peak rate factor is probably too low for the unburned condition. When a mountainous watershed has experienced wildfire, the peak rate factor is likely to be increased even further. Even if data gages existed before the wildfire, the data would not be applicable for developing a post-fire peak rate factor. The work of BAER teams and Emergency Watershed Protection (EWP) efforts generally begins even before a wildfire is completely contained, which precludes the use of gaged data. A method proposed by McCuen and Bondelid (1983) circumvents the availability of data, may be used for both pre- and post-wildfire conditions, and is facilitated by GIS. A time-area histogram of the watershed, provides the proportion of rising limb versus total runoff time, which is needed for equation 16. However, since the time-area histogram is not dimensionless, the calculations should be made using area under the curve (equation 17) which is the proportion of the watershed area that has drained prior to the peak compared to the total watershed area.

$$D_f = \frac{1290.67 A_{rise}}{A_{total}} \quad \text{(eq. 17)}$$

where:

D_f = peak rate factor

A_{rise} = watershed area drained before the peak

A_{total} = total watershed area

Development of a time-area histogram is discussed in the Time-Area Histogram Synthetic Unit Hydrograph section of this technical note.. McCuen and Bondelid (1983) caution that this procedure assumes that watershed storage characteristics are relatively homogeneous. Lacking this prerequisite, one could choose to subdivide the drainage area in a way that retains homogeneity of storage characteristics, or else develop a curve of time-storage rather than time-area, as discussed in McCuen and Bondelid (1983).

The USACE (2013) HEC-HMS model offers several unit hydrograph options. In addition to the SCS Unit Hydrograph transform, other synthetic unit hydrograph methods include Clark, ModClark, and Snyder. Each of these requires a parameter similar to the peak rate factor of the SCS method. For example, the two Clark methods require the input of a "storage coefficient." This factor, which attempts to account for the runoff lag effects of overall watershed storage, is exactly how the function of the peak rate factor is described. The HEC-HMS user manual states that, "many studies have found that the storage coefficient, divided by the sum of the time of concentration and storage coefficient, is reasonably constant over a region." However, the hydrologist working with a burned watershed may not have access to regionally derived storage coefficients.

Similarly, the Snyder synthetic unit hydrograph requires the input of a peaking constant and the HEC-HMS user manual states that "it ranges from 0.4 to 0.8, with lower values associated with steep-rising hydrographs." The user manual also states that the peaking constant. "is estimated using the best judgment of the user, or possibly from locally-developed relationships to watershed physical features."

Time-Area Histogram Synthetic Unit Hydrograph

Another option in HEC-HMS is the "User-Specified Unit Hydrograph Transform." This allows users a way to input an externally derived unit hydrograph, normally developed using streamflow and precipitation records. Although these gaged records may or may not exist for a burned watershed, they would not be applicable shortly after a wildfire event. The option exists, however, to develop a synthetic unit hydrograph using estimated time-area histograms of runoff from the burned watersheds. The procedure can also be used to estimate peak rate factor, as described in the Synthetic Unit Hydrograph Peak Rate Factor section.

To develop this terrain-based synthetic unit hydrograph, the user can create GIS raster information that ultimately allows the estimate of time-bands of cells within a sub-basin. For example, the Manning's roughness raster may be developed based on whether the cell contains overland, shallow-concentrated, or channel flow. Other factors can be taken into account in the derivation of the roughness layer, such as soil types, vegetation types, and burn severity. A flow slope raster can also be easily developed from the DEM layer. Then, using the velocity method procedures (described in the Velocity Method section of this technical note), the hydrologist can derive velocity equations (Figure 13) to be applied to each grid to compute a velocity raster layer. Note that Manning's roughness values vary significantly between overland flow and channel values, as shown in Tables 2 and 3. Further guidance on selection of post-wildfire roughness coefficients is provided in the Post-Wildfire Manning's Roughness Coefficients section. In addition, the velocity equation for stream grids requires the cross-sectional flow area *A* at that location, which may be estimated using hydraulic geometry relations of bankfull flow area as a function of drainage area.

Figure 13. Examples of equations derived using the Velocity Method

$$V_{overland} = \frac{0.04S^{0.5}}{n} \qquad V_{collector} = \frac{0.58S^{0.5}}{n} \qquad V_{stream} = \frac{0.314S^{0.5}A^{0.333}}{n}$$

Once the velocity raster is available for a watershed, then a drainage time raster can be created using a GIS hydrology function. This can be examined to determine the number of cells that

drain to the outlet in successive time bands of, say, five minutes, the basis of a time-area histogram of the watershed. Standard hydrology textbooks such as Bedient, Huber, and Vieux (2012) show how a unit hydrograph can be easily created in a spreadsheet, using a time-area histogram. The Whitewater Creek Case Study demonstrates the derivation of synthetic unit hydrographs by this methodology.

Post-Wildfire Manning's Roughness Coefficients

Manning's roughness coefficients are of a different scale between overland flow and channel flow, due to the phenomenon of relative roughness, which is a measure of flow depth (or hydraulic radius) over surface roughness height. In Limerinos (1970) the same ratio is called relative smoothness. For coarse gravel beds, $3.5D_{84}$ is generally considered a measure of bed roughness height, where D_{84} is the 84^{th} percentile of the particle size distribution (Hey, 1979). Defining overland flow roughness height or vegetation roughness height is much more difficult. The roughness elements may not be fully inundated, as is usually the case with stream channel flow. However, an important concept to understand is that, for a homogeneous channel bed, Manning's roughness will generally remain constant or slightly decrease when flow depth is well above roughness height. However, for shallow depths, roughness height has a bigger impact and Manning's roughness can greatly increase as inundation decreases. This phenomenon is magnified with overland flow roughness. Figure 14 from Lawrence (1997) shows three conditions of roughness height to inundation depth, which are accompanied by rapidly increasing Manning's roughness coefficient. For the partial inundation case, however, and for small depth changes, Lawrence found that roughness can increase with increasing depth (which may be due to increased wetted perimeter within that small depth range).

Steeper mountain channels can have higher roughness for the same reason. (See the Channel Flow Routing section). For overland flow, this is why Manning's roughness coefficients in Table 2 are much higher than channel roughnesses in Table 3.

Figure 14. Overland flow regimes, (Lawrence, 1997) between well inundated (top), marginally inundated (middle), and partially inundated (bottom) accompanied by increasing Manning's roughness.

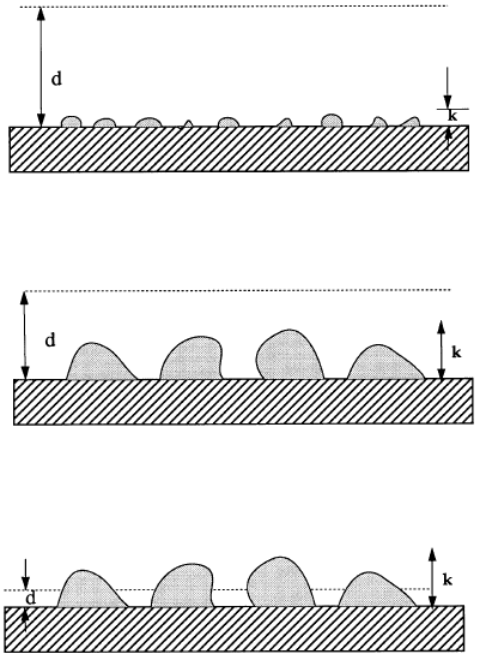

Assignment of Manning's roughness value, even for channel flow, can be challenging, and is best estimated by experienced hydraulic engineers. Roughness is raised by the presence of vegetation and by increasing sediment transport. For post-wildfire overland flow, the analyst must assess the effect of surface condition and rainfall depth. Lack of vegetation generally lowers the roughness, to say, that of bare soil. Hydrophobicity can be considered to lower the roughness even further. Figure 14 shows different roughness conditions for the same hillslope (Canfield, et al. 2005).

Figure 15. Hydrographs from the same hillslope, with different surface conditions (Canfield, et al. 2005).

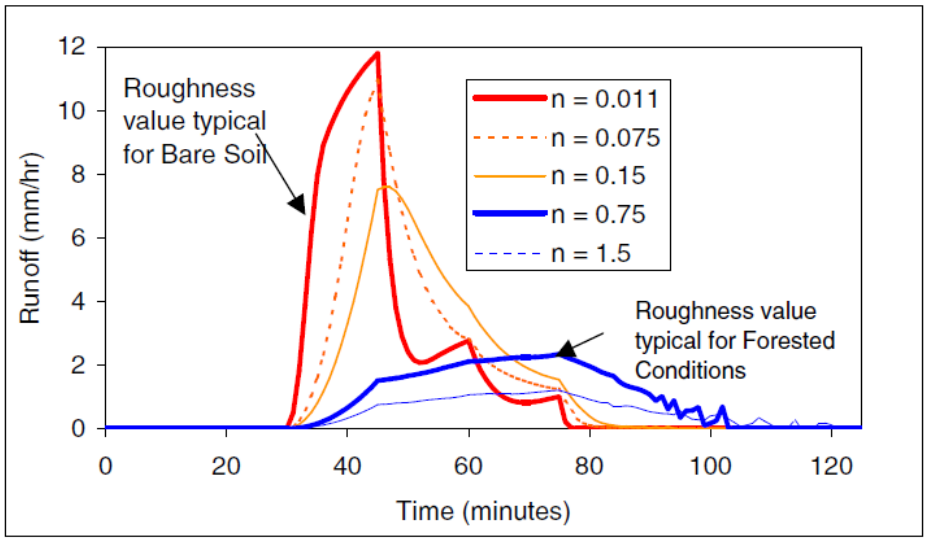

Moody and Kinner (2006) suggest that wildfire basically results in overland flow Manning's roughness values near that of bare soil and that minor variation from this value (0.011) has much less effect on model results than changes in effective rainfall.

Kinematic Wave Transform

Another option available in HEC-HMS is the Kinematic Wave Transform. This is conceptually similar to the procedure to determine a time-area histogram, but does not require as much GIS manipulation. The user must be able to determine flow lengths, flow slopes, and roughnesses, for four types of flow surfaces, overland flow plane, subcollector, collector, and channel, and specify the percentage of the sub-basin composed of each. The sub-basin percentage may be determined in GIS from the flow accumulation layer. The hydrology model takes it from there, allowing the user to avoid the extra steps of creating a GIS-derived estimate of unit hydrograph.

The HEC-HMS Technical Reference Manual (USACE 2013) discusses applicability and limitations of direct runoff models such as the kinematic wave transform. The methodology does not employ a unit hydrograph for transforming runoff from the landscape to an outlet, but performs timestep calculations using differential equations for flow over the various surfaces. Ponce (1991) suggests that the kinematic wave transform should not be applied to sub-areas

larger than one square mile because larger areas subject the differential equation solutions to artificial numerical effects. However, Woolhiser (1992) and Goodrich (1992) point out that difficulties with numerical stability do not render a model inapplicable to larger watersheds, and Goodrich had, at the time, successfully modeled sub-basins up to 2.5 square miles. These discussions alert the user to be aware of numerical stability issues related to watershed size.

Another way to take advantage of GIS is to use the model AGWA (Goodrich, et al. 2005). As shown in Figure 16, the model has both a continuous simulation option (SWAT) and a storm event option (KINEROS). The latter would generally suffice for post-wildfire hydrologic analyses. As implied in the name, the KINEROS model employs the Kinematic Wave flow routing strategy. Similarly, to the HEC-HMS, Kinematic Wave Transform, KINEROS has the user subdivide the watershed into types of flow surfaces. Also similar to one of the HEC-HMS infiltration options, KINEROS uses Smith Parlange, a process-based simplification of Richard's equation for infiltration estimation. In addition to flow runoff estimation, AGWA incorporates the ability to estimate sedimentation, which neither WinTR-20 nor HEC-HMS offer. This is discussed in more detail in the next section.

Figure 16. AGWA model (Goodrich, et al. 2005)

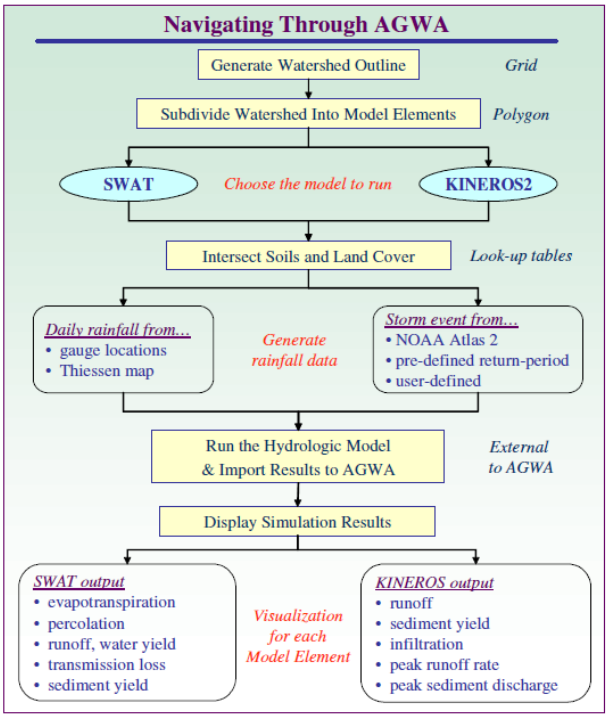

Sediment Modeling

If modeling rainfall runoff is complicated, the difficulties only multiply when considering the phenomena of sediment transport. While the discipline of hydraulics for water flow makes much use of the basic physical conservation laws, sediment transport is almost entirely empirical. So many variables affect whether the movement of a given particle will be initiated, how far it will be transported, and where it will be deposited, that prediction is fraught with uncertainty.

Flowing water flow drives the process, and water is notoriously erosive, referred to sometimes as the universal solvent. At the microscopic level, the polarity of the water molecule contributes to its ability to attract the ions of other substances. At the macroscopic level, water is heavy and exerts considerable force on the land as it flows. Consider a half inch of rain falling on a small roof (Figure 17). The volume of that rainfall would be 1247 gallons and the total weight over five tons. Even a very small stream can carry a lot of power. At a flow rate of a mere five cubic feet per second, a creek sends over nine tons of water past its bank every minute.

Figure 17. Roof of a small house

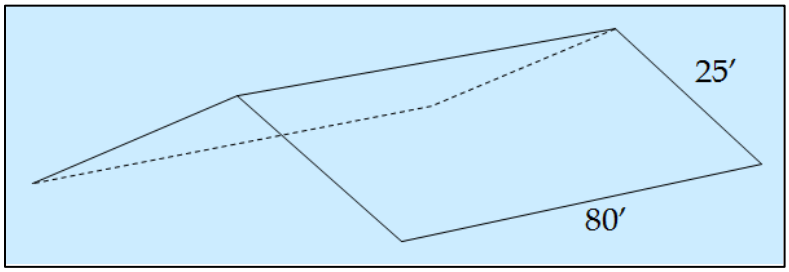

The difficulty in determining how much sediment a stream will transport is that the velocity of flow varies continuously, the potential sediment particles vary widely in size, weight, and cohesiveness, and the protective shielding of vegetation varies widely with species, density, and extent of growth.

Figure 18 shows the result of a steep stream in a canyon emerging onto a plane and losing profile slope. No longer capable of transporting as much sediment, the deposits form an alluvial fan.

Figure 18. Alluvial fan, Death Valley National Park

(photo by Marli Bryant Miller, marlimillerphoto.com)

While the velocity and sediment transport capacity of a stream can vary significantly along its profile, it can also vary considerably within a single cross-section. The fastest flow will generally be over the thalweg and about three-quarters of the maximum depth. (See Figure 19.) Toward the flow boundaries, the velocity is reduced, especially in the presence of vegetation.

Figure 19. A stream cross-section with isolines of velocity, maximized over the thalweg.

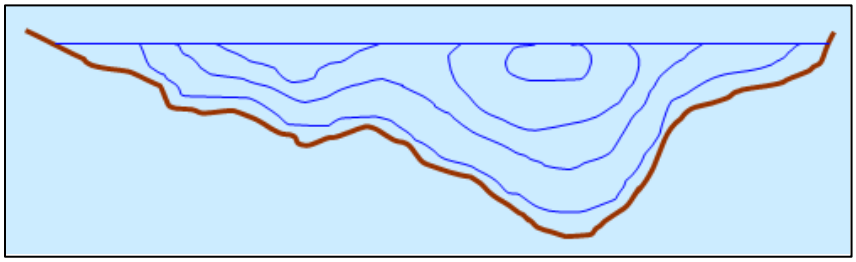

Velocity currents flow not only longitudinally, downstream, but also circulate sideways, in what are termed transverse or secondary currents. This phenomenon is responsible for the meandering

behavior of rivers (Figure 20), as downwelling tends to scour out pools on the outside of bends, while gravel and sand deposition forms bars on the inside of bends.

Figure 20. Riffle-pool morphology

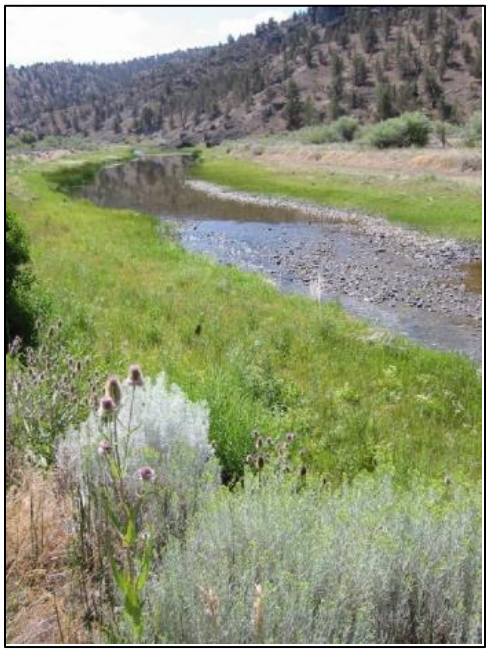

Wildfire removes vegetation and leaves overland flow slopes highly vulnerable to erosion. The swales and gullies may clog with sediment and debris. Hydrophobic soil at a depth of as little as two inches leaves the unconsolidated soil above it vulnerable to erosive flow as if over the asphalt of a parking lot. With wildfire, not only is sediment more vulnerable to erosion, but debris such as logs and partially burned branches can be washed into the streams. Sometimes the flowing water can be so clogged with sediment, that the flowing mass is termed mudflow or debris flow. Having a higher density and viscosity than clear water flow, debris flows can be extremely dangerous.

Debris-flow is defined as "the rapid flow of saturated material consisting of more than 20% gravel and coarse material through a steep channel or over steep hillsides" (Santi, et al. 2006). Because the volume of debris flows can often be correlated with property damage and other hazards, a number of studies have examined size classification (see Table 13, Jakob, 2005) and

prediction (Santi and Morandi, 2012; Prochaska, et al., 2008). As relates to post-wildfire recovery in the Western US, Santi and Morandi (2012) state: "...there is a clear progression in decreasing volume of debris flows as basins recover from the wildfire: it takes approximately 1 year, or at a few locations, as much as 3 years, for debris production to return to pre-fire rates." Note that accelerated sediment transport rates, as opposed to debris-flows, may persist much longer.

Table 13. Size classification and potential consequences of debris flows (Santi and Morandi, 2012)

Size class	Volume (10^3 m^3)	potential consequences
1	< 0.1	localized damage, known to have killed foresters in small gullies, damage small buildings
2	0.1 - 1	could bury cars, destroy small wooden buildings, break trees, block culverts, derail trains
3	1 - 10	could destroy larger buildings, damage concrete bridge piers, damage highways or pipelines
4	10 - 100	could block creeks, destroy parts of villages, destroy bridges, damage infrastructure corridors
5	100 - 1000	could destroy larger urban areas, dam up creeks and small rivers
6 - 10	> 5000	generally restricted to volcanic events, capable of destroying entire cities, damming large rivers

Another interesting finding from Santi, et al. (2006) is that "the majority of material in post-fire debris flows is eroded from the channels—only a small percentage of the total volume is contributed from hillslope rilling and sheetwash." However, again, the analyst must distinguish between the much more sediment-bulked debris flow events and rainfall-runoff events with elevated sediment transport. The latter may well originate on hillslopes subjected to vegetation removal and hydrophobic soils associated with wildfire.

For design of Emergency Watershed Protection (EWP) measures, the hydrologist has basically three options, clear flow modeling, bulked flow modeling, or debris flow estimation. Clear flow modeling has been discussed in the Hydrologic Modeling sections. Bulked flow is discussed in the Sediment Bulking section that follows. Debris flow hazard assessment is not an exact science. Although the two-dimensional flood-routing model FLO-2D (O'Brien, et al. 1993) has been used to model debris flow (Elliott, et al. 2005) rapid post-wildfire assessments preclude its use due to extensive input requirements and model complexity. For estimation of debris flow

impacts, the analyst should consider storm event frequency, source material availability, and location of concern relative to location of source material. Debris flow will generally require a less frequent (higher rainfall peak) storm such as a ten-year event, although immediately after the wildfire a 2-year event may suffice. Availability of source material can be assessed by field observations of channel conditions, primarily, but also steep hillslope conditions. The further the location of concern from the source material the less likely the effect of debris flow (as differentiated from sediment-bulked flow). Cannon, et al. (2003), for example, found that relative degree of debris flow hazard could be assessed by examining the abundance of colluvium available in stream channels, the degree of channel confinement, and channel gradient. The study concluded that further research is needed.

For estimating elevated sediment transport, as opposed to debris-flow, two models are discussed herein, GeoWEPP and AGWA. The former is a geo-spatial interface for the Water Erosion Prediction Project (WEPP) model (Flanagan, et al. 2001), which can be downloaded for ArcGIS from: https://lesami.geog.buffalo.edu/projects/active/geowepp/. The WEPP model itself can be downloaded from: http://www.ars.usda.gov/Research/docs.htm?docid=10621. This is a continuous simulation process-based model, applicable to hillslope erosion processes (sheet and rill erosion). It uses stochastically derived climate data from the CLIGEN model (Zhang and Garbrecht, 2003). Two distinct disadvantages of this model should be considered. As WEPP is designed for continuous simulation, it is less applicable to storm events, which tend to drive post-fire runoff and sediment transport. Secondly, existing climate generator models such as CLIGEN and GEM6 are not designed to produce less frequent storm event peaks (Theurer, et al. 2010) but rather the day-to-day kinds of rainfall events evaluated by continuous simulation models.

The KINEROS option of the Automated Geospatial Watershed Assessment (AGWA) modeling tool (Goodrich, et al. 2005) may be best for sediment transport estimation. The KINEROS model is applicable to storm events and AGWA has had recent improvements for post-wildfire use (Canfield and Goodrich, and Burns, 2005). The AGWA model and documentation can be downloaded from: http://www.tucson.ars.ag.gov/agwa/.

Concerning sediment, the modeler may be advised to pay attention to burn severity. One study (Benavides-Solorio and MacDonald, 2001) in Colorado found relatively small differences in runoff rates as a function of burn severity, but a much higher correlation for sediment yield. That study stated, "...percent ground cover accounted for 81% of the observed variability in sediment yields" and "...large differences in sediment yields with burn severity should be attributed primarily to the differences in ground cover rather than the differences in runoff, water repellency, or antecedent soil moisture." These results imply that watershed recovery and return of sediment yield to unburned rates should be a function of vegetation and ground cover, and the study indicates that full recovery may take from three to nine years.

Sediment Bulking

The post-fire hydrographs produced by the models discussed herein do not take into account the phenomenon of sediment bulking. As defined above, debris flow is considered that which entrains at least 20% gravel and coarse material. Elliott, et al. (2005) delineates hyperconcentrated flows as ranging from 20 to 47 percent sediment concentration and mudflows as having a greater than 47% sediment concentration.

A flood of rare recurrence interval, such as the 50-year event, occurring shortly after wildfire, may cause hyperconcentrated sediment flows or mudflows. One study (Cannon, et al. 2003) found significant post-wildfire debris flows occurring with storms as frequent as the two-year event. That study suggests that the generation of high sediment concentrated flows is made possible by progressive sediment bulking over time. Other studies (Giraud and McDonald, 2007) found that debris flows tend to result from channel incision rather than hillslope erosion, but agree with Cannon, et al. (2003) that smaller events, merely bulked rather than hyperconcentrated. may transport enough sediment from overland flow surfaces to channels to then be available for later debris flow events.

Post wildfire flows that do not reach the 20% threshold nevertheless transport considerable sediment loads. This entrained sediment raises (or bulks) the overall flow rate and, at any particular location, raises the flood depth. For a hydrograph, the total bulked flow rate is the sum of the water discharge and the sediment discharge.

$$Q_{bulked} = Q_w + Q_{sed} \quad \text{(eq. 18)}$$

One way to account for sediment bulking in post-wildfire hydrograph analyses is to apply a bulking factor to the flood peak (O'Brien and Fullerton 1989, Elliott et al. 2005):

$$BF = \frac{Q_w + Q_{sed}}{Q_s} = \frac{1}{1 - C_v} \quad \text{(eq. 19)}$$

where C_v is the maximum sediment concentration by volume in percent.

As discussed in Elliott, et al. (2005), if the event is assumed to with sediment concentration just under hyperconcentrated (20 percent) then the resulting bulking factor would be 1.25:

$$BF = \frac{1}{1 - 0.2} = 1.25 \quad \text{(eq. 20)}$$

The sediment concentration varies during a storm and generally peaks before that of the water discharge. One way researchers have estimated sediment discharge over time has been to measure data and derive simple regression equations. For example, Moody and Martin (2001) found for
two recently burned Colorado watersheds,

$$Q_{sed} = 4.4 {Q_w}^{1.5} \quad \text{(eq. 21a)}$$

$$Q_{sed} = 23 {Q_w}^{1.1.3} \quad \text{(eq. 21b)}$$

where:

Q_w = water flow (cfs)

Q_{sed} = sediment flow (kg/s)

The study reported statistical correlations of r^2=0.89 for equation 21a and r^2=0.96 for equation 21b.

Using a hypothetical storm hydrograph, with a peak of about 580 cfs in the second watershed, and translating both discharges into cfs, a bulk factor for the peak of 1.06 is derived (Figure 21).

Figure 21. Hypothetical storm using equation 21b (all discharges converted to cfs).

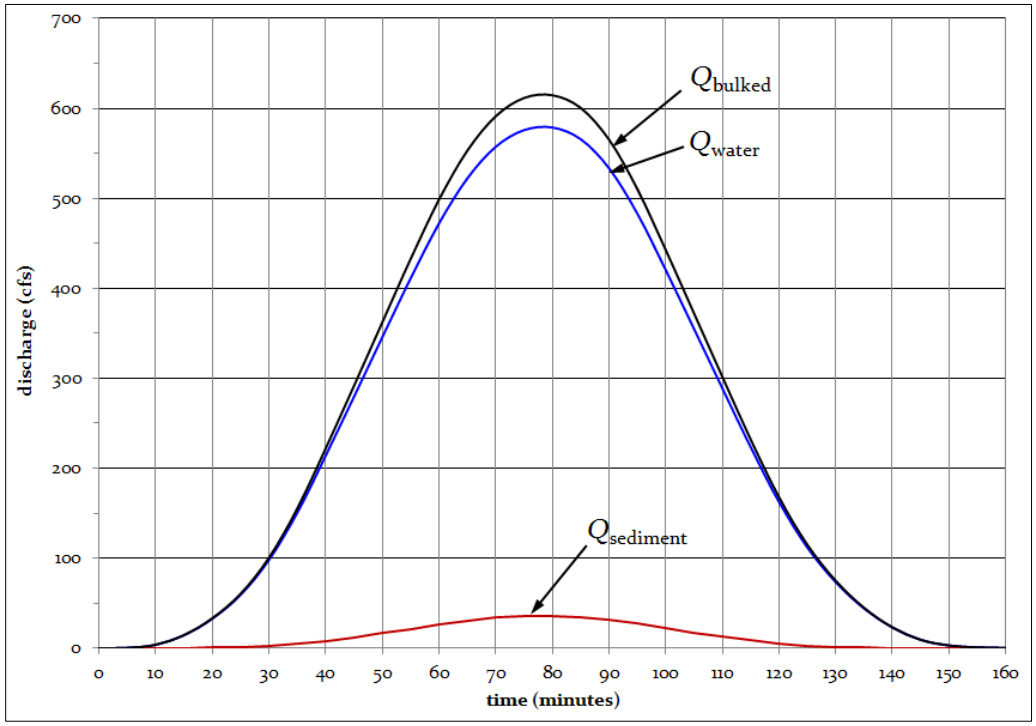

For post-fire hydrologic analyses, if previous studies for the watershed of concern exist, then maximum sediment concentrations and bulk factors can be better estimated. The bulk factor can be much higher than the hypothetical one from above. For example, LACDPW (2006) has compiled curves for debris production and bulk factors for the Los Angeles River, Santa Clara River, and Antelope Valley watersheds, with wide variation from place to place. Figure 22 shows the data for one of their lower "debris production areas" with bulking factors in the range of 1.5.

A handy factsheet from the USGS (Pierson, 2005) provides guidance on field investigations to distinguish between debris flows and normal flow sediment deposits. The reference suggests that normal suspended sediment concentrations are five to ten percent by volume, but that even with hyperconcentrated flow (volumes between 20 and 60 percent) the flow behavior is

controlled by water, whereas mud flows (even higher sediment concentrations) have behavior controlled by the entrained sediment.

Among the field indicators listed are, for water flow deposits, most grains are rounded, beds are stratified with good sorting both horizontally and vertically, with loose consistency when dry. Debris flow deposits, on the other hand, tend to be angular sand and fine gravel (indicating a hillslope source), non-stratified, and extremely poorly sorted, with coherent consistency rather than loose.

Note that, when post-wildfire streamflow records are available to help calibrate modeled hydrographs, that these measurements will already be bulked.

Figure 22. Sediment production and bulking factors for debris production area 7 (LACDPW 2006)

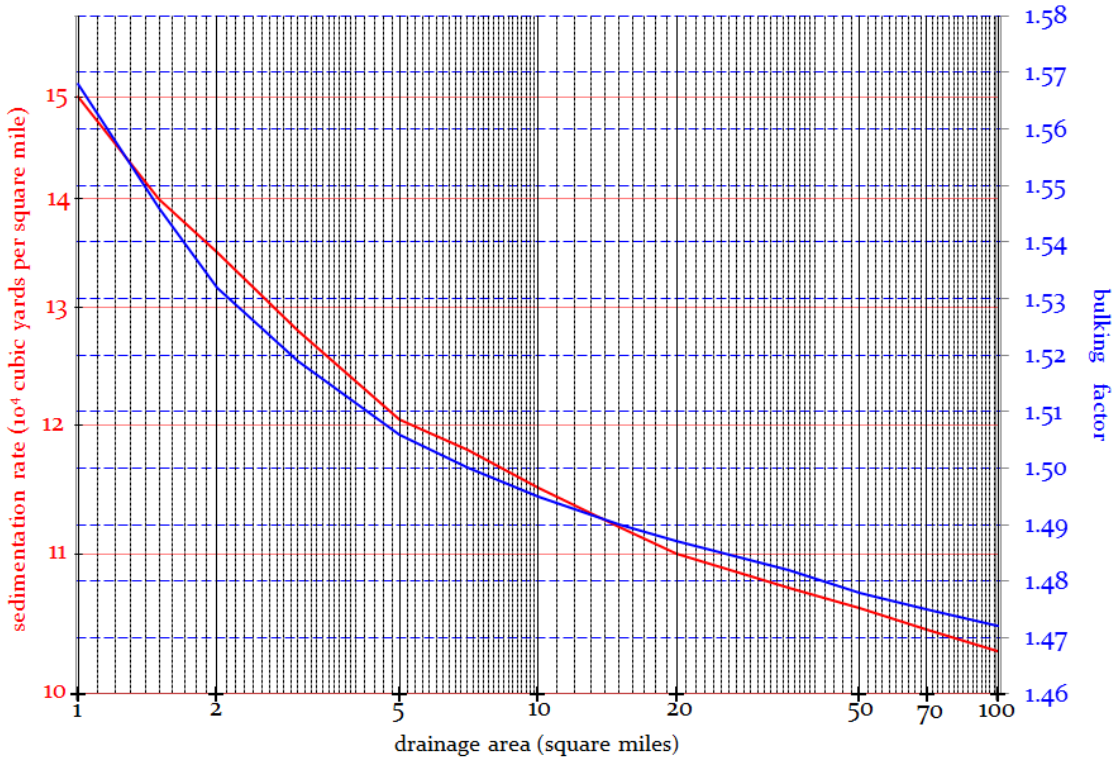

Channel Flow Routing

Larger wildfires are likely to have watershed areas too large to be modeled using a single catchment methodology. Using the CN method, it is generally recommended that watershed areas be limited to 2000 acres (3.1 square miles) or smaller. For larger drainage areas, more than one catchment (sub-area) can be delineated and runoff hydrographs estimated for each, as illustrated by the Rist Canyon portion of the High Park Fire (Figure 23). This watershed has an overall area of 8.2 square miles. Upstream hydrographs are routed downstream, with hydrographs from the lower catchments added to the routed hydrograph. This sum is then routed downstream to the next junction where the process repeats. Besides honoring recommended watershed area limitations, sub-delineation allows the computation of expected flooding at upstream points of interest, such as road crossings and flood-threatened homes. This process is simulated within many modeling packages; however, WILDCAT and FIRE HYDRO do not include this feature.

Figure 23. Rist Canyon portion of the High Park Fire model

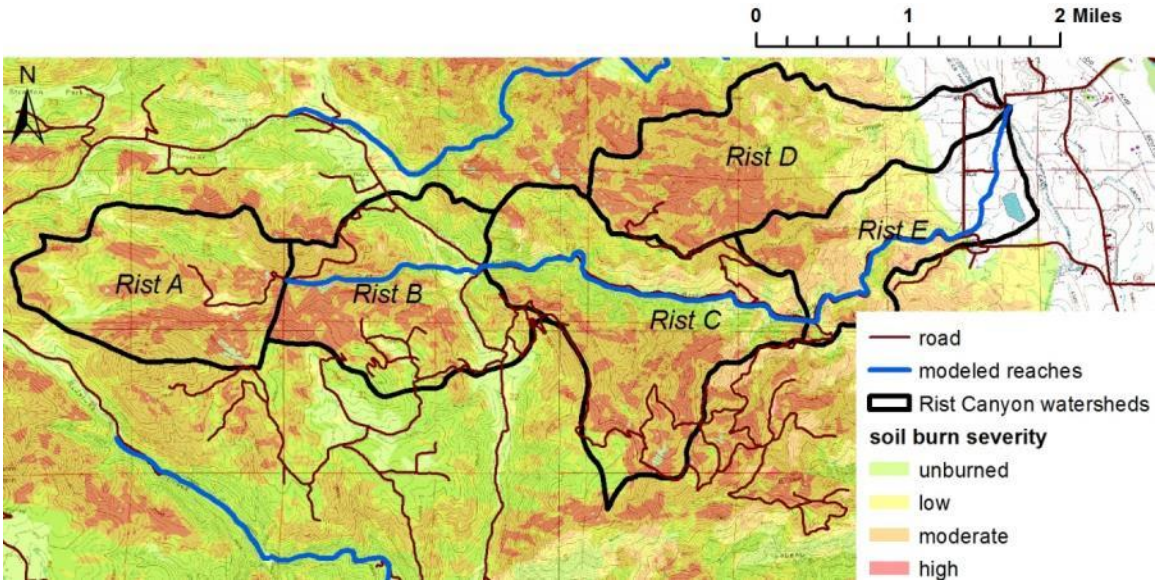

Routing algorithms are integrated into such models as HEC-HMS. This model includes six routing methodologies, including kinematic wave, lag, modified Puls, Muskingum, and

Muskingum-Cunge. Routing methods that simulate attenuation should be implemented, such as the Muskingum-Cunge procedure.

It is essential that flow resistance is appropriately estimated in the steep channels often encountered below wildfire areas. Models typically use Manning's n as the resistance coefficient. It is common for high-gradient channels to have Manning's n values between 0.1 and 0.2 (Yochum et al. 2012), although reaches where the riparian area has been severely burned may have lower Manning's n than normal. Resistance is the result of roughness due to the bed and bank grain material, bedforms (such as step pools), plan form, vegetation, instream wood, and other obstructions. In-channel resistance typically decreases as stage and discharge increase; resistance coefficients need to be selected for the discharge of interest. In higher-gradient channels, bedforms can be the dominant source of flow resistance. In intermittently flowing channels, in-channel riparian vegetation can be extensive, adding to the flow resistance. Both photographic guidance (Barnes 1967, Aldridge and Garrett 1973, Hicks and Mason 1998, Yochum and Bledsoe 2010, Yochum et al. in press) and quantitative prediction tools (Limerinos 1970, Hey 1979, Jarrett 1984, Bathurst 1985, Yochum et al. 2012) are helpful for selecting appropriate flow resistance coefficients.

References

Aldridge, B. N., and J. M. Garrett, 1973. Roughness coefficients for stream channels in Arizona. U.S. Geological Survey Open-File Report, Tucson, Arizona.

Bathurst, J.C. 1985. Flow resistance estimation in mountain rivers. Journal of Hydraulic Engineering 111(4), 625-643.

Bedient, P.B., Huber, W.C., and Vieux, B.E. 2012. Hydrology and Floodplain Analysis, Prentice Hall, NJ, 5th Edition, 801 pages.

Benavides-Solario, J.D., and MacDonald, L.H. 2001. Post-fire runoff and erosion from simulated rainfall on small plots, Colorado Front Range. Hydrological Processes, 15, 2931-2952.

Beven, K.J. 1989. Changing ideas in hydrology -- the case of physically-based models. Journal of Hydrology 105, 157-172.

Beven, K.J. 2001. How far can we go in distributed hydological modelling? Hydrology and Earth System Sciences 5, 1-12.

Canfield, H.E., Goodrich, D.C. 2005. Suggested changes to AGWA to account for fire (V. 2.1). Southwest Watershed Research Center, USDA-ARS, Tucson, Arizona.

Canfield, H.E., Goodrich, D.C., and Burns, I.S. 2005. Selection of parameters values to model post-fire runoff and sediment transport at the watershed scale in Southwestern forests.

Cannon, S.H., Gartner, J.E., Parrett, C., and Parise, M. 2003. Wildfire-related debris-flow generation through episodic progressive sediment-bulking processes, western USA. In Proceedings: Debris-Flow Hazards Mitigation: Mechanics, Prediction, and Assessment.

Cerrelli, G.A. 2005. FIRE HYDRO, a simplified method for predicting peak discharges to assist in the design of flood protection measures western wildfires. In Proceedings of the ASCE 2005 Watershed Management Conference, July 2005, Williamsburg VA. pp. 935-941.

CFR (Code of Federal Regulations), 2005. Emergency watershed protection program. 7 CFR Part 624.4.

Chen, L., Berli, M., Karletta, C. 2013. Examining modeling approaches for the rainfall-runoff process in wildfire-affected watersheds: using San Dimas Experimental Forest. Journal of the American Water Resources Association 1-16.

Conedera, M., Peter, L., Marxer, P., Forster, F., Rickenmann, D., Re, L. 2003. Consequences of forest fires on the hydrogeological response of mountain catchments: a case study of the Riale Buffaga, Ticino, Switzerland. Earth Surface Processes and Landforms 28, 117-129.

Debano, L.F., Osborn, J.F., Krammes, J.S., Letey, J. 1967. Soil wettability and wetting agents: our current knowledge of the problem. USDA Forest Service Research Paper PSW-43: 13.

DeBano, L.F. 1981. Water repellent soils: a state-of-the art. USDA Forest Service, General Technical Report PSW-46.

Dendy, G.S. 1987. A 24-hour rainfall distribution and peak rate factors for use in Southwest Florida. Masters Thesis, University of Central Florida, Orlando Florida, 172 pages.

Doerr, S.H. 1998. On standardizing the 'Water Drop Penetration Time' and the 'Molarity of an Ethanol Droplet' techniques to classify soil hydrophobicity: A case study using medium textured soils. Earth Surface Processes and Landforms 23, 663-668.

Doerr. S.H., Shakesby, R.A., Walsh, R.P.D. 2000. Soil water repellency: its causes, characteristics and hydro-geomorphological significance. Earth Science Reviews, 51, 33-65.

Dyrness, C.T. 1976. Effect of wildfire on soil wettability in the high cascades of Oregon. USDA Forest Service, Pacific Northwest Research Station, Research Paper PNW-202, 19 p.

Elliott, J.G., Smith, M.E., Friedel, M.J., Stevens, M.R., Bossong, C.R., Litke, D.W., Parker, R.S., Costello, C., Wagner, J., Char, S.J., Bauer, M.A., and Wilds, S.R. 2005. Analysis and mapping of post-fire hydrologic hazards for the 2002 Hayman, Coal Seam, and Missionary Ridge wildfires, Colorado. USGS Scientific Investigations Report 2004-5300, 80 pages.

Engman, E.T. 1986. Roughness coefficients for routing surface runoff. Journal of Irrigation and Drainage Engineering 112 (1). Amer. Soc. of Civil Eng., New York, NY. pp. 39-53.

Fang, X., etal. 2005. Revisit of NRCS unit hydrograph procedures. In Proceedings of the ASCE Texas Section Spring Meeting, Austin TX, April 2005, 21 pages.

Garen, D.C., Moore, D.S. 2005 Curve number hydrology in water quality modeling: uses, abuses and future directions. Journal of the American Water Resources Association 42(2), 377-388.

Giraud, R.E., and McDonald, G.N. 2007. The 2000-2004 fire-related debris flows in northern Utah. In: Proceedings 1st North American Landslide Conference, AEG Special Publication 23, 1522-1531.

Flanagan, D.C., etal. 2001. Chapter 7: The Water Erosion Prediction Project (WEPP) model. In Landscape Erosion and Evolution Modeling. Kluwer Academic Publishers, Norwell MA. 51 pages.

Foltz, R.B., Robichaud, P.R., and Rhee, H. 2009. A synthesis of post-fire road treatments for BAER teams: methods, treatment effectiveness, and decisionmaking tools for rehabilitation. USDA Forest Service General Technical Report RMRS-GTR-228.

Goodrich, D.C. 1992. Discussion of "The kinematic wave controversy" by Victor M. Ponce (April, 1991, Vol. 117, No. 4). ASCE Journal of Hydraulic Engineering 118(9): 1334-1335.

Goodrich, D.C., etal. 2005. Rapid post-fire hydrologic watershed assessment using the AGUA GIS-based hydrologic modeling tool. In Proceedings of the ASCE 2005 Watershed Management Conference, July 2005, Williamsburg VA. pp. 1-12.

Hawkins, R.H., Woodward, D.E., Hjelmfelt, A.T., Van Mullem, J.A., and Quan, Q.D. 2002. Runoff curve number method: examination of the initial abstraction ratio. Proceedings Federal Interagency Hydrologic Modeling Conference, Las Vegas NV. 12pp.

Hawkins, R.H. 1993 Asymptotic determination of runoff curve numbers from data. Journal of Irrigation and Drainage Engineering 119, 334-345.

Hawkins, R.H., Greenberg, R.J. 1990. WILDCAT4 flow model. School of Renewable Natural Resources, University of Arizona, Tucson, AZ. BLM contact: Dan Muller, Denver, CO.

Henkle, J.E., Wohl, E., Beckman, N. 2011. Locations of channel heads in the semiarid Colorado Front Range, USA Geomorphology 129, 309-319.

Hey, R.D. 1979. Flow resistance in gravel bed rivers, ASCE Journal of the Hydraulics Division, 105(4), 365-379.

Hicks, D.M., Mason, P.D. 1998. Roughness characteristics of New Zealand rivers, 2nd Edition, Water Resource Publications.

Hudak, A.T., Robichaud, P.R., Evans, J.S., Clark, J., Lannom, K., Morgan, P., Stone, C. 2004. Field validation of burned area reflectance classification (BARC) products for post fire assessment. Remote Sensing for Field Users: Proceedings of the Tenth Forest Service Remote Sensing Applications Conference, Salt Lake City, Utah, April 5-9 2004.

Huffman, E.L., MacDonald, L.H., and Stednick, J.D. 2001. Strength and persistence of fire-induced soil hydrophobicity under ponderosa and lodgepole pine, Colorado Front Range. Hydrologic Processes, 15, 2877-2892.

Jakob, M. 2005. A size classification for debris flows. Engineering Geology, 79, 151-161.

Jarrett, R.D. 1984. Hydraulics of high-gradient streams. Journal of Hydraulic Engineering 110 (11), 1519–1539.

Keeley, J.E. 2009. Fire intensity, fire severity and burn severity: a brief review and suggested usage. International Journal of Wildland Fire, 18, 116-126.

LACDPW (Los Angeles County Department of Public Works), 2006. Sedimentation Manual, 2nd Edition.

LandFire 2010. LandFire Fact Sheet, http://www.landfire.gov/.

Lawrence, D. S. L. 1997. Macroscale surface roughness and frictional resistance in overland flow. Earth Surface Processes and Landforms 22: 365-382.

Limerinos J.T. 1970. Determination of the Manning coefficient from measured bed roughness in natural channels. U.S. Geological Survey Water Supply Paper 1898-B, 52 pages.

Livingston, R.K., etal. 2005. Los Alamos post-fire watershed recovery: a curve-number-based evaluation. In Proceedings of the ASCE 2005 Watershed Management Conference, July 2005, Williamsburg VA. pp. 471-481.

Maidment, D.R. 1992. Handbook of Hydrology McGraw-Hill, Inc.

McCuen, R.H. and Bondelid, T.R. 1983. Estimating Unit Hydrograph Peak Rate Factors. ASCE Journal of Irrigation and Drainage Engineering 109(2), 238-250.

Miller, J.D., and Thode, A.E. 2007. Quantifying burn severity in a heterogeneous landscape with a relative version of the delta Normalized Burn Ratio (dNBR). Remote Sensing of Environment 109, 66-80.

Moody, J.A., etal. 2013. Current research issues related to post-wildfire runoff and erosion processes. Earth Science Reviews, (in publication).

Moody, J.A., and Martin, D.A. 2009. Synthesis of sediment yields after wildfire in different rainfall regimes in the western United States. International Journal of Wildland Fire, 18, 96-115.

Moody, J. A., and Kinner, D.A. 2006. Spatial structure of stream and hillslope drainage networks following gully erosion after wildfire. Earth Surface Processes and Landforms 31(3): 319-337.

Moody, J.A., and Martin, D.A. 2001. Hydrologic and sedimentologic response of two burned watersheds in Colorado, USGS Water-Resources Investigations Report 01-4122, 146 pages.

NASA 2012. NOAA National Aeronautics and Space Administration , Water and Energy Cycle website: http://science.nasa.gov/earth-science/oceanography/ocean-earth-system/ocean-water-cycle/

NWCG 2006. Glossary of wildland fire terminology. National Wildfire Coordinating Group, Incident Operations Standards Working Team.

O'Brien, J. S., Julien, P.Y., and Fullerton, W.T. (1993). Two-dimensional water flood and mudflow simulation. ASCE Journal of Hydraulic Engineering 119(2): 244-261.

O'Brien, J.S., and Fullerton, W.T. 1989. Hydraulic and sediment transport study of Crown Pointe flood wall: Breckenridge, Colo., Lenzotti and Fullerton Consulting Engineers, Inc., 34 p.

Parsons, A., Lewis, S.A., Napper, C., and Clark, J.T. 2010. Field guide for mapping post-fire soil burn severity. USDA Forest Service General Technical Report RMRS-GTR-243, 49 pages.

Pierson, T.C. 2005. Distinguishing between debris flows and floods from field evidence in small watersheds. USGS factsheet 2004-3142.

Ponce, V.M. 1991. The kinematic wave controversy. ASCE Journal of Hydraulic Engineering 117(4): 511-525.

Prochaska, A.B., Santi, P.M., Higgins, J.D., and Cannon, S.H. 2008. Debris-flow runout predictions based on the average channel slope (ACS). Engineering Geology, 98, 29-40.

Rallison, R.E. 1980. Origin and evolution of the SCS runoff equation. Proceedings of the Symposium on Watershed Management; American Society of Civil Engineers, Boise, ID.

Rallison, R.E., and Miller, N. 1982. Past, present, and future SCS runoff procedure. *In* Rainfall-Runoff Relationships, V.P. Singh, ed., Water Resources Publ., Littleton, CO, pp. 353-364.

Rawls, W.J., Brakensiek, D.L., and Miller, N. 1983. Green-Ampt infiltration parameters from soils data. ASCE Journal of Hydraulic Engineering. 109: 62-70.

Robichaud, P.R., Lewis, S.A., Ashmum, L.E. 2008. New procedure for sampling infiltration to assess post-fire soil water repellency. USDA Forest Service, Rocky Mountain Research Station, Research Note RMRS-RN-33.

Safford, H.D., etal. 2008. BAER Soil Burn Severity Maps Do Not Measure Fire Effects to Vegetation: A Comment on Odion and Hanson (2006). Ecosystems, 11:1, 1-11.

Santi, P. and Morandi, L. 2012. Comparison of debris-flow volumes from burned and un-burned areas. Landslides, 9, 1-13.

Santi, P. etal. 2006. Evaluation of post-wildfire debris flow mitigation methods and development of decision-support tools. Report to USGS and the Joint Fire Science Program, 78 pages.

Saxton, K.E., Rawls, W.J., Romberger, J.S., and Papendick, R.I. (1986) Estimating generalized soil-water characteristics from texture. Transactions of the American Society of Agricultural Engineers 50(4): 1031-1035.

Scott, D.F. 2000. Soil wettability in forested catchments of South Africa; as measured by different methods and as affected by vegetation cover and soil characteristics. Journal of Hydrology 231-232, 87-104.

Smith, R.E., Goodrich, D.C., Woolhiser, D.A., Unkrich, C.L. 2005. KINEROS – A kinematic runoff and erosion model. In: Computer Models of Watershed Hydrology, V.J. Singh (Editor). Water Resource Publications, Highland Ranch, Colorado, pp. 597-632.

Springer, E.P., Hawkins, R.H. 2005. Curve number and peakflow responses following the Cerro Grande Fire on a small watershed. In: Moglen, G.E., ed. Proceedings of Managing Watersheds for Human and Natural Impacts: Engineering, Ecological, and Economic Challenges, July 19-22, 2005, Williamsburg, VA, USA. American Society of Civil Engineers, Alexandria, VA.

Stoof, C.R., Vervoort, R.W., Iwema, J., van den Elsen, E., Ferreira, A.J.D., Ritsema, C.J. 2011. Hydrological response of a small catchment burned by an experimental fire. Hydrology and Earth System Sciences Discussions 8, 4053-4098.

Tedela, N.H., McCutcheon, S.C., Rasmussen, T.C., Hawkins, R.H., Swank, W.T., Campbell, J.L, Adams, M.B., Jackson, C.R., and Tollner, E.W. 2012. Runoff curve numbers for 10 small forested watersheds in the mountains of the Eastern United States. ASCE Journal of Hydrologic Engineering, 17, 1188-1198.

Theurer, F.D. etal. 2010. Comparison of historical versus synthetic weather inputs to watershed models and their effect on pollutant loads. In Proceedings of the Federal Interagency Sedimentation Conference.

USCOE-HEC (U.S. Army Corps of Engineers, Hydrologic Engineering Center), 2013. Hec-HMS. Available at http://www.hec.usace.army.mil/software/hec-hms/. Accessed in April, 2013.

USDA-ARS (U.S. Department of Agriculture-Agricultural Research Service), 2013a. AGNPS. National Sedimentation Laboratory, ARS, USDA, Oxford MS. Available at http://go.usa.gov/KFO. Accessed in April, 2013.

USDA-ARS (U.S. Department of Agriculture-Agricultural Research Service), 2013b. Soil and Water Assessment Tool: SWAT. Grassland Soil and Water Research Laboratory, ARS, USDA, Temple TX. Available at http://swat.tamu.edu/. Accessed in April, 2013.

USDA-NRCS (U.S. Department of Agriculture-Natural Resources Conservation Service), 2013. WinTR-20 and WinTR-55 hydrologic models. Available at http://go.usa.gov/KoZ/. Accessed in April 2013.

USDA-NRCS (U.S. Department of Agriculture-Natural Resources Conservation Service), 2004a. NRCS National Engineering Handbook, Part 630 Hydrology, Chapter 9, Hydrologic soil cover complexes. Available at http://go.usa.gov/T3eV/. Accessed in April 2013.

USDA-NRCS (U.S. Department of Agriculture-Natural Resources Conservation Service), 2004b. NRCS National Engineering Handbook, Part 630 Hydrology, Chapter 10, Estimation of direct runoff from storm rainfall. Available at http://go.usa.gov/T3eV/. Accessed in April 2013.

USDA-NRCS (U.S. Department of Agriculture-Natural Resources Conservation Service), 2010. NRCS National Engineering Handbook, Part 630 Hydrology, Chapter 15, Time of Concentration. Available at http://go.usa.gov/T3eV/. Accessed in April 2013.

USDA-NRCS (U.S. Department of Agriculture-Natural Resources Conservation Service), 2007. NRCS National Engineering Handbook, Part 630 Hydrology, Chapter 16, Hydrographs. Available at http://go.usa.gov/T3eV/. Accessed in April 2013.

USDA-SCS (U.S. Department of Agriculture-Soil Conservation Service), 1991. Engineering Field Handbook, Chapter 2, Estimating Runoff. Available at ftp://ftp-fc.sc.egov.usda.gov/NHQ/pub/outgoing/jbernard/CED-Directives/efh/EFH-Ch02.pdf/. Accessed in April 2013.

Woolhiser, D.A. 1992. Discussion of "The kinematic wave controversy" by Victor M. Ponce (April, 1991, Vol. 117, No. 4). ASCE Journal of Hydraulic Engineering 118(9): 1337-1339.

Yochum, S., Bledsoe, B. 2010. Flow resistance estimation in high-gradient streams. 2nd Joint Federal Interagency Conference, Las Vegas, NV, June 27- July 1.

Yochum, S.E., Bledsoe, B.P., David, G.C.L., Wohl, E. 2012. Velocity prediction in high-gradient channels. Journal of Hydrology. 424-425, 84-98, doi:10.1016/j.jhydrol.2011.12.031.

Yochum, S.E., Comiti, F., Wohl, E., David, G.C.L., Mao, L. In Press. Photographic guidance for selecting flow resistance coefficients in high-gradient channels. U.S. Department of Agriculture, Forest Service, Rocky Mountain Research Station, General Technical Report.

Zhang, X.C. and Garbrecht, J.D. 2003. Evaluation of CLIGEN precipitation parameters and their implication on WEPP runoff and erosion prediction. In Transactions of the American Society of Agricultural Engineers, 46, 311-320.

Case Study 1: Estimating Increased Flood Potential from the High Park Fire Area

Background

The High Park Fire, in the foothills west of Fort Collins, Colorado (Figures 1 and 2), burned within an area of 88,600 acres between June 9th and July 1st, 2012, the day containment was declared. The fire burned primarily in steep, forested terrain, with average slopes ranging from 14 to 49% and elevations ranging from 5300 to 10,200 feet. It was a fast burning fire – about 37,000 acres burned in the first three days. It was also a dirty burn, with a substantial amount of unburned area (21,100 acres, 23%) distributed as a patchy mosaic throughout the fire extent. Of the impacted area, 9800 acres burned at high soil burn severity (11%), 36,300 acres burned at moderate severity (40%), and 21,300 acres burned at low severity (23%). As the fire was contained, the summer monsoon season started. Increased flooding and debris flows were observed in streams draining numerous portions of the fire, with local residents noting that some of these floods were the most severe since the Big Thomson Flood of 1976. Ash mobilized through the enhanced runoff flowed into the Cache la Poudre River, a primary source of drinking and irrigation water for the northern Colorado Front Range. Since part of the Horsetooth Reservoir watershed was also burned, water supply storage in this reservoir was also threatened with contamination. As expected, the most severe flooding was in catchments with the highest percentages of high soil burn severity. In these areas the vegetation cover and soil litter were consumed, leaving surfaces dominated by a bare mineral condition, reduced surface roughness, and perhaps hydrophobicity. These high severity burn areas also likely had substantial destruction of seed banks, forcing longer vegetative recovery rates and resulting in longer periods of enhanced flooding. Increased flood peaks, flow volumes, sediment transport, nutrient enrichment, and stream channel destabilization are expected for a number of years in many streams draining the fire area, threatening life, property, infrastructure, and water quality.

Noting the increased flood potential and resulting risks, as well as the limitations of the initial hydrologic analyses performed for the Burned Area Emergency Response (BAER) report for the large catchments draining this fire, the Natural Resources Conservation Service (NRCS) was

asked by local and state officials to provide flow frequency estimates for post fire conditions. This case study provides an overview of the analyses performed to provide these estimates.

Figure CS1- 1. Sunset through smoke plumes, from Fort Collins on Day 1 of the High Park Fire (7/9/2012).

Figure CS1- 2. Aerial extent and soil burn severity of the High Park Fire, based on a BARC image generated from 7/20/2012 Landsat 7 imagery.

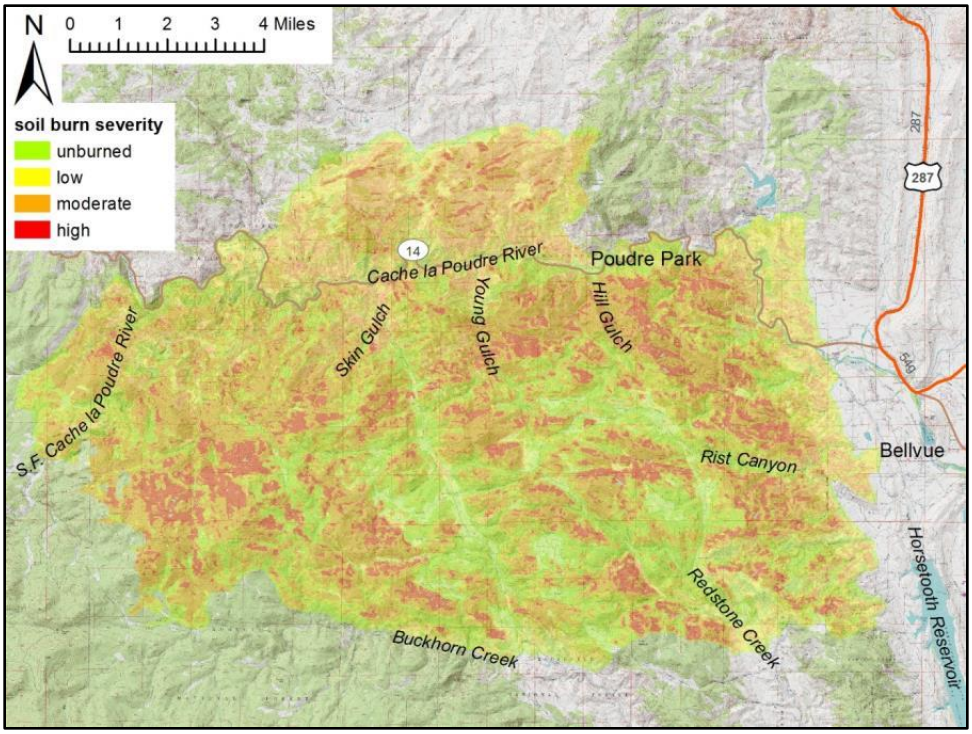

Methods

A rainfall-runoff model was developed to simulate the expected runoff response for both pre- and post-fire conditions, for the 2-, 10-, 25-, 50-, and 100-year 1-hour rainfall events. Hydrologic modeling was performed using the program HEC-HMS (version 3.5), developed by the U.S. Army Corps of Engineers' Hydrologic Engineering Center. The NRCS curve number (CN) technique for estimating direct runoff from rain events was used in this analysis. As quality control, peak flows estimated using U.S. Geological Survey (USGS) regression equations (Capesius and Stephens 2009), embedded in USGS StreamStats, and were compared to the CN runoff results for unburned conditions.

Hydrologic modeling performed as a part of the BAER assessment that the U.S. Forest Service (USFS) spearheaded for the High Park Fire provided initial peak flow estimates used for post-fire flood mitigation planning activities (BAER 2012). This analysis used the WILDCAT model (Hawkins and Greenberg 1990), which also relies on the CN method. This hydrologic analysis needed to be completed within a week of fire containment, per USFS requirements. Due to this time constraint, the modeling is relatively coarse, ignoring relevant hydrologic mechanisms such as variability in lag time between pre- and post-fire conditions, vegetation type, differences in runoff between moderate and high soil burn severity areas, as well as flood attenuation in larger catchments. Additionally, the BAER modeling used relatively large catchments in some areas. These simplifications are compounded by the large burn area of the High Park Fire, where mechanisms such as flood attenuation can substantially impact results. The NRCS initiated more detailed modeling of streams draining the High Park Fire area, likely enhancing the accuracy of predictions for flood mitigation efforts. Initial results of this modeling was obtained for key catchments just before the monsoon season started in early July, to provide preliminary results to local and state officials as flooding initiated, and was refined throughout the summer before providing flood estimates for most streams draining the fire extent (Yochum 2012a, Yochum 2012b). While these results do appear to provide reasonable simulations of flood enhancement to be expected from the burn areas, monitoring and research being performed in some areas may prompt more refined modeling using more mechanistic rainfall-runoff simulations than the CN method. Hence, flood simulation modeling from burn areas, especially large fires with substantial private land ownership, more dense settlement, and higher risks to life, property, and

infrastructure, should be viewed as an iterative process with models of varying complexity developed over time to satisfy specific needs.

Runoff was simulated using the CN procedure (NRCS 2004b). The CN is a simple catchment-scale method that gives estimates of flood peaks and volumes at watershed outlets, with more accurate results expected for larger, higher-intensity rain events. The method is documented in the NRCS National Engineering Handbook, Section 4, Hydrology, Chapters 9 and 10 (NRCS 2004a, NRCS 2004b), in Rallison (1980), as well as in numerous other publications. However, little quantitative information has been published of the database on which it was developed (Maidment 1992) and many of the curves used in the development have been misplaced (Woodward 2005). In general, the method was developed for rural watersheds in various parts of the United States, within 24 states; was developed for single storms, not continuous or partial storm simulation; and was not intended to recreate a specific response from an actual storm (Rallison, 1980).

Catchments and modeled stream channels implemented in the analyses are presented in Figure 3. Overall, 105 delineated catchments were utilized in the modeling. The average catchment area was 1.6 mi^2, with the individual sizes determined by required computation points (to provide needed flood predictions at roadway crossing, homes at risk, etc.…), catchment morphologic characteristics, and the need for simulating flood routing and attenuation in the modeled stream channels.

Figure CS1- 3. Modeled catchments and stream channels, with flow computation points.

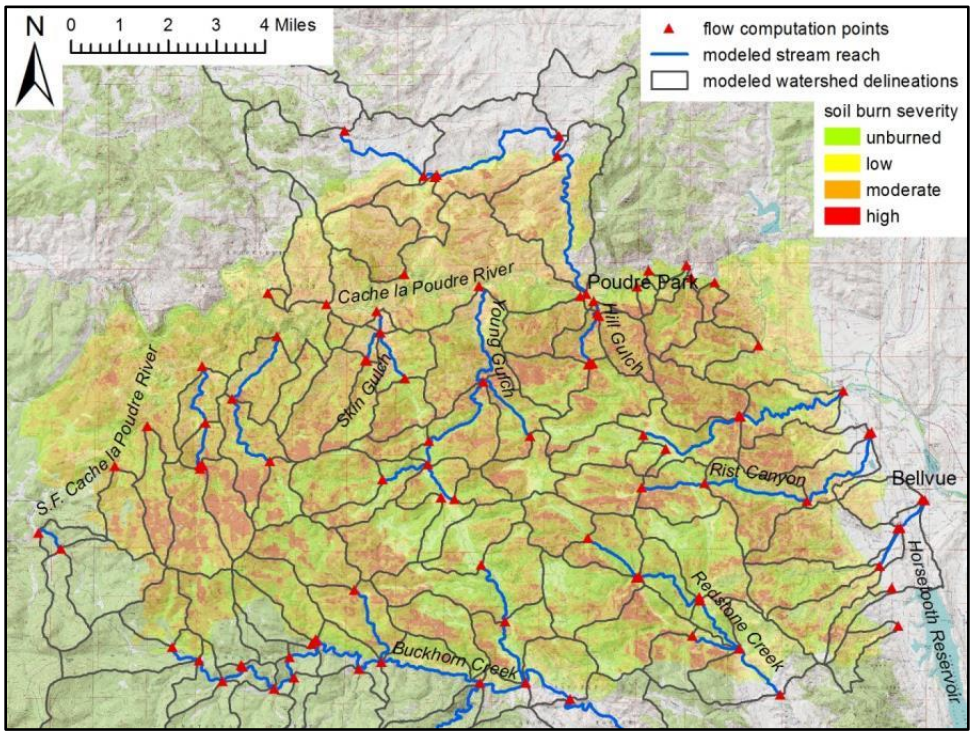

CN

The CNs were assigned to the modeled catchments according to hydrologic soil group, vegetative type, soil burn severity, and ground cover condition (percent cover). The average catchment CN was computed using an aerial averaging methodology in GIS, with more than 51,000 polygons computed for the entire modeled extent.

Soil burn severity (Figure 3) is the principle driver for increasing flow in runoff predictions. For this modeling, soil burn severity was measured using the Burned Area Reflectance Classification (BARC) process from satellite data collected on 7/20/2012, by researchers at Colorado State University. BARC uses reflectance recorded in satellite images to quantify soil burn severity. For defining soil burn severity, BARC images have the advantage of being comprehensive and relatively-rapidly developable. However, comparison with field-collected data has indicated that this remotely sensed product can be more indicative of post-fire vegetative condition than soil condition, especially in low to moderately burned areas (Hudak et al. 2004). Qualitative field assessment of this High Park Fire BARC image indicates that it appears to reasonably predict

burn severity in high and moderate areas. The soil burn severity imagery depicted in Figure 3 was developed by the USGS Earth Resources Observation and Science Center (from the same 7/20 satellite data), rather than the CSU interpretation implemented in the hydrologic modeling. This BARC interpretation was not available at the time of the analysis, though the burn severity estimates are relatively comparable and substantial variations in flood peaks are not expected.

Hydrologic soil group (HSG) classification was selected using soils data published in the NRCS SSURGO (Soil Survey Geographic) database. Two soil surveys cover the fire extent: NRCS Larimer County survey (CO644), published in 1980; and USFS Arapahoe-Roosevelt survey (CO 645), published in 2001. The USFS survey covers the western 1/3 of the fire area.

Vegetation type, from SWReGAP (Southwest Regional Gap Analysis Project) land cover mapping, was included in the CN assignments used for the modeling. The dominant vegetation types within the fire boundary were lodge pole, mixed conifer, ponderosa, shrubs and grass.

The assigned CN values are provided in Table 1. Using a fair ground cover condition, NRCS recommended values (NRCS 2004a) were applied by hydrologic soil group for unburned conditions. The CN values for low, moderate and high severity burn areas, at the four hydrologic conductivity classifications, were estimated based on CN values developed from post-fire runoff measurements (Livingston et al. 2005), with additional guidance from Wright et al. (2005) and Goodrich et al. (2005).

Table CS1- 1. CN assignments implemented in the High Park Fire hydrologic modeling

Highlighted columns indicate values extracted from NRCS (2004a).

Cover Description	Ground Cover Condition	**A** HSG				**B** HSG				**C** HSG				**D** HSG			
		Unburned	Low	Moderate	High	Unburned	Low	Moderate	High	Unburned	Low	Moderate	High	Unburned	Low	Moderate	High
Herbaceous—mixture of grass, weeds and low-growing brush, with brush the minor element	Fair	49	55	67	77	71	75	80	86	81	85	88	89	89	90	90	95
Oak-aspen—mountain brush mixture of oak brush, aspen, mountain mahogany, bitter brush, maple, and other brush	Fair	35	45	65	77	48	55	65	86	57	75	75	89	63	70	80	92
Ponderosa pine-juniper (grass understory)	Fair	36	45	65	77	58	65	75	86	73	80	80	89	80	85	90	92
Sagebrush (grass understory)	Fair	35	45	65	77	51	60	75	86	63	70	75	89	70	75	85	92
Lodgepole Pine Forest	Fair	36	45	65	77	60	65	70	86	73	80	80	89	79	85	85	92
Bare soil	n/a	77	77	77	77	86	86	86	86	91	91	91	91	94	94	94	94
Wetland	n/a	98	98	98	98	98	98	98	98	98	98	98	98	98	98	98	98

Rainfall

Since the High Park Fire area is most susceptible to flooding from relatively short duration monsoonal rain events, a 1-hour storm duration was implemented. Rainfall depths were extracted from NOAA Atlas 2, Volume 3 (Miller et al. 1973) for the 2-, 10-, 25-, 50- and 100-year rainfall events. The rainfall duration and distribution was identical to that used in the BAER modeling (BAER 2012), and is provided in the project report (Yochum 2012b). For catchments with drainages areas ≥ 6 mi^2, an aerial reduction factor was applied as detailed in Miller et al. (1973). Reduction varied from 0.95 to 0.78. When applied, this area reduction was implemented in all catchments; flow may be underpredicted in the smaller, upper catchments of such drainages.

Lag Time

Lag time (L) was computed using the watershed lag method (NRCS 2010). This equation is:

$$L = \frac{l^{0.8}(S+1)^{0.7}}{1900Y^{0.5}} \qquad \text{(equation cs1-1)}$$

, where l is the flow length (ft), Y is the average watershed land slope (%), and S is the maximum potential retention (in),

$$S = {}^{1000}\!/_{cn'} - 10 \qquad \text{(equation cs1-2)}$$

, where *cn'* is the retardance factor and is approximately equal to the *CN*. This method allows the computation of differing lag times for pre- and post-fire simulations, reflecting the actual physical mechanism of more rapid flow response during post-fire conditions. The method was developed under a wide range of conditions, including steep, heavily forested watersheds (NRCS 2010).

Flow Routing

A Muskingum-Cunge procedure was used to route flow from upper catchments to stream outlets, along the modeled stream reaches (Figure 3). This 1-dimensional method simulates flow attenuation but does not provide a numerical solution of the full unsteady flow routing equations, as provided in such computational models as HEC-RAS. Instead, in each reach flow routing was estimated using a single simplified cross section, channel slope, and Manning's *n* estimates. Photographic guidance (Yochum and Bledsoe 2010) was used to help select flow resistance coefficients, and these values were checked by inspecting the model solutions to verify that the selected Manning's *n* values resulted in subcritical or approximately critical flow velocity. Hence, it was assumed that bedform development prevents reach-average supercritical flow in these alluvial channels.

Sediment Bulking

A simple multiplication factor was applied to the post-fire flood predictions to account for sediment bulking in the debris flows. For burned catchments, this multiplication factor was assumed to be 1.25 if the (severe + moderate) soil burn severity aerial extent was greater than 50%, and 1.1 for catchments with between 10 and 50 % (severe + moderate) soil burn severity.

StreamStats

The regional USGS regression equations for peak flow prediction (Capesius and Stephens 2009), embedded in StreamStats, were used to assess the reasonableness of pre-fire peak flow predictions. The predictions are based on drainage area and the 6-hour, 100-year precipitation depth and provide expected runoff from rain events, reflecting the expectation that floods are expected to result from summer monsoons. The error bars associated with these predictions are substantial – typically about 140 percent.

These predictions are based on stream gage data and, hence, provide a level of ground truthing, but this method accounts for only drainage area and precipitation regime. Other physical characteristics and processes that are relevant in runoff processes, such as infiltration capacity, vegetative type, ground cover condition, watershed shape, and flow attenuation, are not accounted for. However, due to its foundation in field-collected data within similar watersheds, this method is valuable for assessing the general reasonableness of the model predictions for pre-fire conditions.

Results and Discussion

Hydrologic modeling was performed to develop estimates of increased flood hazard and potential threats to life and property along streams draining the High Park Fire. For several key catchments, at locations where there are threats to residences, example hydrographs (Figures 4) show the expected response to a 10-year rainfall depth over each entire catchment. Substantially increased flow peaks and runoff volumes were estimated. Using a map presentation style (Figure 5) that is simple for planners, designers, and emergency response officials to utilize, results were provided at 96 computation points over the fire extent. Results were also provided as attributes in ArcGIS shapefiles. In addition to simulated flood peaks, time-to-peak estimates were provided to give emergency response personnel estimates of the expected flood response times. For detailed results, refer to Appendix A of the project report (Yochum 2012b) and the accompanying poster (Yochum 2012a).

Substantially higher peak flows and flood volumes are predicted for post-fire conditions. In many catchments, post fire conditions were predicted to cause a 50- or 100-year (pre-fire) flood to result from a 10-year rain event on burned landscapes, similar to measured fire runoff responses (Conedera et al. 2003). If it is assumed that the fire impacts on runoff in each of these catchments will be substantial for at least 5 years, the risk of a 10-year rainfall event over each point in these catchments over those 5 years of destabilization is 41 percent, with resulting (pre-fire) 50- to 100-year floods. If a 10-year recovery is expected, the risk increases to 65 percent. However, as catchment size increases the small spatial extent of typical convective storms will reduce the severity of the flood effects.

Due to their simplicity, peak flow enhancement ratios (Q_{post}/Q_{pre}) can be a preferred method for communicating flood enhancement predictions. Predicted values for the 25-year rain event are provided (Figure 6). Peak flow enhancement ratios are higher for more frequent rain events (2- and 10-year storms) and lower for less frequent events (50- and 100-year storms), with this same pattern observed with field-collected data (Moody and Martin 2001). This method only provides meaningful results where the pre-fire peak flow is greater than zero for the rainfall event of interest.

Figure CS1- 4. Example estimated pre- and post-fire hydrographs for the 10-year rain event.

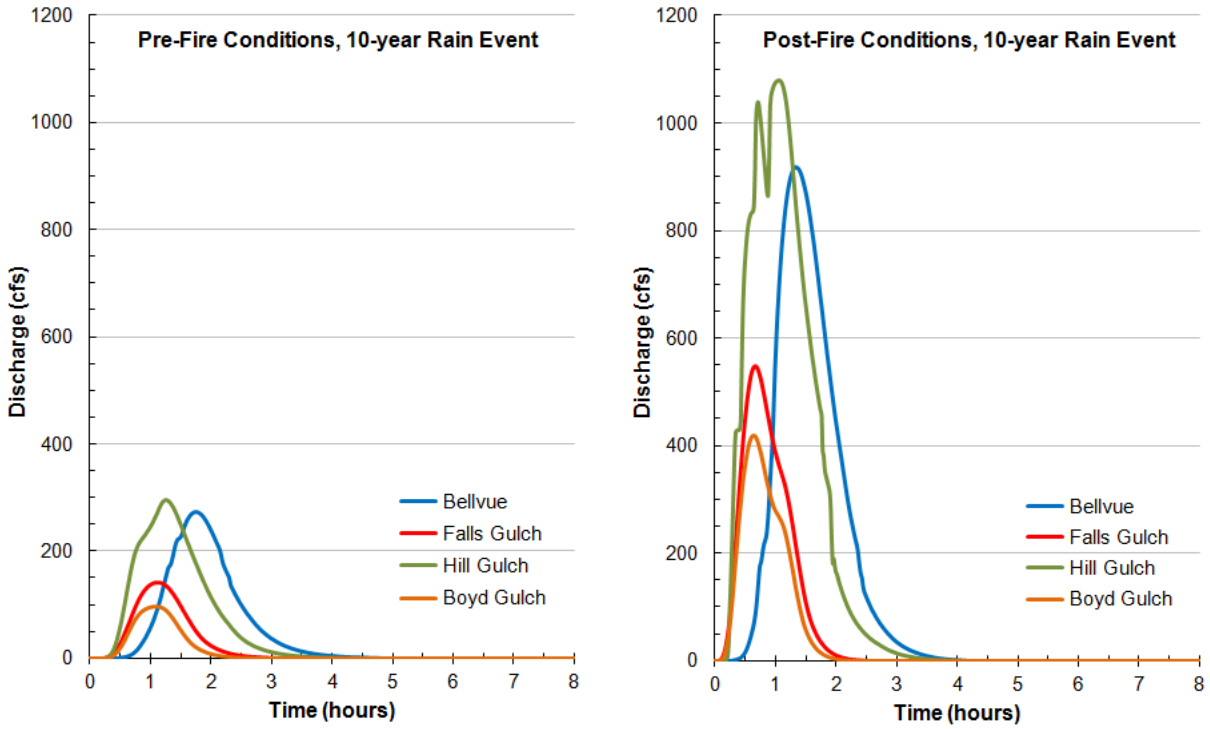

Figure CS1- 5. Example map providing pre- and post-fire flood prediction estimates for the Poudre Park area.

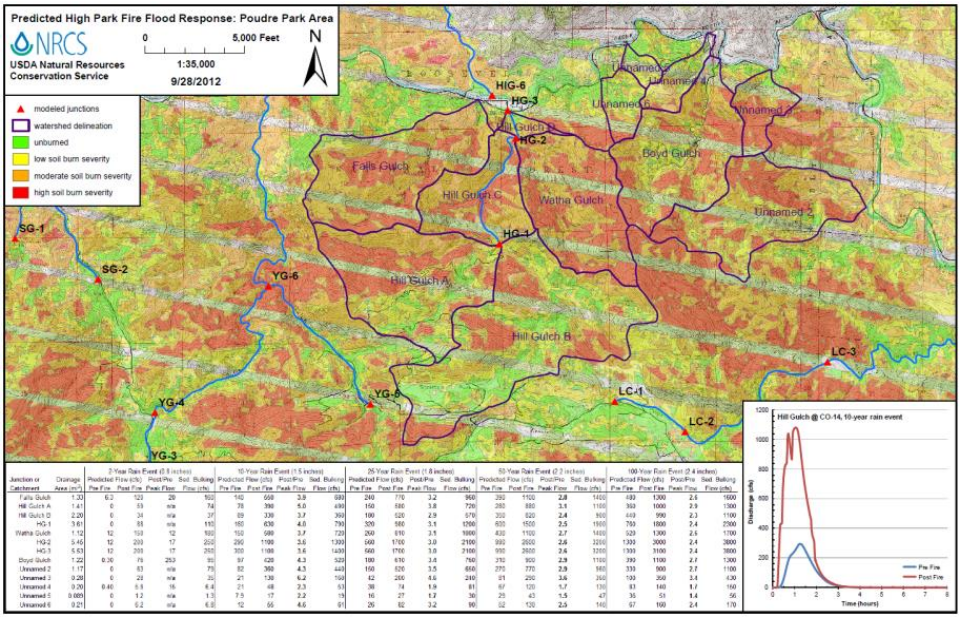

Figure CS1- 6. Estimated 25-year peak flow enhancement ratios for the High Park Fire

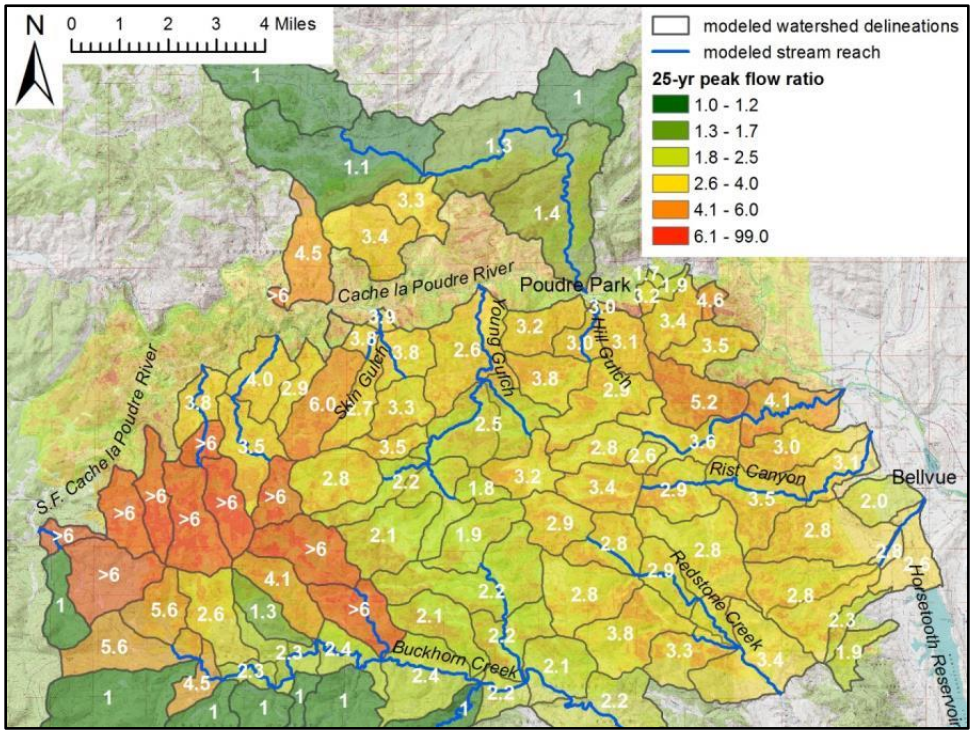

Comparison with Regression Predictions

Table 2 illustrates USGS regression modeling results (from StreamStats) compared to CN modeling results at a number of locations, for the 10- and 25-year events. Considering the large expected prediction errors of the USGS regression equations in this area (typically 140%), the results are reasonably comparable. The greatest differences in prediction are typically in the largest catchments. Differences in the results are likely due to limited data available for selecting CN values for post fire conditions, questionable CN model appropriateness in forested watersheds, and possible inaccurate rainfall depths and aerial reduction factors. Additionally, the regression technique does not account for relevant hydrologic processes, such as variable soil infiltration capacity, vegetative type, ground cover condition, and stream flow attenuation.

Table CS1- 2. Comparison example of CN modeling with USGS regressions published in StreamStats. Reg: regression results.

	Area	10-yr flow (cfs)		25-yr flow (cfs)			Area	10-yr flow (cfs)		25-yr flow (cfs)	
Point	(mi^2)	CN	Reg	CN	Reg	Point	(mi^2)	CN	Reg	CN	Reg
MC-2	3.33	119	212	249	360	BG	1.22	97	95	177	151
MC-5	6.61	272	335	588	574	UN-3	0.28	21	40	42	61
BC-8	23.2	44	407	119	650	RdC-2	5.05	131	231	284	382
BC-13	42.9	244	599	474	974	RdC-5	13.2	180	445	479	764
BC-18	55.0	332	741	729	1230	RdC-6	16.2	168	512	478	885
HlG-3	10.9	207	248	446	387	RC-2	3.00	172	170	334	277
HlG-5	21.8	210	348	466	554	RC-4	8.16	282	316	549	531
LC-1	1.20	23	96	60	152	SG-1	3.09	103	120	216	183
LC-4	6.97	168	277	354	460	SG-2	1.19	45	73	96	111
CG	2.00	89	92	178	139	SG-4	5.99	191	182	395	283

Accuracy and Limitations

As with all hydrologic modeling, the results provided by these simulations are approximate. Comparisons with flood peaks estimated using the USGS regression equations (Table 2) indicate that the pre-fire runoff simulations are more-or-less reasonable overall, but that the modeling often provides estimates that might be inaccurate, especially as catchment size increases. Post fire runoff prediction using the CN technique is hampered by the very little available field data available to reliably select CN values from measured rainfall and runoff in burned catchments.

Additionally, the use of dated rainfall depths and aerial reduction factors (Miller et al. 1973) in orographic-forced mountainous watersheds adds an additional layer of uncertainty to the estimates.

Additionally, greater infiltration is indicated by the USFS soil survey than the adjacent NRCS survey, with infiltration commonly increasing by a step at the survey boundary and a large area with HSG A indicated. In the most problematic areas zero runoff is predicted for pre-fire conditions in some catchments during the 10- and 25-year rain events. This problem may be due to shallow, permeable soils over bedrock dominating the USFS soil survey classification methodology, but the true reason for this inconsistency is unknown. As a result, the modeling may be underpredicting runoff and overestimating flood response ratios in catchments draining the Arapaho-Roosevelt soil survey area, especially for more frequent (shallower) rainfall events.

More fundamentally, the reliability of the CN method for predicting peak flow from forested, mountainous watersheds is questionable, due to questionable appropriateness of the CN method and shifting streamflow generation processes between and pre- and post-fire conditions. This issue is discussed in the body of this technical note under the CN Methodology Limitations in Forested Watersheds section.

Despite these shortcomings, due to its relative simplicity, achievable data requirements on large scales, and the lack of a viable alternative, the CN method is a preferred tool for predicting flood responses of wildfire areas. The modeling performed for the High Park Fire has substantial value for identifying areas of greatest threat to life, property and infrastructure. Peak flow ratios provide an excellent tool for communicating expected increases in runoff with agencies, first responders, and the public. In addition, peak flow and runoff volume estimates are still required for sizing infrastructure improvements. Unknown uncertainties in the estimates needs to be effectively communicated to provide assurances that involved parties use the estimates with caution. Research and technical guidance is needed to develop and communicate more robust methods for flood prediction from wildfire-impacted landscapes.

Conclusions

Using the NRCS Curve Number method, peak flow predictions were made for streams draining the High Park Fire area, for both pre-fire and post-fire conditions. Watershed maps for each modeled catchment were developed, illustrating computation points, peak discharges, peak flow enhancement ratios, soil burn severity, and stream outlet hydrographs. While many relevant hydrologic mechanisms were simulated, including rainfall depth and spatial extent; variation in runoff by soil burn severity, vegetation type and soil conductivity; variable lag times; and stream attenuation, the questionable reliability of the CN method in forested watersheds, for both post- and pre- fire conditions, adds a level of undefined uncertainty to the estimates. Research is needed to address this uncertainty, especially since lives are often at risk. In the meantime, wildfires will occur and methods need to be available to predict the expected flood response from burned watersheds. This case study provides an example of one such approach.

Acknowledgements

Appreciation is expressed to High Park Fire BAER team, for their initial analyses, Brandon Stone and Colorado State University for the utilized BARC soil burn severity interpretation, and Randy McKinley of the USGS and Eric Schroder of the USFS for the presented soil burn severity interpretation. Appreciation is also expressed to John Andrews for his contributions to the post-fire CN assignment compilation, John Norman for GIS analysis assistance and soils expertise, and Kari Sever and Sam Streeter for field data collection.

References

BAER 2012 High Park Fire Burned Area Emergency Response Report. USDA USFS and NRCS, Larimer County, Colorado Department of Transportation, July 17th.

Capesius, J.P., Stephens, V.C. 2009 Regional Regression Equations for Estimation of Natural Streamflow Statistics in Colorado. U.S. Department of Interior, U.S. Geological Survey, Scientific Investigations Report 2009-5136.

Conedera, M., Peter, L., Marxer, P., Forster, F., Rickenmann, D., Re, L. 2003 Consequences of Forest Fires on the Hydrogeological Response of Mountain Catchments: A Case Study of the

Riale Buffaga, Ticino, Switzerland. Earth Surface Processes and Landforms 28, 117-129.Maidment, D.R. 1992 Handbook of Hydrology McGraw-Hill, Inc.

Garen, D.C., Moore, D.S. 2005 Curve Number Hydrology in Water Quality Modeling: Uses, Abuses and Future Directions. Journal of the American Water Resources Association 42(2), 377-388.

Goodrich, D.C., Canfield, H.E., Burns, I.S., Semmens, D.J., Miller, S.N., Hernandez, M., Levick, L.R., Guertin, D.P., Kepner, W.G. 2005 Rapid Post-Fire Hydrologic Watershed Assessment Using the AGWA GIS-Based Hydrologic Modeling Tool. In: Moglen, G.E., ed. Proceedings of Managing Watersheds for Human and Natural Impacts: Engineering, Ecological, and Economic Challenges, July 19-22, 2005, Williamsburg, VA, USA. American Society of Civil Engineers, Alexandria, VA.

Hawkins, R.H. 1993 Asymptotic Determination of Runoff Curve Numbers from Data. Journal of Irrigation and Drainage Engineering 119, 334-345.

Hawkins, R.H., Greenberg, R.J. 1990 WILDCAT4 Flow Model. School of Renewable Natural Resources, University of Arizona, Tucson, AZ. BLM contact: Dan Muller, Denver, CO.

Hudak, A.T., Robichaud, P.R., Evans, J.S., Clark, J., Lannom, K., Morgan, P., Stone, C. 2004 Field Validation of Burned Area Reflectance Classification (BARC) Products for Post Fire Assessment. Remote Sensing for Field Users: Proceedings of the Tenth Forest Service Remote Sensing Applications Conference, Salt Lake City, Utah, April 5-9 2004.

Livingston, R.K., Earles, T.A., Wright, K.R. 2005 Los Alamos Post-Fire Watershed Recovery: A Curve-Number-Based Evaluation. In: Moglen, G.E., ed. Proceedings of Managing Watersheds for Human and Natural Impacts: Engineering, Ecological, and Economic Challenges, July 19-22, 2005, Williamsburg, VA, USA. American Society of Civil Engineers, Alexandria, VA.

Moody, J.A., Martin, D.A. 2001 Post-Fire, Rainfall-Intensity-Peak Discharge Relations for Three Mountainous Watersheds in the Western USA. Hydrological Processes 15, 2981-2993.

Miller, J.F., Frederick, R.H., Tracey, R.J. 1973 Precipitation-Frequency Atlas of the Western United States. U.S. Department of Commerce, National Oceanic and Atmospheric Administration, National Weather Service, NOAA Atlas 2, Vol 3, Silver Spring, Maryland.

NRCS 2004a Hydrologic Soil Cover Complexes. USDA Natural Resources Conservation Service, National Engineering Manual, Chapter 9, 210-VI-NEH, July.

NRCS 2004b Estimation of Direct Runoff from Storm Rainfall. USDA Natural Resources Conservation Service, National Engineering Manual, Chapter 10, 210-VI-NEH.

NRCS 2010 Time of Concentration. USDA Natural Resources Conservation Service, National Engineering Manual, Chapter 15, 210-VI-NEH.

Rallison, R.E. 1980 Origin and Evolution of the SCS Runoff Equation. Proceedings of the Symposium on Watershed Management; American Society of Civil Engineers, Boise, ID.

Springer, E.P., Hawkins, R.H. 2005 Curve Number and Peakflow Responses Following the Cerro Grande Fire on a Small Watershed. In: Moglen, G.E., ed. Proceedings of Managing Watersheds for Human and Natural Impacts: Engineering, Ecological, and Economic Challenges, July 19-22, 2005, Williamsburg, VA, USA. American Society of Civil Engineers, Alexandria, VA.

Tedela, N.H., McCutcheon, S.C., Rasmussen, T.C., Hawkins, R.H., Swank, W.T., Campbell, J.L., Adams, M.B., Jackson, C.R., Tollner, E.W. 2012 Runoff Curve Numbers for 10 Small Forested Watersheds in the Mountains of the Eastern United States. Journal of Hydrologic Engineering, 17(11), 1188-1198.

Woodward, D 2005 Personal Communications (email). Retired National Hydraulic Engineer, USDA Natural Resources Conservation Service, Washington D.C.

Wright, K.R., Earles, T.A., Pemberton, E. 2005 Mesa Verde Bircher Fire Hydrological Impact. In: Moglen, G.E., ed. Proceedings of Managing Watersheds for Human and Natural Impacts: Engineering, Ecological, and Economic Challenges, July 19-22, 2005, Williamsburg, VA, USA. American Society of Civil Engineers, Alexandria, VA.

Yochum, S.E. 2012a Poster: Increased Flood Potential of Steams Draining the High Park Fire, with Ratios of Predicted Post/Pre Fire Peak Flows for the 1-Hour, 25-Year Rain Event. U.S. Department of Agriculture, Natural Resources Conservation Service, Colorado State Office, 9/2012.

Yochum, S.E. 2012b High Park Fire: Increased Flood Potential Analysis. U.S. Department of Agriculture, Natural Resources Conservation Service, Colorado State Office, 10/2012.

Yochum, S., Bledsoe, B. 2010 Flow resistance in high-gradient streams. Proceedings of 4th Interagency Hydraulic Modeling Conference, June 21 – July 1st, 2010, Las Vegas, NV, USA.

2162

2163 (This page intentionally blank)

Case Study 2: The 2000 Montana Bitterroot Wildfires and the Development of the MT NRCS FIRE HYDRO Method

Background

Southwestern Montana was in the midst of a severe climatic drought in the late summer of 2000 when wildfires raged through that corner of the state. Various fires hit the area around the Bitterroot National Forest particularly hard. These fires were largely started by lightning strikes. The total area damaged by these fires included 244,000 acres on USDA National Forest lands as well as 49,000 acres of state-owned and private land. The severity of the fires ranged from low that meant some under-story destroyed but minimal tree canopy impacts, to high, signifying complete destruction by fire of all living plant material.

A significant effort was put forth after the fires by USDA personnel, including both Forest Service (FS) and Natural Resources Conservation Service (NRCS) employees, to evaluate the potential hydrologic impacts to the area's residents and infrastructure. NRCS got involved with this work by use of the Emergency Watershed Protection Program (EWP). The work was complicated by the fact that traditional agency hydrologic evaluation methods did not address the conditions found in the burn areas. An expedited search for any existing simple and expedited procedures to handle this need did not reveal suitable results. NRCS in Montana made a decision to pursue the development of a simple but accurate hydrologic evaluation method for use by USDA personnel working on post-wildfire watershed protection projects. An adherence to the Runoff Curve Number (RCN) methodology described in NRCS National Engineering Handbook, Part 630- Hydrology, Chapter 10 (1972), was desired since NRCS employees were most familiar with this. The difficulty with this concept was establishing the correct RCNs applicable to various land covers burned by wildfires of differing severities. The analytical routine used to determine the times of concentration for the burn areas also required consideration during the development of this new method.

The goal was to create a simplistic method that USDA field engineers were readily familiar with and could perform using laptop computers on location so that they could quickly determine the appropriate practices and their required sizes in order to reduce the impacts of runoff and debris

coming from the burn areas. The Emergency Watershed Protection program (NRCS, applied to private landowners typically downhill and adjacent to National Forest lands) and the Burn Area Emergency Rehabilitation program (Forest Service work focused on National Forests lands) that were being administered for this recovery work are typically executed in an expedient manner. Within these programs, projects must be evaluated, designed, contracted, and constructed in a short time or they will not be considered for funding by these agencies.

Photos

Figure CS2- 1. Lightning strikes in the Bitterroot Valley of Montana caused the outbreak of wildfires in 2000.

Figure CS2- 2. One of the most poignant scenes ever captured of a wildfire was this image taken in the 2000 Bitterroot Valley Complex.

Figure CS2- 3. Satellite imagery used to detail burn severity found in the 2000 Bitterroot Valley Complex wildfire.

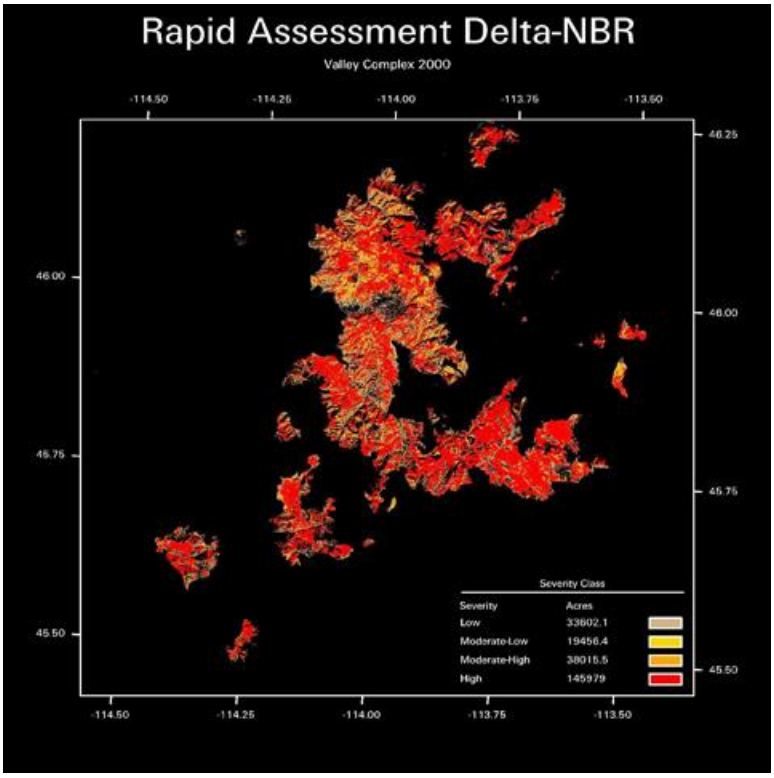

Figure CS2- 4. Burn severity map and rain gage data for a rain event that happened a year after the 2000 Bitterroot Valley Complex wildfire

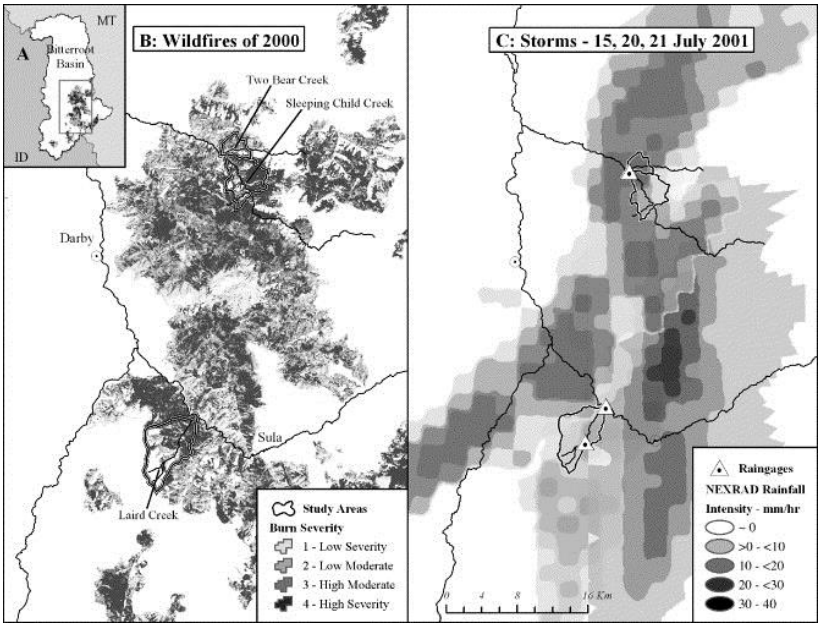

Figure CS2- 5. This is Laird Creek in 2001 within what was the Bitterroot Fire Valley Complex.

This photo (figure CS2-5) was taken the year after the fire with obvious high runoff issues. Alluvial deposition of sediments and debris are clearly evident. This area was subject to a high severity burn. Grass cover is largely the benefit of helicopter seeding done the previous fall, after the fire.

Figure CS2- 6. Fully loaded silt fence placed in the aftermath of the 2000 Bitterroot Valley Complex wildfire.

Figure CS2- 7. Sheafman Point in October 2008.

Eight years after the 2000 Bitterroot Valley Complex wildfire. Note that viable woody vegetation is still not evident.

Figure CS2- 8. Glen Lake trail in the summer of 2012.

Twelve years after the 2000 Bitterroot Valley Complex wildfire.

Figure CS2- 9. The landscape around Glen Lake in the summer of 2012.

Twelve years after the 2000 Bitterroot Valley Complex wildfire shows good grass cover but little woody vegetation.

Methods

The hydrologic principles found within the SCS Engineering Field Handbook, Chapter 2, Estimating Runoff and Peak Discharge(EFH-2, Aug. 1989) were considered appropriate to meet the needs for this simple but accurate analysis of the wildfire areas. At the time (2000), EFH-2 was only available as a manual method that required the user to look to the tabular and graphical

listings within the method to determine the volume and peak discharge of runoff for the singular watershed under investigation. The EFH-2 peak discharge analysis requires the user to specify the design rainfall distribution type (defined by NRCS into four categories nationwide) that is appropriate for the project area under investigation. The NRCS in MT has its own criteria for determining the appropriate selection of design rainfall distribution based on the project area's ratio of the 6-hour to 24-hour rainfall amounts for the desired recurrence event. The FIRE HYDRO method was created as an EXCEL spreadsheet that incorporated NRCS RCN technology and EFH-2's peak discharge graphical solution in conjunction with the MT NRCS design rainfall selection criterion. Trend curve function equations were developed from the graphs of Ia/P vs. Tc shown in EFH-2. These equations were installed in the EXCEL file to help solve for predicted peak discharge.

Several issues related to the proper hydrologic evaluation of the project area were considered in the creation of this method. These include the proper selection of RCN for burn areas (which were and still are not available) and time of concentration analysis. The time of concentration and its related flow length were analyzed assuming a rectangular watershed shape (watershed height equal to 2 times the watershed width for a total area equal to the watershed area stated by the designer). Another related issue considered was the fire-induced soil hydrophobicity (water repelling soil property, detailed later).

The FIRE HYDRO method involves an analysis of four different watershed conditions. They are as follows:

Condition 1- Pre-Fire.

Condition 2- Post-Fire. Immediately after the fire with hydrophobic soil properties included.

Condition 3- Post-Fire. Little emergent vegetation from that destroyed by fire but hydrophobic soil properties have ceased. The diminished influence with time of the hydrophobic soil properties is discussed on the next page. The assumption here is that hydrophobic properties are considered to wane prior to significant post-fire vegetal recovery.

Condition 4- Post-Fire. Estimated conditions based on anticipated re-growth of vegetation after the next growing season following the fire.

These four conditions were evaluated to give the designer a greater feel for the range of runoff conditions that were, are and will be present for the watershed being investigated. This information helps the designer better understand the change in relative risk over time on various alternative hydrologic control measures considered for installation including the "do nothing" alternative.

Runoff Curve Numbers for Burn Areas

The FIRE HYDRO method is used to evaluate individual watersheds by treating all land use/soil conditions as a composite homogeneous collection. This assumption contains inherent problems when widely varying runoff conditions exist in the watershed being modeled. A literature search for recommended RCNs for wildfire burn areas specifically related to southwestern MT's climate and vegetation types yielded nothing. Consequently, select MT NRCS engineers created the following guidance for selection of RCN based on burn severity and hydrologic soil grouping (HSG) specific to the Bitterroot wildfire vicinity:

For High Severity Burn Areas*- HSG A soils = RCN 64
HSG B soils = RCN 78
HSG C soils = RCN 85
HSG D soils = RCN 88

For Moderate Severity Burn Areas-Use Cover Type in FAIR Condition

For Low and Unburned Areas- Use Cover Type in GOOD Condition for North & East facing slopes

Use Cover Type between FAIR & GOOD for South & West facing slopes

* High Severity Burn Areas were assumed to have attained a minimum of 30% ground cover consisting of vegetation, duff, thick ash, or woody debris by June of the following year. These recommended RCNs (for all burn severity types listed) were arrived at by consensus amongst three MT NRCS engineers with hydrologic evaluation experience. Their basic premise was to establish a logical fit for burn area RCN values within the existing accepted NRCS RCN/land use table. There was no time between when the fires were occurring and exigency runoff protection work was to take place for any gauging or calibrating to take place to verify or improve upon these recommendations. Rainfall events that occurred the following spring and summer, approximately the 2-year to 5-year, 24 hour storms did not produce failure-causing runoff for the protection practices installed using these RCN values.

Hydrophobic Soils

Hydrophobicity in soils can be induced by wildfire. It requires certain soil textures and certain plant types to be burned in order to create this condition of significant water repellency. In brief, this condition can be found in more moderately coarse soils that have a deep plant litter mat and experience a severe burn. The resulting "waxy gas" that is created then permeates and coats the upper soil layer making it water repellent. Runoff rates and volumes from these previously absorptive soils can become extremely high once they have become hydrophobic. The engineer must make their best estimate as to how much and to what degree hydrophobicity has occurred after the fire in conjunction with how long this changed runoff condition can be expected to occur when assigning a design RCN for the watershed (also consider timing of next normal rain season compared to hydrophobic abatement recovery time). Field-testing is called for by applying water to the mineral soil (below the ash layer) and checking for infiltration with time. One rule of thumb arrived at by MT NRCS was to give all hydrophobic soils a runoff curve number (RCN) of 94. It is important to consider the window of time to which hydrophobic conditions are expected to occur. Hydrophobicity in the soils tends to breakdown over time as the soil surface is disrupted through either plant growth activity or water action (freeze/thaw or dew and desiccation). These two processes occur very typically in MT but may not be so prominent in other states.

Experience gained from the Bitterroot EWP effort while considering hydrophobic soils properties for effective RCN assignment yielded some interesting findings. Significant field reconnaissance, largely by Forest Service personnel, was dedicated to evaluating the water-repellent properties of the soils in the fire-affected watersheds. Certain conditions yielded estimated 50-70% water-repellent tendencies in high severity burn areas. Similar tests in adjacent unburned areas often yielded 40-60% water repellency. It was thought that the drought that was prevalent throughout the area in the summer of 2000 created a "tightening effect" of drought-affected soils, which created water-repelling properties within the soil. Since the burned and unburned water repelling rates seemed so similar it was determined that the fire had not induced a significant increase in hydrophobicity and that any added runoff effect should not be attributed to the weighted watershed RCNs. The resulting runoff from rainfall events subsequent to the fire did not display any tendencies towards large hydrophobicity induced increases above pre-fire conditions as would be expected if indeed the soil hydrophobicity was actually a major factor in the post-fire hydrology.

Time of Concentration (T_c) and Assumed Watershed Shape

The engineers and technicians assigned to perform the watershed hydrologic evaluations within the wildfire area were not often offered detailed topographic mapping of the site. They were given GIS data that included total watershed area as well as percentages of which experienced low, moderate, or high severity burns along with soils data that included land slopes within the dominant soil classes found. An assumption was needed within the FIRE HYDRO method that provided an estimate of watershed length based on its area. An assumed rectangular shape watershed with dimensions of one unit wide by two units long was made to produce the area stated for the watershed in the GIS data report. The T_c flow path was taken as the longitudinal line down the center of this rectangle with a bend towards a corner at the upper third. The T_c was calculated using the Lag Method found in EFM-2. This method used RCN, flow length, and average watershed slope (based on values from the soils data in the GIS data) as its basis. The post-fire T_c was assumed to stay equal to the pre-fire T_c even though there was a reduction in plant cover (therefore reduced flow friction leading to higher flow velocities) after the fire that should logically allow a faster T_c to develop. The assumption here though was that the excessive

amount of available debris after the fire would cause blockages in the flowpath, a kind of debris dam, which would serve to attenuate the flows. The degree of flow attenuation after the fire may vary tremendously from one area to another or one watershed to another but it was felt that a reasonable estimate was to maintain post T_cs equal to that found in the pre-fire condition.

Results and Discussion

The FIRE HYDRO method was utilized to a great extent by engineers and technicians involved with the 2000 Bitterroot Wildfire recovery operations. NRCS personnel designed many runoff diversion practices to protect homes from the anticipated increased rainfall runoff brought about by changes in watershed conditions due to the wildfires. FS personnel designed for the enlargement of culverts to provide capacity for the anticipated increase in runoff and also to allow for fish passage. All of the practices designed for by use of the FIRE HYDRO method were able to satisfactorily withstand the rigors of rainfall runoff in the following years without any notable failures being reported.

It should be noted that the typical setting applicable to a home being protected by diversion practices in this event was that the home was situated on the only reasonably flat land around, being surrounded by steep mountainous land. The reason that the land was near level there was because it happened to be on an alluvial fan brought about by deposition of sediments from previous historic wildfires through time. So in effect, the homes were situated as prime targets to receive heavy depositions of sediment and debris if not for the successful functioning of the diversion practices (most typically in the form of concrete highway dividers placed slightly down the slope and above the area of interest).

One key feature that should be considered in establishing the proper design RCN for post wildfire hydrologic evaluations is the anticipated recovery time of the watershed towards its pre-fire value. As the burn severity worsens the resulting RCN increases. This leads to higher estimated predicted runoff from the various design rainfalls used for sizing runoff control practices that in turn leads to higher costs to control the runoff. Nevertheless, in the seasons that follow the wildfire there is a recovery of the hydrologic processes towards that of pre-fire thereby lessening the design RCN from that used immediately after the fire. It is incumbent

upon the key figure in charge of assigning the recommended design RCNs for various land covers and burn severities that they consider both the risk of failure versus storm frequency. Design RCNs based on recovery of the land cover can vary greatly in the seasons following a wildfire.

There was concern for selection of the proper design storm recurrence interval for design purposes of various post-fire runoff control practices. The concern stemmed from the idea that the notable increase in RCN value as the result of a fire would be short-lived and recovery of the ground cover would start to decrease the RCN in the seasons following the wildfire. The EFH-2 method that FIRE HYDRO is based on is very sensitive to the selected design RCN. It was thought that to base all designs, including those for low hazard structures, on the accepted storm recurrence interval (25-yr for most practices) would produce costly results that may not be needed. The MT State Conservation Engineer (SCE) issued a guidance letter to all EWP engineers and technicians relating to the selection of recurrence interval design storms to be used for the statewide EWP effort. Low hazard scenarios were to be designed for non-damaging passage of flows of the 25-year pre-fire peak discharge or post-fire 10-year peak, whichever was greater. High hazard scenarios were to be dealt with on a case-by-case basis in consultation with the SCE.

The assumption for maintaining the pre-fire T_c as that used for post-fire analysis should be more thoroughly investigated to determine its validity. As previously mentioned, this assumption was based on the idea that the added debris and sediment load from the burn would create increased opportunity for flow blockages to occur thereby slowing the runoff process from what might initially be expected from a higher RCN setting. This assumption should be inspected for consideration on improvements to this method or similar ones in the future. Onsite inspection of the burn area during a prominent runoff event should reveal the reality of this assumption or not. There may be visible evidence of flow blockages and their potentially eventual breaches after a storm has occurred. The most ideal setting would be to have gaged (time-based recording style) rainfall and runoff response for various watersheds affected by the fire with records from storms both before and after a wildfire. This would provide the most accurate assessment of wildfire influence to T_c and storm runoff volume and rate.

There are some complex issues that should be recognized when attempting to model hydrology post wildfire. One of the biggest issues is the time varying RCN value. It is obvious that the effective RCN for the watershed where the burn occurred will have increased drastically. The question becomes how long and at what rate does the recovery to pre-fire RCN take. It might not be economically proper to assume the worst case RCN (immediately after the fire) for all hydrologic modeling related to design of runoff control practices in these areas. An accurate assessment of how the RCN changes with time would help decision makers develop a sensible strategy for setting proper design parameters. Peter Robichaud, USFS, has spent considerable time investigating and monitoring post wildfire watershed. His findings indicate a tremendous increase in sheet erosion taking place on the landscape the year following the fire but then cutting back drastically each year thereafter. It seems that the growth of grass on the bare ground provides abatement to raindrop impact on the soil thereby stemming erosion about a year or two after the fire. The question may still exist as to whether the runoff amount has significantly decreased as well in this window of time. In other words, the soil may not be suffering from raindrop impact yet it may still be yielding runoff considerably greater than it did prior to the fire (indicating a higher RCN and greater potential for flooding downstream).

The answer to the question above can only be answered by gaging of the watershed runoff or possibly by visible indicators of stream flow levels along the stream bank from various rainfall events. Optimally these records would be compared to those kept from the same area prior to the fire. This would begin to show how RCN changes with time in the watershed landscape recovery process. One option here might be to seek out watersheds that have been used for USGS predictive peak discharge regression equation development that have also experienced a wildfire. These areas could then be similarly analyzed for newly developed equations to reveal what trends have become apparent. RCNs could perhaps then be assigned within the NRCS hydrology models that produce results in line with the USGS gaged watersheds.

Limitations

Sound hydrologic judgment is called for in utilizing FIRE HYDRO. It is based on the NRCS runoff equation. It is subject to all of the assumptions pertaining to that method. The selection

of appropriate (and likely weighted) RCN should be based on the best information available (pre-fire land cover/condition and fire severity distribution in the watershed being evaluated). The predicted peak discharges from this model are quite sensitive to the RCN used. The RCNs listed in this paper were refined from existing tables in EFM-2 and altered by the judgment of MT NRCS engineers to address the conditions found in western MT. Other areas may require similar scrutiny to best define appropriate RCN usage. The decision of whether or not it is appropriate to weight the various RCN attributed sub-areas and treat them as one homogeneous area is left to the designer. If a more refined modeling approach for radically different (and typically large scale drainage areas, over 2000 acres) RCN defined sub-areas is desired, the designer should consider using either the NRCS Win TR55 or Win TR20 programs. Consultation with experienced users of these programs is warranted to assure accurate assessments. One other possible way to handle "non-homogeneous" watersheds utilizing this tool would be to analyze the pre-fire scenario and determine a csm (cubic feet per second per sq. mile) delivery to the outlet for the various recurrence events. Then analyze the severely affected (RCN-wise) areas for the post-fire condition but using only the reduced area attributed this burn (not the entire drainage area used in the pre-fire analysis). Then for each recurrence event in the post-fire analysis add the peak discharge from the high RCN area to the discharge estimated for the remaining area (assumed unburned) by multiplying the pre-fire csm x the remaining area (in sq. mi units). For instance if a 5.0 sq. mile watershed is analyzed resulting in a pre-fire 10 year (24hr.) peak discharge estimate of 25 cfs, this would yield a pre-fire delivery of 25/5 or 5 csm. Assuming the post fire analysis of the area revealed an area of 2 sq. miles that were severely burned and went from an RCN=58 (pre-fire) to RCN=82 (post-fire) and 3 sq. miles were found to be unchanged by the fire. The analysis of the 2 sq. mile high severity burn yields a 10-year peak discharge of 90 cfs (but only for the 2 sq. miles). An estimate for the total 10-year (24hr) for the entire watershed would be 90cfs+(3sq. mi x 5csm)= 105 cfs. A wide mosaic of burns (and resultant varying RCNs) could not be handled in this way but may fit the homogenous assumption that the spreadsheet utilizes. Again, sound judgment is called for, by the designer, to ensure that accurate modeling procedures are followed.

Though the drainage area is limited to 2000 acres by the parent method (EFM-2) of FIRE HYDRO, some of the burn areas are much larger than this. The results of FIRE HYDRO were

compared to those from a more detailed method (TR-20) and found to be reasonably close for watersheds in the 5-10 square mile range. Consequently, no limit on drainage area was imposed on FIRE HYDRO. The user is cautioned to exercise judgment in the appropriate use of FIRE HYDRO to make sure that sound principles of hydrology are being modeled properly for the conditions present in the watershed. The assumptions for rectangular watershed shape, which effects T_c, and maintaining the same T_c from pre-fire to post-fire conditions should not be overlooked.

Acknowledgement

The development of FIRE HYDRO was largely a joint venture between MT NRCS Hydraulic Engineers Geoffrey Cerrelli, PE (retired) and Ralph Bergantine, PE (retired). This method was created in a short time window between when the fires broke out and it became apparent that EWP would be implemented. Cerrelli and Bergantine matched wits to arrive at the strategies for development of the burned area RCNs and the Tc. Cerrelli then created the EXCEL file to capture these ideas. SCE, D. James Suit, PE (retired) provided oversight and approval to the process.

Further Reading

"Avoiding the Disaster After the Disaster", NRCS September 2001
http://www.nrcs.usda.gov/Internet/FSE_DOCUMENTS/nrcs143_007760.pdf

"A Synthesis of Post-Fire Road Treatments for BAER Teams: Methods, Treatment Effectiveness, and
Decisionmaking Tools for Rehabilitation", USFS, R. Foltz, P. Robichaud, H. Rhee, 2009
http://www.firescience.gov/projects/06-3-4-03/project/06-3-4-03_BAER_Road_Treat_Main.pdf

"Effects on the Forest Ecosystem"
http://library.thinkquest.org/C0119184/english/historical_fires_2000_fire_season_effects_of_2000_forest.shtml

"FIRE HYDRO: A Simplified Method for Predicting Peak Discharges to Assist in the Design of Flood Protection Measures for Western Wildfires", ASCE paper by G. Cerrelli, 2005
http://ascelibrary.org/doi/abs/10.1061/40763(178)80

References (for the development of FIRE HYDRO)

Engineering Field Handbook, Chapter 2, Hydrology, National Engineering Handbook Series Part 650, USDA-Natural Resources Conservation Service

National Engineering Handbook, Part 630, Hydrology, USDA-Natural Resources Conservation Service (various chapters dating from 1971-2001)

WinTR-20, USDA Natural Resources Conservation Service, October 2004
Formerly Technical Release No. 20, Computer Program For Project Formulation

Case Study 3: Post fire analysis for the 2012 Saratoga Fire

Introduction

As part of the 2012 fire season, analysis of the Dump Fire was conducted to design a sediment basin. The event is estimated to be a 1.25-inch storm that lasted 25 minutes and dropped an estimated bedload of 70,000 tons of material, which damaged houses, inundated basements and overtopped a small basin. The event is comparable to two times the 100-year flow. The "Dump Fire" was analyzed as a part of the United States Department of Agriculture Natural Resources Conservation Service Emergency Watershed Protection Program.

The Dump Fire is located near Saratoga Springs, Utah, on the eastern edge of the basin and range. It was analyzed using the United State Department of Agriculture Agricultural Research Service Automated Geospatial Watershed Assessment Tool (USDA-ARS AGWA), Pacific Southwestern Inter Agency Committee (PSIAC) models, and the methods described below. Although PSIAC is an annual estimate tool, it is used to estimate 25-year post fire hydrology cross check. The runoff curve number (RCN) and derived hydrologic characteristics were calibrated using local stream gage networks, regression equations (USGS StreamStats), NOAA Atlas 14 rainfall distribution, and modified cumulative Karmic time of concentration methods.

Furthermore, specific papers and their methods will be analyzed and compared for modifications to Runoff Curve Number, changes to lag time, and other basin characteristics. Traditional methods and their extracted methods will also be taken into consideration to determine sediment yield and changes to peak discharges as presented below:

- Methodology as outlined in Cannon and Gartner paper "Wildfire-related debris flow from a hazard perspective" that is comparison of 1) peak discharge, area of basin burned, and lithology, and 2) peak discharge, area of basin burned, average basin gradient, and storm rainfall.
- Modifications to RCN pending reduction of cover and severity of burns, as outlined in Goodrich et al, (2000) "Rapid Post Fire Hydrologic Watershed Assessment using the AGWA GIS-based Hydrologic Modeling Tool".

- Changes in lag time related to relative increases in CN from McLin et al. (2001) "Predicting floodplain boundary changes following the Cerro Grande wildfire".
- Fire related debris flow volumes as estimated by Gartner et al. (2008) using the Western U.S. Regression model.

As part of this analysis, sediment supply will be estimated by accumulated area concerning measured width and depth of channel and potential estimate material available to determine future risk. The results will be compared to Giraud and Castleton (2009) "Estimation of potential Debris-flow volumes for Centerville Canyon, Davis County, Utah" and measured as cubic yards/yard of river reach.

Typically, the ratio of sands and colloidal to bedload is estimated at 10:1 or 3:1 ratios. Since the AGWA value was within reason for the total sediment and sands as a percentage (i.e. 10%), it is assumed to be comparable to total bedload in this case. Overall, AGWA is a reliable to tool for sedimentation / bulking values.

The upper watershed of the Dump Fire outlets onto an alluvial fan that slopes into a development where mud slurry, small boulders, cobbles and gravel were deposited during a storm event on (September 1, 2012) following the 2012 fire. Advanced GIS was used to assemble GIS data such as 5 meter auto correlated DEMs, National Land Cover Data Set (NLCD), and SSURGO data. The upper watershed has the potential to erode and transport large material due to high entrenchment and the steep gradient of the channel.

Concerning the severity of burn analyzed for the Dump fire, it was assumed that the entire watershed had a moderate burn.

Initial Sediment Predictions - pre fire conditions and range of post fire predictions

According to the United State Department of Agricultural Soil Conservation Service (SCS) (1973) study the range of sediment yield for the Saratoga watershed ranges between 0.1-0.2 acre-feet/square mile/year with a 60% sheet and rill erosion and 40% channel and gully erosion (see figure cs3-1, (SCS, 1973).

Figure CS3- 1. SCS 1973 annual sedimentation map with Saratoga watershed.

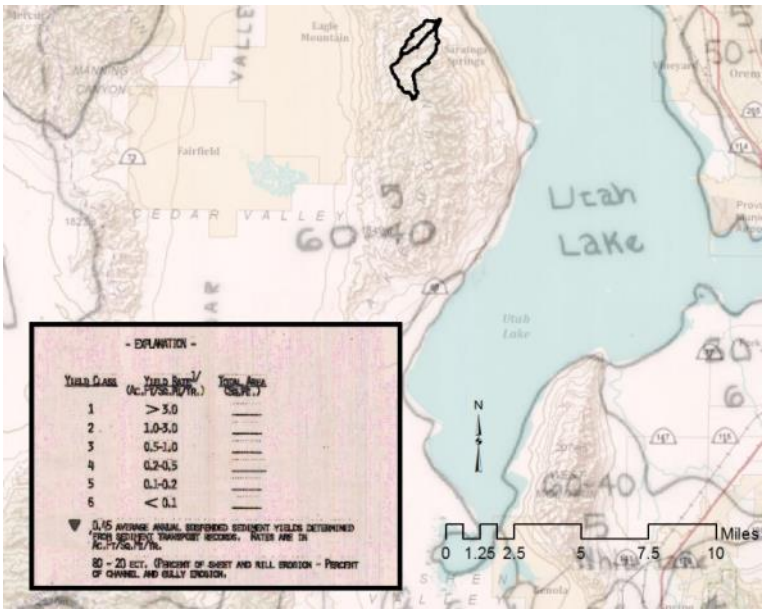

Below in figure cs3-2 is the range of erosion rates from the SCS (1973) study. First plotted is the acre-feet/square mile/year rate that correlates to the tons for 2.5 square miles, pre-burn condition. Second, the SCS (1973) reports shows 45% of the measures sites plotted on the map. This range of values assuming a 0.45 acre feet/square mile/year rate illustrated the total tons, a conservative pre-fire condition. Finally the 60-60-40 illustrates the total tons and including the 60% sheet / rill erosion, 60% other colloidal material surmised by the fire, and 40% channel and gully erosion, a post fire condition.

The sediment rates for the different scenarios this watershed are as follows: @ 0.2 acre-feet/square mile/year for 2.5 square miles →0.45 – 620 tons/year, total –1379 tons, and 60-60-40 – 2206 tons. These numbers will be taken into consideration later in the report.

Figure CS3- 2. Range of annual erosion rats from SCS 1973 study.

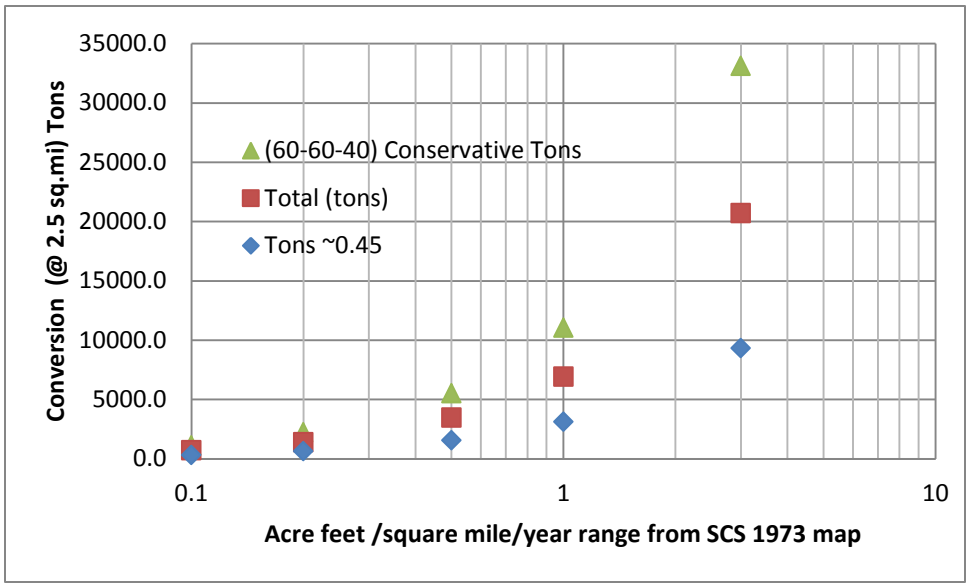

Whitewater-Baldy Fire New Mexico 2012

Stream Gage Analysis / range to Calibrate Ungaged Hydrology

A total of six stream gages were analyzed in the vicinity the study area, see figure CS3-3. The stream gage statistics were taken from the StreamStats report appendix (Kenny et. al, 2007) and a discharge / unit area conversion was applied to analysis cubic feet/second per square mile (csm) uniformly. The top 100-year csm is near 63 csm and the average 25 year csm is approximately 20 csm, see figure CS3-4.

The ungaged hydrology of the Saratoga Watershed (unnamed tributary and Israel Canyon) is described later in the report. Pre-fire time-on-concentration of 1 hour or average velocity of 5.99 fps and RCN of 65 gives a CSM at the 25 year of 28.28 and at the 100 year a CSM of 100.6. The 100-year csm of 100.6 is high and conservative. Pre-fire hydrology is estimated to be 70.7 cfs (25 year event) and 251.5 cfs (100 year event). NOAA Atlas 14 rainfall distribution was generated for the scenario and WinTR-20 was used to model this scenario. The 25-year csm and more so, the 100-year csm is both higher than the csm derived from the six stream gages. The RCN and T_c both seem to be appropriate, therefore numbers will not be changed.

Figure CS3- 3. Location of Stream Gages and study are for CSM analysis

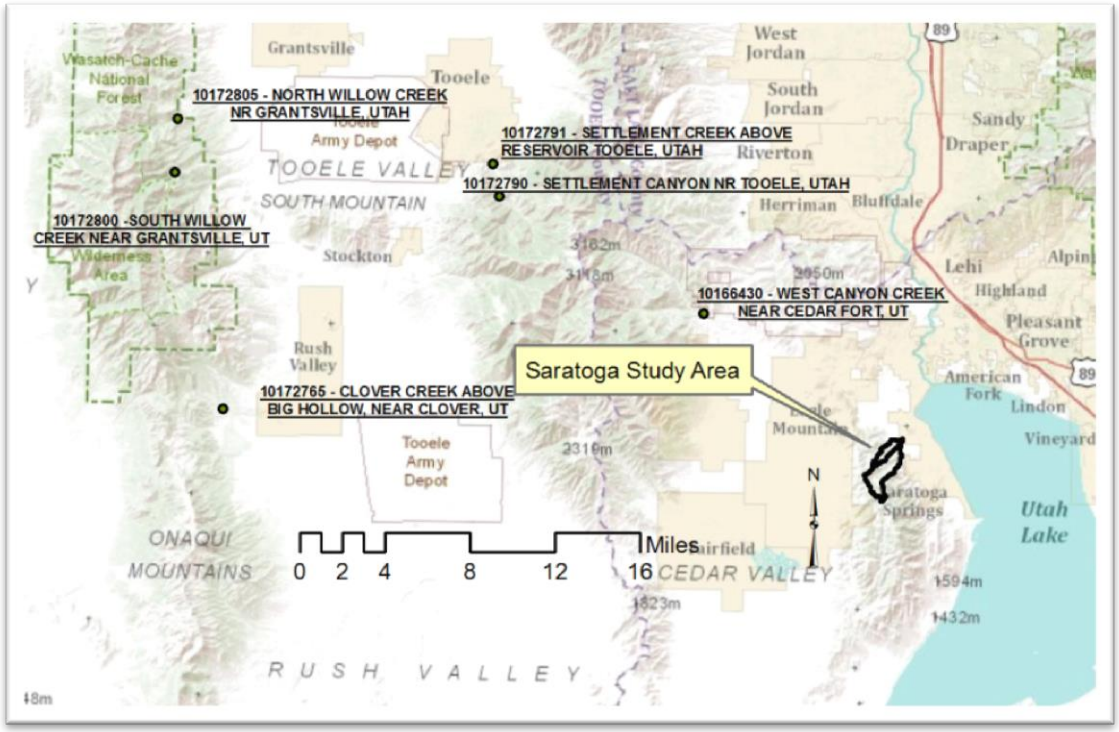

Figure CS3- 4. Stream Gage discharges converted to CSM

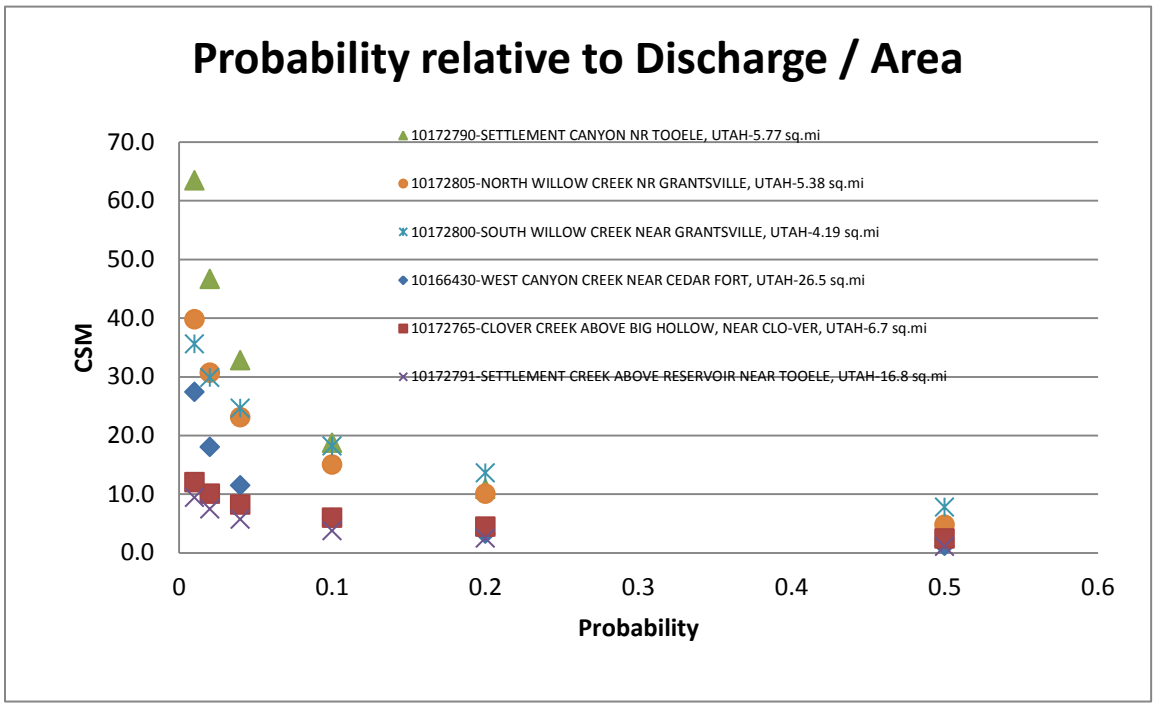

Runoff Curve Number Generation

Taken from the example, Goodrich et. al (2005), it is assumed that "there a 15% reduction in cover for low-severity burns, a 32% reduction for moderate-severity burns, and a 50% reduction for high-severity burns and a 32% reduction for moderate-severity burns (as is assumed in Disturbed WEPP - http://forest.moscowfsl.wsu.edu/cgi-bin/fswepp/wd/weppdist.pl)". This is reference in figure cs3-5.

Figure CS3- 5. Relationship between Cover and Curve Number for Each Hydrologic Soils Group

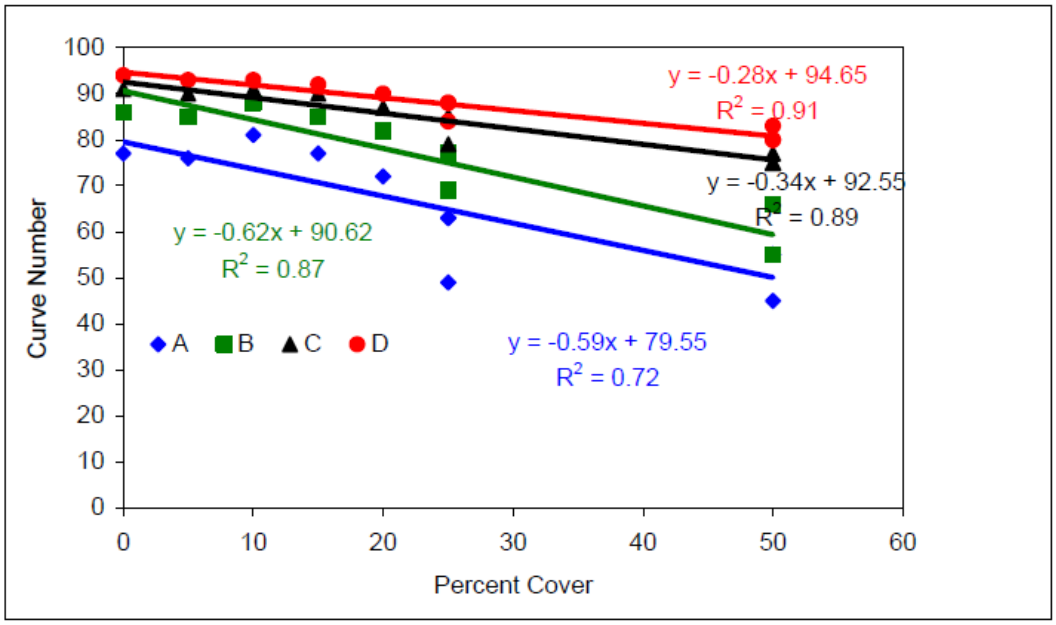

Located below in table CS3-6 is the difference between pre and post RCN Fire Condition with associated National Land Cover Data Set. These changes in runoff curve number were generated with the Relationship Between Cover and Curve Number for Each Hydrologic Soils Group - reduction to cover concept (Goodrich et. al, 2005).

Table CS3- 1. Difference of RCN from pre to post fire conditions with Associated NLCD

	CLASS	NAME	A	B	C	D
Low Severity Burn	41	Deciduous Forest	4	5	3	2
	42	Evergreen Forest		16	10	8
	43	Mixed Forest	4	5	3	2
	51	Shrubland	2	2	1	1
Moderate Severity Burn	41	Deciduous Forest	10	10	5	5
	42	Evergreen Forest		21	12	11
	43	Mixed Forest	10	10	5	5
	51	Shrubland	5	5	3	2
High Severity Burn	41	Deciduous Forest	15	16	8	7
	42	Evergreen Forest		27	15	13
	43	Mixed Forest	15	16	8	7
	51	Shrubland	10	11	6	3

Time of Concentration changes from Pre to Post Fire

As describe in McLin et. al (2001) the lag time decreases from the pre burn to post burn as a result of the runoff curve number increasing. This illustrated in the figure CS3-6 below.

Figure CS3- 6. Cerro Grande wildfire changes in CN and basin lag times.

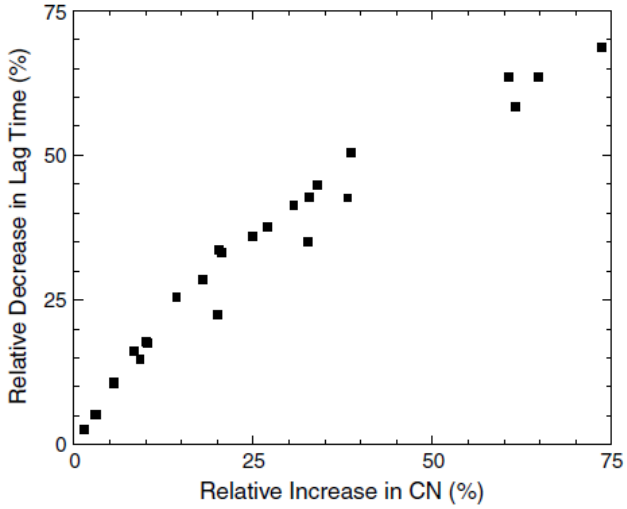

Relative change is defined as (pre-fire value – post-fire value)/(pre-fire value).

Note this is dependent on the available material and how often the watershed has burned. It is conceivable that channel blockages could result in long lag times. In this case since the watershed had mixed and deciduous forest and low-lying shrubs, it was assumed no channel blockages were present. Furthermore, it assumed that the roughness of the watershed had decreased as a result of fire. In this case, a rule of thumb for changes in velocities that result in changes of time of concentration are as follows: increase 0.5 fps for low severity burns, 1 fps for moderate severity burns, and 1.5 fps for high severity burns. This could be compared to both the Synders Lag equation (US-DOI-BOR, 2004) and Chapter 15 Time of Concentration (USDA NRCS, 2010), see figure 15-4. The Snyder's Lag (US-DOI-BOR, 2004) equation is as follows:

$$T_L = LL_{ca} / \sqrt{S} \qquad \text{(equation cs3-1)}$$

The Design of Small Dams 3rd edition changed to equation 2.

$$T_L = C * LL_{ca} / \sqrt{S} \qquad \text{(equation cs3-2)}$$

this was expanded to

$$T_L = 26 * K_n * LL_{ca} / \sqrt{S} \qquad \text{(equation cs3-3)}$$

K_n = C/26 – associated to Manning's roughness of entire drainage

L = Length (miles) of longest watercourse

L_{ca} = Length (miles) along the longest watercourse from the point of concentration

S = Overall slope (feet/miles) of longest watercourse

T_L = Lag Time (hours)

Figure CS3- 7. Velocity versus slope for shallow concentrated flow.

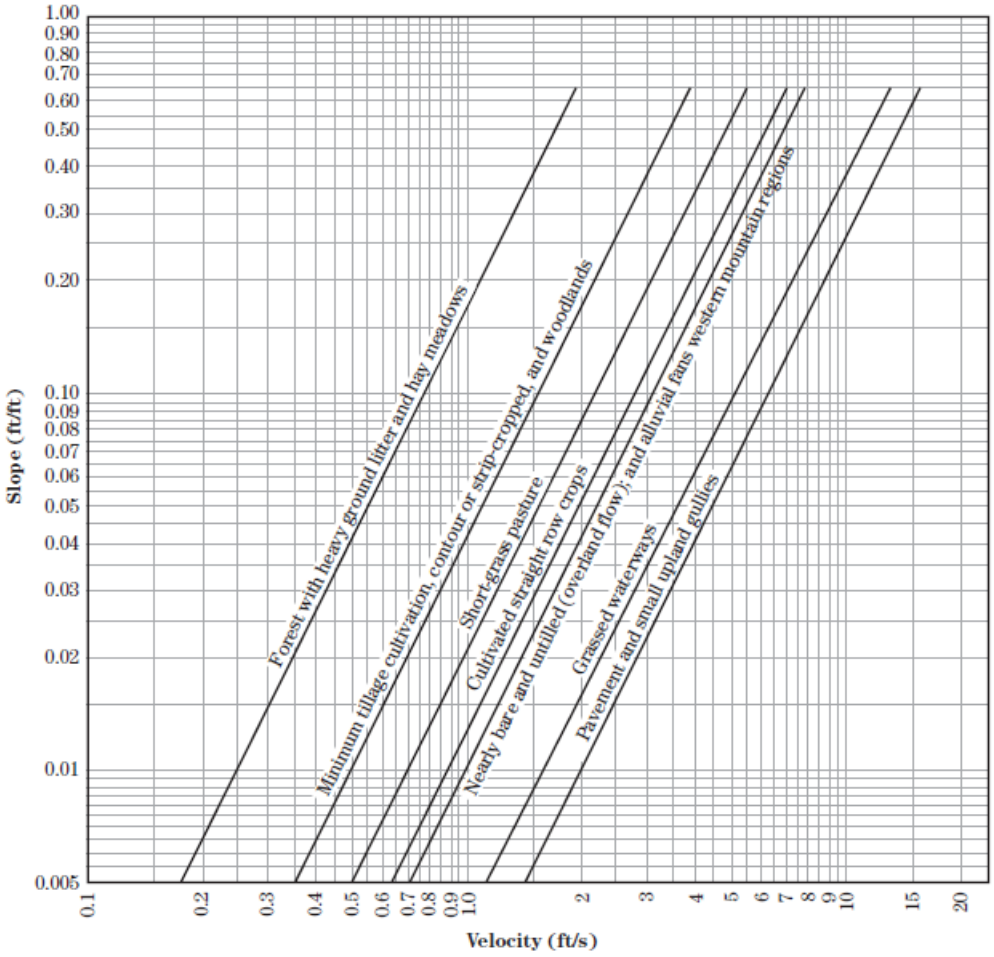

Precipitation

NOAA Atlas 14 Data was used to derive depth of precipitation and WinTR-20 is used to convert the NOAA Atlas 14 depths to rainfall distributions. Table CS3-2 has the NOAA Atlas rainfall depths.

Table CS3- 2. NOAA Atlas 14 Rainfall Depths (inches)

	1 year	2 year	5 year	10 year	25 year	50 year	100 year
24-hr	**1.09** (1.01-1.18)	**1.34** (1.24-1.45)	**1.61** (1.49-1.74)	**1.83** (1.69-1.97)	**2.12** (1.95-2.29)	**2.35** (2.15-2.53)	**2.57** (2.35-2.78

Pre and Post Fire discharges

Below in tables CS3-3 and CS3-4 are the WinTR-20 input data and output data for estimated peak flows for pre and post fire.

Table CS3- 3. WinTR-20 input data

Subbasin ID	Gage ID	Area (sq.mi)	Runoff CN	Time

```
SUB-AREA:
          Area65pre Outlet    Gage15    2.50      65.       1.00      YY
          Area75postOutlet    Gage15    2.50      75.       0.92      YY
          Isrl_pre  Outlet    Gage15    1.81      62.       0.92      YY
          Isrl_post Outlet    Gage15    1.81      74.       0.85      YY
          Btwn_pre  Outlet    Gage15    0.60      74.       0.40      YY
          Btwn_post Outlet    Gage15    0.60      80.       0.37      YY


STORM ANALYSIS:
          1_yr_stm  GAGE15              1.03     1_yr_tbl  2          1.26
          2_yr_stm  GAGE15              1.26     2_yr_tbl  2
          5_yr_stm  GAGE15              1.51     5_yr_tbl  2
          10_yr_stm GAGE15              1.72     10_yr_tbl 2
          25_yr_stm GAGE15              1.99     25_yr_tbl 2
          50_yr_stm GAGE15              2.20     50_yr_tbl 2
          100_yr_stmGAGE15              2.42     100_yr_tbl2
          200_yr_stmGAGE15              2.63     200_yr_tbl2
          500_yr_stmGAGE15              2.94     500_yr_tbl2
```

Table CS3- 4. WinTR-20 Output

Area or Reach Identifier	Drainage Area (sq. mi)	Peak Flow by Storm					
		2_yr_stm (cfs)	5_yr_stm (cfs)	10_yr_stm (cfs)	25_yr_stm (cfs)	50_yr_stm (cfs)	100_yr_st (cfs)
Area65pre	2.5	0	6	17.1	70.7	145.1	251.5
Area75post	2.5	26.1	91.7	179.4	341.8	515.6	727.8
Isrl_pre	1.81	0	0	0	25.1	64.9	127.1
Isrl_post	1.81	13.9	56.9	117.7	233.8	359	514.1
Btwn_pre	0.6	6.1	29.2	62.5	126.1	194.7	279.8
Btwn_post	0.6	38.6	92	149.4	247.5	346.8	465.5

The Israel watershed changed from 25 cfs pre-fire to 234 cfs post fire, an 831% difference for the 25-year event. And the 100-year changed from 127 cfs pre-fire to 514 cfs post fire, a 96% difference. The unnamed tributary changed from 126 cfs pre fire to 247 cfs post fire, a 96% difference for the 25 year event. And the 100 year changed from 280 cfs pre-fire to 465 cfs post-fire, a 66% difference. As illustrated in the below graph, figure 8, from McLin and Lane (2001) the change in peak discharge per unit area can have a percent difference as high a 60,000 % (i.e. 1 csm pre-fire to 600 csm post-fire, a 60,000% difference). The lower csm are currently low from the WinTR-20 results, but reasonable.

Figure CS3- 8. Comparison of observed and simulated pre-and post-fire peak discharges per unit drainage basin area. The La Mesa and Dome wildfires occurred south of the Cerro Grande wildfire in the years indicated.

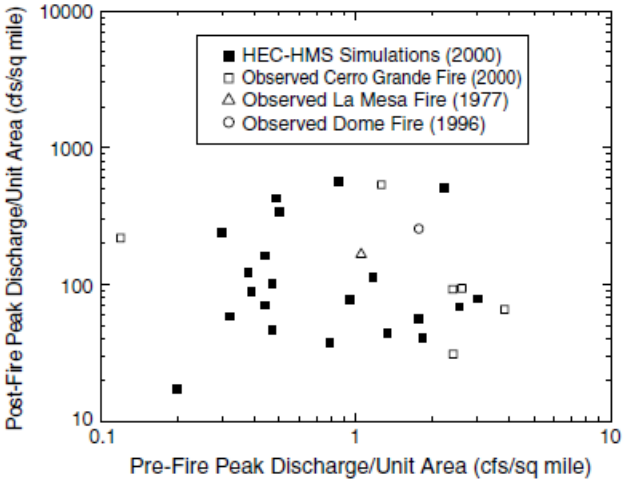

The Cannon and Gartner (2005) was also review. The slopes of the study are much steeper than the Saratoga watershed. This is shown in Figure 15.9 of the report and below as figure CS3-9.

Figure CS3- 9. Relations between basin area and average basin gradient relative to lithology of basins reported to have produced fire-related debris flows.

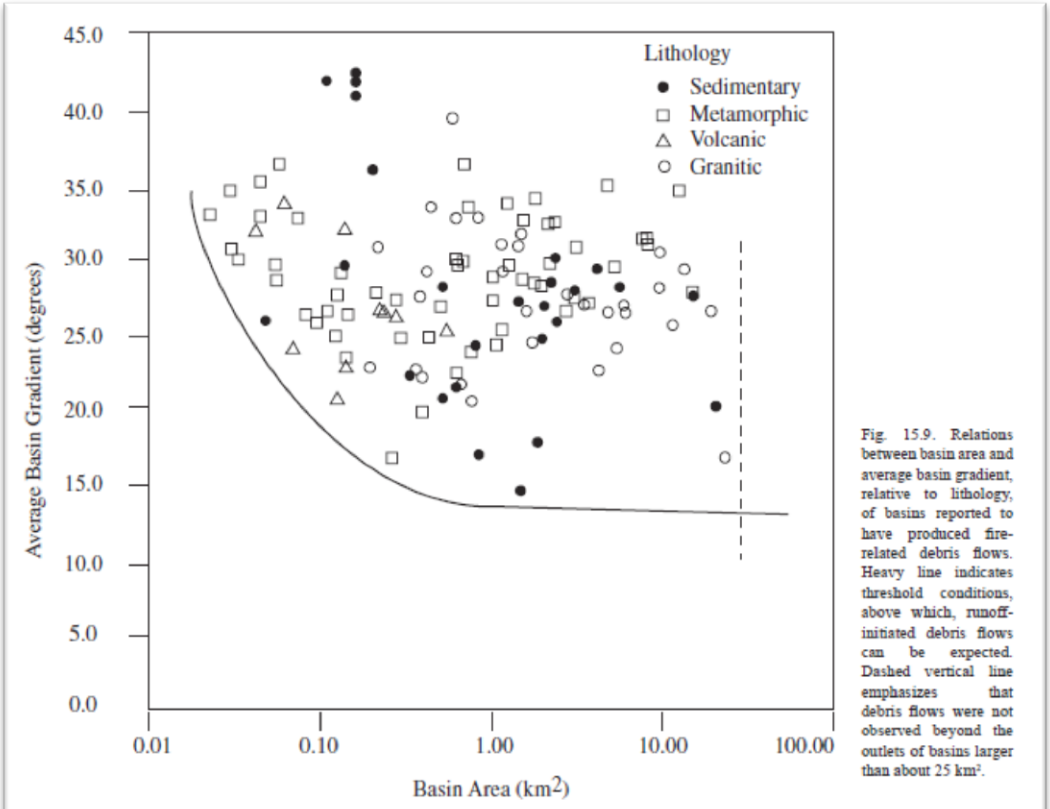

Fig. 15.9. Relations between basin area and average basin gradient, relative to lithology, of basins reported to have produced fire-related debris flows. Heavy line indicates threshold conditions, above which, runoff-initiated debris flows can be expected. Dashed vertical line emphasizes that debris flows were not observed beyond the outlets of basins larger than about 25 km².

[1] Dry ravel is the process of rapid, downhill movement of individual regolith and organic particles solely under the influence of gravity, and without the effect of water (Swanson, 1981). This process occurs in response to drying of the soil and combustion of soil-binding organisms and has been observed occurring both during and after the passage of the fire.

The equations were followed through as outlined in Cannon and Gartner (2005), figure 15.11 (shown below as figure cs3-10). Two of the three equations are listed in the figure. When applying the metamorphic lithology equation $Q_p=188A_b^{0.8}$ the discharge is estimated to be over 29,000 cfs. When applying the sedimentary lithology equation $Q_p=174A_b^{0.4}$ the discharge is estimated to be 1266 cfs, which is 74% difference from the WinTR-20 post-fire result. This calculated number should be substantially bigger since the Cannon and Gartner (2005) has steep slopes. Note the squared correlation coefficient is 0.42, which is reasonable plausible equation for this area. Below in figure cs3-11 is an image of Israel Canyon with geologic unit code with description.

Figure CS3- 10. Relation between peak debris-flow discharge estimates (Q_p) and area of basins burned at high and moderate severities ($A_{??}$), identified by lithology.

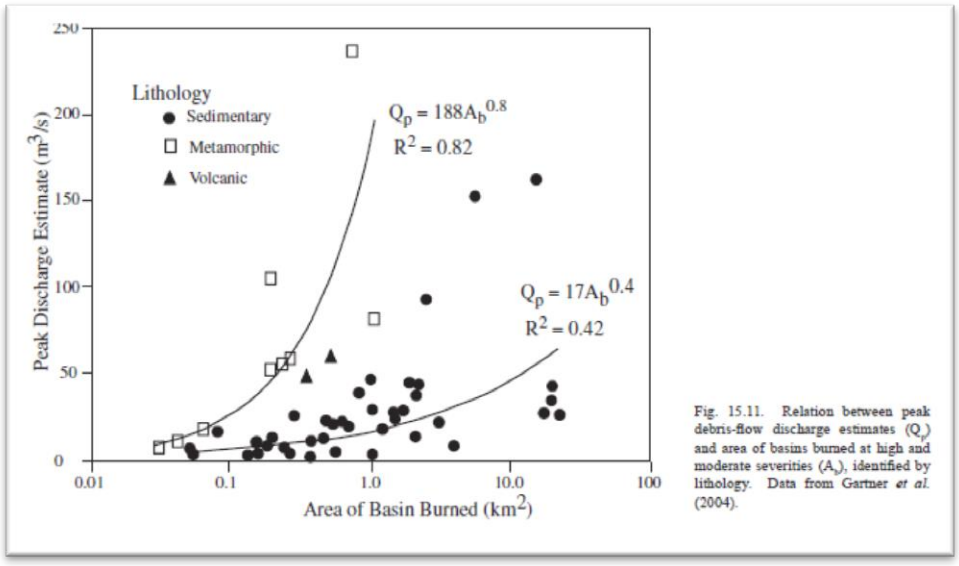

Fig. 15.11. Relation between peak debris-flow discharge estimates (Q_p) and area of basins burned at high and moderate severities (A_b), identified by lithology. Data from Gartner *et al.* (2004).

Figure CS3- 11. Map of Israel Canyon with geologic unit code with description

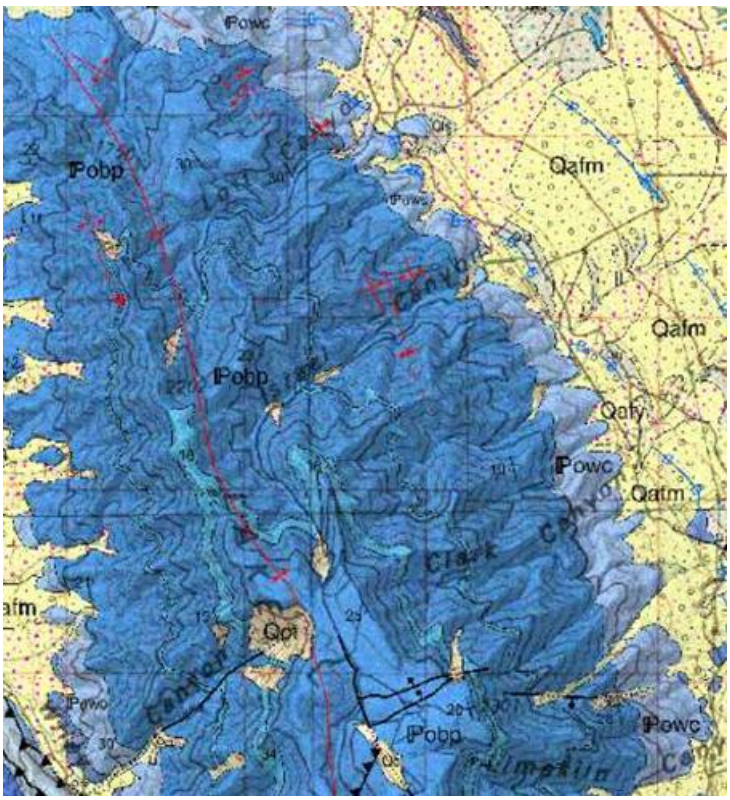

IPobp: Oquirrh Group, Butterfield Peaks Formation (Pennsylvanian, Desmoinesian-Atokan- Morrowan)

Interbedded, brown-weathering, fine-grained calcareous sandstone, medium-gray, fine-grained sandy limestone, minor orthoquartzite, and several limestone intervals (some mapped as IPobl); typically cyclically interbedded with several tens of feet of calcareous sandstone capped by gray limestone several feet thick; minor siltstone and shale interbeds form some poorly exposed slopes; unit typically forms ledgey to cliffy slopes; limestone intervals are locally fossiliferous with Chaetetes (coral) present in lower part of unit; fusulinid and conodont fossils provide some age control (Clark, 2009); queried on southwest end of South Mountain because extensive fracturing makes identification uncertain, though a single sample contained Atokan fusulinids; more than 4500 feet (1370 m) thick, top not exposed, in Lake Mountains (Biek, 2004) and more than 7300 feet (2200 m) thick, base not exposed, in West Mountain (Clark, 2009); complete thickness 9070 feet (2765 m) in Oquirrh Mountains (Tooker and Roberts, 1970); lithologically and near-age correlative with Bear Canyon Member of Oquirrh Formation. Limestone units (IPobl), locally mapped to show structural geology, commonly contain spherical or irregularly shaped, black chert; about 40 to 300 feet (12- 90 m) thick in Lake Mountains and West Mountain (see Biek, 2004; Biek and others, 2009; Clark, 2009).
http://geology.utah.gov/maps/geomap/interactive/viewer/index.html

Bulking and Sedimentation

The first estimated of the debris flow was taking a 20% bulking factor of the 25 year and 100 year events. The post fire peak Q for the 25-year event is 342 cfs and the 100-year event is 728 cfs, with runoff volumes for the 25-year event being 0.374 inches and the 100-year event being 0.603 inches. This gives an estimate 21,700 tons of material for the 25-year event and 35,022 tons of material for the 100-year event. This was derived from taking 20% of the runoff volume and converting this volume to tons of material.

In hopes of taking the SCS 1973 annual average acre-feet/square mile/year an applying a correlation to post fire sediment rates, it was hypothesis that an episodic storm might correlated to an annual rate. This was not the case. But to put the 21,700 and 35,000 tons of material mentioned above into range the acre-feet/square mile/year would need to change from 0.1-0.2 to 3 acre feet/square mile/year. This is taking the idea 60% sheet / rill erosion, 60% other colloidal material surmised by the fire, and 40% channel and gully erosion, a post fire condition, 60-60-40. These numbers are still a reasonable estimate.

Figure CS3- 12. Western U.S. regression Equation and Variables

$$\ln V = 0.59(\ln S) + 0.65(B)^{1/2} + 0.18(R)^{1/2} + 7.21$$

where:

V = volume (cubic meters),

S = basin area with slopes greater than or equal to 30% (square kilometers),

B = basin area burned at moderate and high severity (square kilometers), and

R = total storm rainfall (millimeters).

Third, the empirical Western U.S. regression model to estimate fire-related debris-flow volumes (Gartner et.al, 2008) is estimated to be between 34550 – 51182 tons for the 2-100 year rainfall events. This numbers are high since the model assumes that watersheds moderate to high severity burns. The Western U.S. regression model to estimated fire-related debris-flow volumes (Gartner et.al, 2008) was taken from Giraud and Castleton (2009) investigation.

Finally, the Automated Geospatial Watershed Assessment tool (AGWA) was used to determine sediment rates. More information about AGWA is located in Appendix C. Although the program gave peak discharges, these values were not used. The runoff curve numbers from above were used in the model. The model uses hydrologic geomorphic relations for channel routing. The results are located in Appendix A. Also the map generate in AGWA is located in Appendix A. The sediment for the 25-year storm is estimated to be 10,303 tons and the 100-year storm is estimated to be 27,897 tons.

To recap, table CS3-5 puts all sediment methods calculations into on table.

Table CS3- 5. Post fire Sediment Methods

Method	25 year	100 year
20% volume converted to tons	21,700 tons	35,022 tons
SCS 1973 Study	12,410 tons*	33094 tons**
Western U.S. regression (Gartner et. al, 2008)	44,875 tons	51,182 tons
AGWA	10,303 tons	27,897 tons

**total assuming 1973 study results are 0.45 (3 acre-feet/square mile/year*

***60-60-40*

References:

Cannon, S.H., and Gartner, J.E., 2005, Wildfire-related de-bris flow from a hazards perspective, in Jakob, M., and Hungr, O., Debris-flows hazards and related phenomena: Chichester, United Kingdom, Springer-Praxis Books, p. 362–385.

Gartner, J.E., Cannon, S.H., Santi, P.M., and deWolfe, V.G., 2008. Empirical models to predict the volumes of debris flows generated by recently burned basins in the western U.S.: Geomorphology, v. 96, p. 339-354.

Giraud, R.E., and Castleton, J.J., 2009. Estimation of Potential Debris-Flow volumes for Centerville Canyon, Davis County, Utah. Report of Investigation 267 Utah Geological Survey, A division of Utah Department of Natural Resources, Salt Lake City, Utah.

Goodrich, D.C., H. E. Canfield, I.S. Burns, D.J. Semmens, S.N. Miller, M. Hernandez, L.R. Levick, D.P. Guertin, and W.G. Kepner. 2005. Rapid Post-Fire Hydrologic Watershed Assessment using the AGWA GISbased Hydrologic Modeling Tool. Proc. ASCE Watershed Manage. Conf., July 19-22, Williamsburg, VA.*

Kenney, T.A., Wilkowske, C.D., and Wright, S.J., 2007, Methods for estimating magnitude and frequency of peak flows for natural streams in Utah: U.S. Geological Survey Scientific Investigations Report 2007-5158, 28 p.

McLin, S. G., Springer, E. P., and Lane, L. J. (2001). "Predicting Floodplain Boundary Changes Following the Cerro Grande Wildfire." Hydrological Proc., 15(15): 2967-2980.

USDA Natural Resource Conservation Service (USDA NRCS), 2010. National Engineering Handbook - Part 630, Hydrology, Chapter 15, Time of Concentration. ftp://ftp.wcc.nrcs.usda.gov/wntsc/H&H/NEHhydrology/ch15.pdf

United States Department of Interior Bureau of Reclamation (US-DOI-BOR) 1987 3rd Edition (Reprint, 2004). Design of Small Dams. A Water Resources Technical Publication.

Appendix A -- AGWA Results

Figure CS3- 13. (Needs a caption)

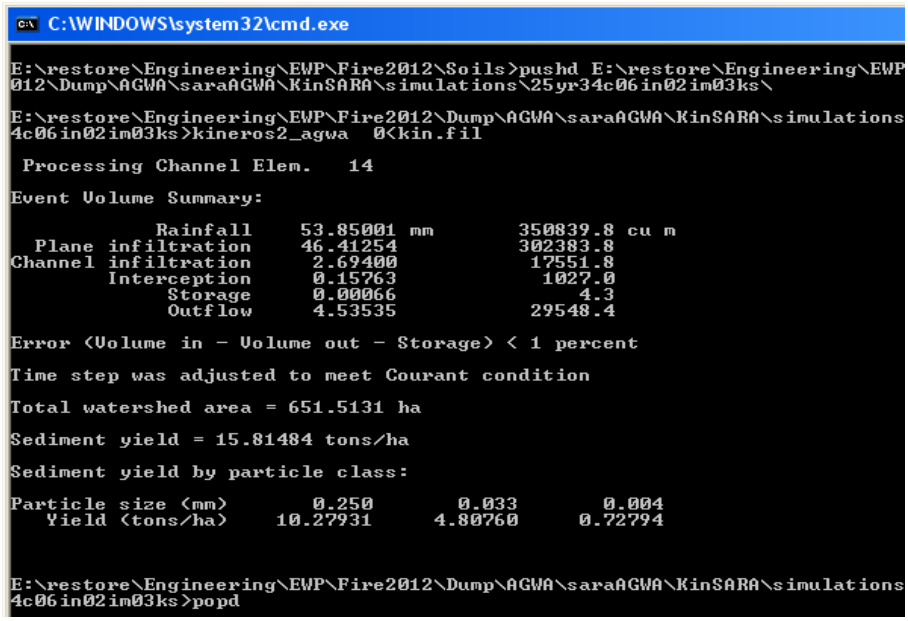

100% of sediment yield and particles was assumed to be correlated to bedload. Note the low runoff.

Figure CS3- 14, (Needs a caption)

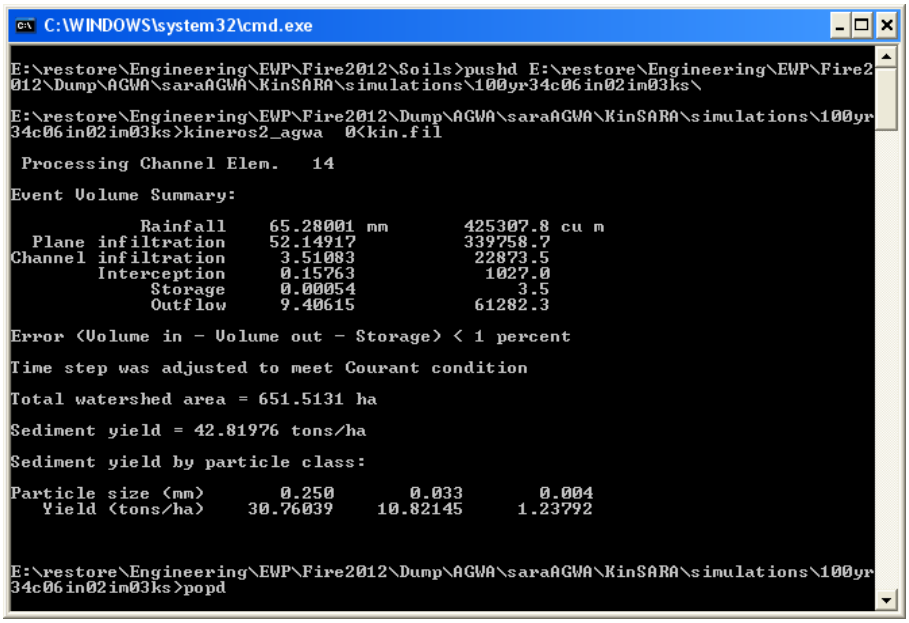

Figure CS3- 15. (Needs a caption).

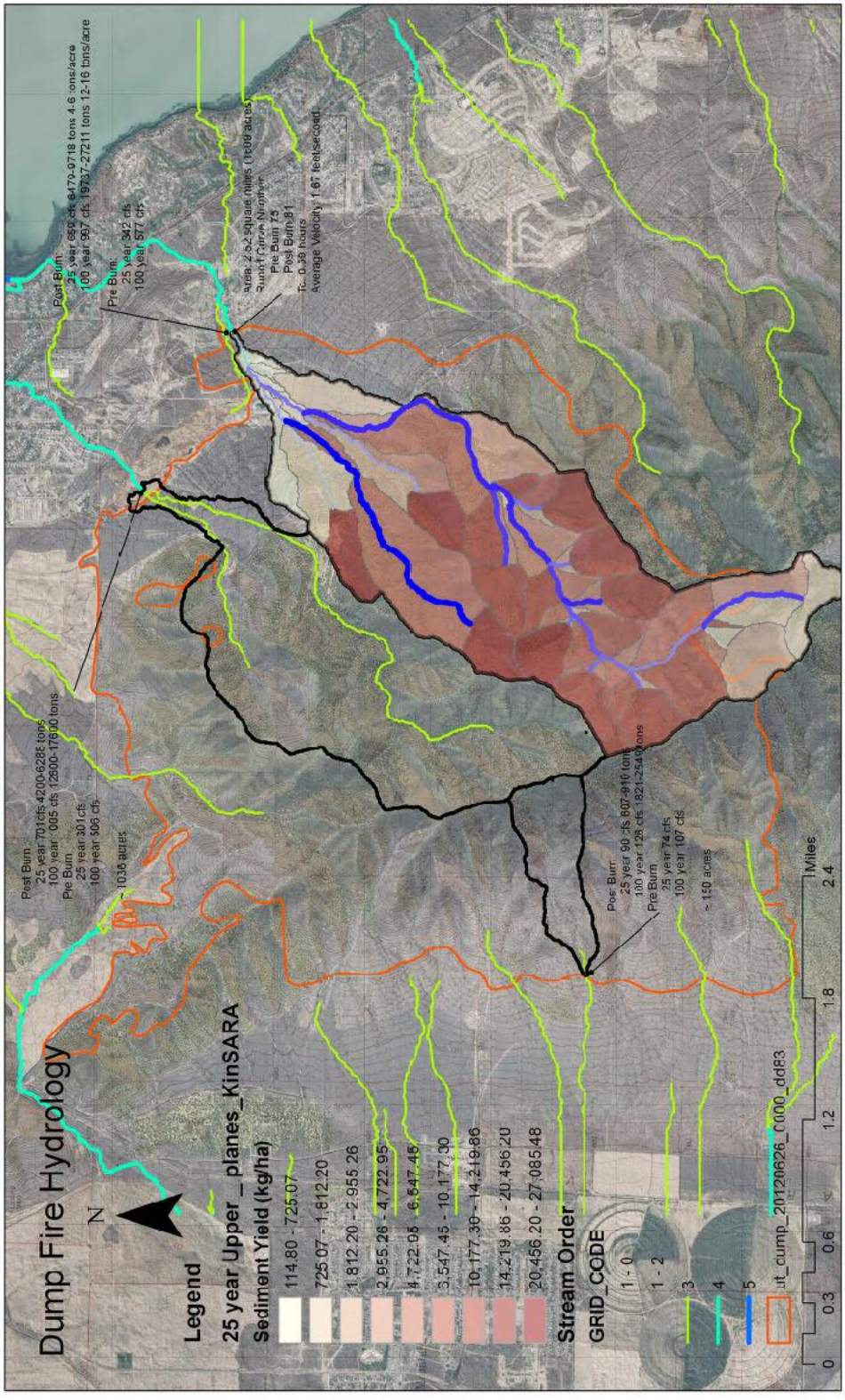
Dump Fire Hydrology
N
Legend
25 year Upper__planes_KinSARA
Sediment Yield (kg/ha)
114.80 - 725.07
725.07 - 1,812.20
1,812.20 - 2,955.26
2,955.26 - 4,722.95
4,722.95 - 6,547.45
6,547.45 - 10,177.30
10,177.30 - 14,219.86
14,219.86 - 20,456.20
20,456.20 - 27,085.48
Stream Order
GRID_CODE
1 - 0
1 - 2
3
4
5
ut_dump_20120626_1000_dd83
0
0.3
0.6
1.2
1.8
2.4
Miles
Post Burn
25 year 701cfs 4200-6285 tons
100 year 005 cfs 12600-17600 tons
Pre Burn
25 year 301cfs
100 year 506 cfs
~1036 acres
Post Burn
25 year 650 cfs 6479-9718 tons 4-6 tons/acre
100 year 997 cfs 19737-27211 tons 12-16 tons/acre
Pre Burn
25 year 342 cfs
100 year 577 cfs
Pre Burn 75
Post Burn 91
Average Velocity 1.67 feet/second
Post Burn
25 year 90 cfs 807-810 tons
100 year 126 cfs 1821-2540 tons
Pre Burn
25 year 74 cfs
100 year 107 cfs
~150 acres

2847

Appendix B – Hydrologic Characteristics, results

Figure CS3- 16. (Needs a caption)

Appendix C -- About AGWA

http://www.tucson.ars.ag.gov/agwa/index.php?option=com_content&view=article&id=5&Itemid=26

Background Planning and assessment in land and water resource management are evolving from simple, local-scale problems toward complex, spatially explicit regional ones. Such problems have to be addressed with distributed models that can compute runoff and erosion at different spatial and temporal scales. The extensive data requirements and the difficult task of building input parameter files, however, have long represented an obstacle to the timely and cost-effective use of such complex models by resource managers.

The USDA-ARS Southwest Watershed Research Center, in cooperation with the U.S. EPA Office of Research and Development Landscape Ecology Branch, has developed a GIS tool to facilitate this process. A geographic information system (GIS) provides the framework within which spatially-distributed data are collected and used to prepare model input files and evaluate model results.

Figure CS3- 17. (Needs title – reference in text?)

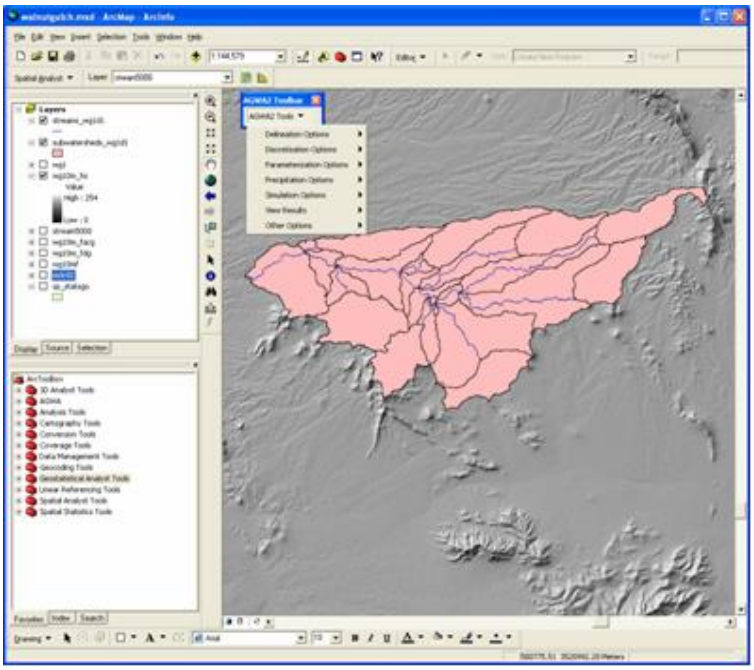

AGWA uses widely available standardized spatial datasets that can be obtained via internet. The data used to develop input parameter files for two watershed runoff and erosion models: KINEROS2 and SWAT.

KINEROS2

The Kinematic Runoff and Erosion Model is an event oriented, physically-based model developed at the USDA-ARS to describe the processes of interception, infiltration, surface runoff and erosion from small (less than about 100 km^2) watersheds. The watershed is represented by a cascade of planes and channels, thereby allowing rainfall, infiltration, runoff, and erosion parameters to vary spatially. KINEROS2 may be used to determine the effects of various artificial features such as urban developments, small detention reservoirs, or lined channels on flood hydrographs and sediment yield. For more information on KINEROS2, please visit www.tucson.ars.ag.gov/kineros.

SWAT

The Soil and Water Assessment Tool is a quasi-distributed model developed at the USDA-ARS to predict the impact of land management practices on water, sediment and agricultural chemical yields in large (basin scale) complex watersheds with varying soils, land use and management conditions over long periods of time (> 1 year). SWAT is a continuous-time model, i.e. a long-term yield model, using daily average input values, and is not designed to simulate detailed, single-event flood routing. For more information on SWAT, please visit www.brc.tamus.edu/swat.

Table CS3- 6. Output Variables Available in AGWA

KINEROS	SWAT
Infiltration (mm; m^3/km)	Channel Discharge (m^3/day)
Infiltration (in; ac-ft/mi)	ET (mm)
Runoff (mm)	Percolation (mm)
Runoff (m3)	Surface runoff (mm)
Sediment yield (kg/ha)	Transmission loss (mm)
Peak flow (m^3/s)	Water yield (mm)
Peak flow (mm/hr)	Sediment yield (t/ha)
Sediment discharge (kg/s)	Precipitation (mm)

AGWA Description and Uses

Using digital data in combination with the automated functionality of AGWA greatly reduces the time required to use these two watershed models. Through a robust and intuitive interface the user selects an outlet from which AGWA delineates and discretizes the watershed using the DEM. The watershed elements are then intersected with soil, land cover, and precipitation (uniform or distributed) data layers to derive the requisite model input parameters. The model is then run, and the results are imported back into AGWA for visual display.

Model results that can be displayed in AGWA are shown in the table to the right. This option allows managers to identify problem areas where management activities can be focused, or to anticipate sensitive areas in association with planning efforts.

AGWA is designed to evaluate relative change and can only provide qualitative estimates of runoff and erosion. It cannot provide reliable quantitative estimates of runoff and erosion without careful calibration. It is also subject to the assumptions and limitations of its component models, and should always be applied with these in mind.

Availability

AGWA is publicly available for download in two different versions: AGWA 2.0 for ArcGIS and AGWA 1.5 for ArcView. Additionally, DotAGWA, an internet version sharing the AGWA 2.0 codebase, is under development.

AGWA 2.0 requires ArcGIS 9.x, Spatial Analyst 9.x, and the .Net Framework. AGWA 1.5 requires ArcView 3.1 or later and version 1.1 of the Spatial Analyst extension.

KINEROS Parameters

Int: interception depth (mm)

Cover: fraction of surface covered by intercepting cover – the rainfall intensity is reduced by this fraction until the specified interception depth has been accumulated (0-1)

Mann_n: Manning roughness coefficient (0-1)

Pave: fraction of surface covered by erosion pavement (0-1)

Splash: Rainsplash coefficient (0-1)

Rock: Volumetric rock fraction, if any. If Ksat is estimated based on textural class, it should be multiplied by (1- rock) to reflect this rock volume.

Ks: Saturated hydraulic conductivity (mm/hr)

G: mean capillary drive – a zero value sets the infiltration at a constant value of Ks (mm)

Por: porosity (cm3/cm3)

Smax: maximum relative saturation (0-1)

Cv: coefficient of variation of Ks

Fract_sand: fractional sand content (0-1)

Fract_silt: fractional silt content (0-1)

Fract_clay: fractional clay content (0-1)

Dist: pore size distribution index. Used for redistribution of soil moisture during unponded intervals

Coh: Soil cohesion coefficients

Ks_final: area-weighted Ks value

Pct_imperv: percent of watershed covered by impervious materials

SWAT Parameters

CN: area-weighted curve number based on soil type and land cover

Cover: fraction of surface covered by intercepting cover – rainfall intensity is reduced by this fraction until the specified interception depth has been accumulated (0-1)

HydValue: weighted hydrologic group value used to determine curve number

Ks: saturated hydraulic conductivity (mm/hr)

Soil_id: value of the soil ID field (MUID, MUKEY or SNUM) of the dominant soil type

Appendix D -- Pertinent picture of Saratoga Fire/Flooding/Damages

Figure CS3- 18. (Needs caption)

http://www.youtube.com/watch?v=mAZZP12nWc8

Overtopping reservoir Debris Flow

http://www.youtube.com/watch?v=6bylJ-B6DxA

Figure CS3- 19. House foreground

http://www.youtube.com/watch?v=0QUpTkA_THg

Figure CS3- 20. Bypass reservoir near houses

http://www.youtube.com/watch?v=M7JnV0dcxB0

Figure CS3- 21. Side channel north of main tributary – debris flow through streets

http://www.youtube.com/watch?v=tfykDiNd7z0

Figure CS3- 22. Flood flow through main conveyance area --

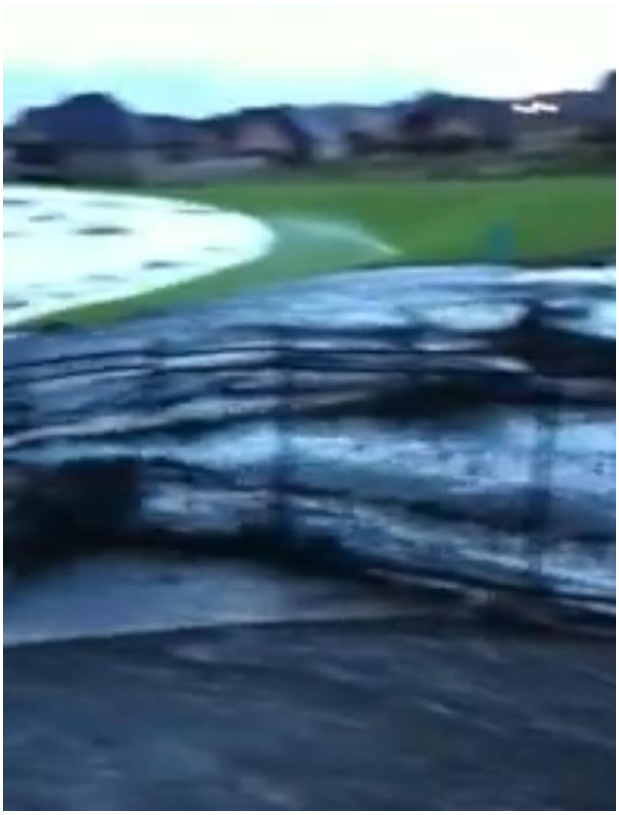

http://www.youtube.com/watch?v=ypnNFZqwF8o

AFTERMATH

Figure CS3- 23. Downstream of reservoir that was plugged and diverted flows. Size of material deposited downstream

http://www.youtube.com/watch?v=dMhaP0avRbc

Figure CS3- 24. Dredging basements –

http://www.youtube.com/watch?v=tHy2EnJSd1s&feature=endscreen&NR=1

2990

2991 (This page intentionally blank)

Case Study 4: Whitewater Creek, Gila Wilderness New Mexico

Background

Lightning sparked a wildfire in early May 2012 that became the largest in New Mexico recorded history. This first strike, in the rugged Gila Wilderness, was named the Baldy Fire, and lack of access hampered containment efforts. In mid-May, a second lightning-initiated fire started several miles to the west. In the Whitewater Creek basin, also part of the rugged Gila Wilderness, this wildfire was extremely hazardous to fire-fighting crews. By the end of May, the two fires joined to become the Whitewater-Baldy Complex.

The rugged landscape was not the only reason this fire got out of hand. The watershed had already been experiencing extreme drought conditions, with the two previous winters recording very low snowfall. At the time of the outbreak, air temperatures were well above average and high winds contributed to the merging of the two fires. By early June, the Whitewater-Baldy Complex was only about 18 percent contained; by mid-June 56% contained. It burned all through that month, at relatively low burn temperatures and mostly in Ponderosa, Piñon/Juniper, and mixed conifer forests. Mid-July rainfall finally helped the fire fighters gain momentum. In late July, at 95% confinement, the wildfire had burned about 465 square miles.

Figure CS4- 1. Location of concern: State of New Mexico with county boundaries, USFS Gila National Forest in green, Gila Wilderness area in yellow.

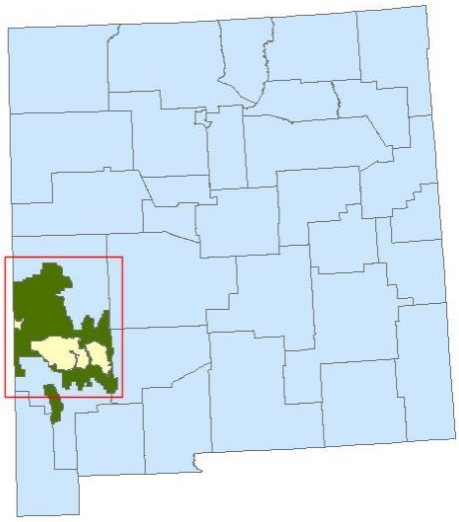

Inset shown in Figure 2.

Figure CS4- 2. Inset from Figure 1. Location of concern, with Whitewater-Baldy Complex Fire location in red.

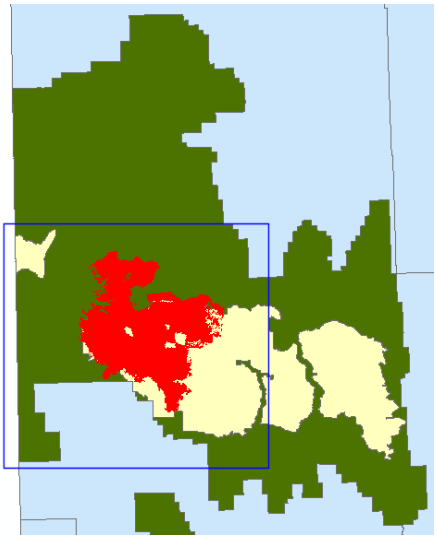

Blue inset shown in Figure 3.

Figure CS4- 3. Location of concern, showing fire location in red, nearby communities and highways.

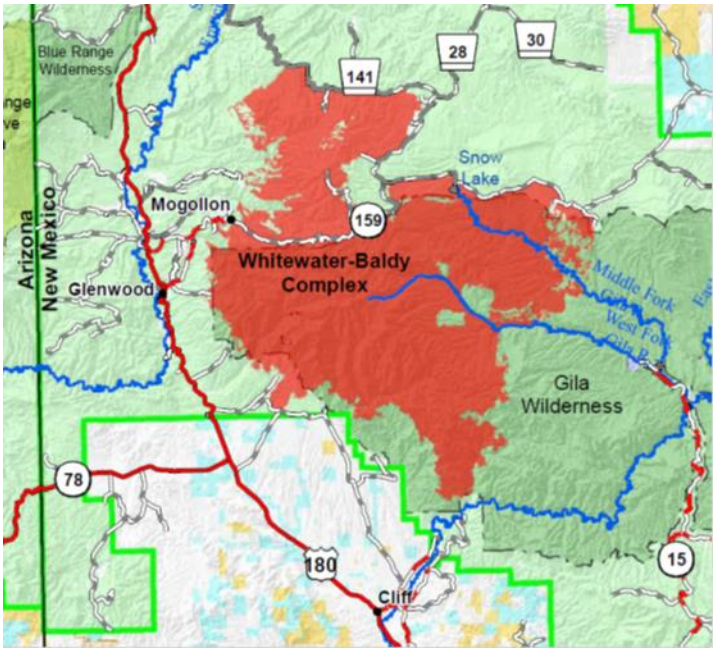

Inset from Figure 2. (Map provided by USFS Gila National Forest.)

The Forest Service estimated the final burn severity for the area within the fire perimeter to be 14% high, 12% moderate, 55% low or unburned, and 20% unknown (due to inadequate satellite imagery).

This case study is a hydrologic analysis of the flood potential of Whitewater Creek and possible hazard to the community of Glenwood NM. As shown in figure CS4-4, Glenwood is at the mouth of Whitewater Creek as it enters the San Francisco River. The percent of the watershed burned was 34% high severity, 21% medium severity, and 13% low severity.

Figure CS4- 4. Whitewater Creek watershed and the community of Glenwood NM.

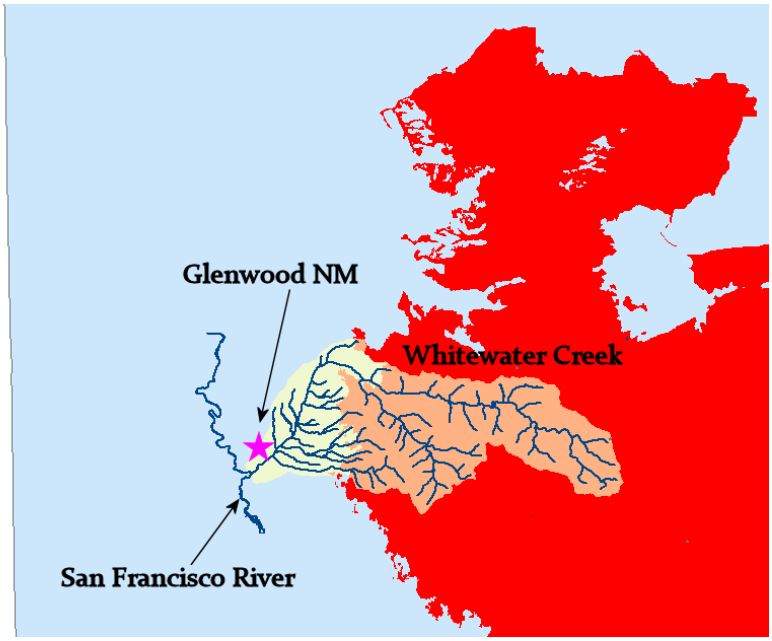

NRCS Involvement

The NRCS Emergency Watershed Protection program (EWP) was implemented for the installation of monitoring gages in the Whitewater-Baldy Complex burn area, to provide early warning to downstream communities of flood potential. The intensity of the wildfire and its large area prompted the USDA Forest Service, in cooperation with the United States Geological Survey (USGS), to seek EWP funding from NRCS. The New Mexico State office of NRCS worked with the New Mexico Department of Homeland Security & Emergency Management, which acted as the EWP local sponsor. USGS installed a streamflow gage on Whitewater Creek, near the Catwalk Recreational Area. (See figure CS4-5.) That station also received a precipitation gage. Additional gages in the area are shown in Figure CS4-5.

NRCS also performed a hydrologic analysis to assess flood potential for the community of Glenwood. In recent years, New Mexico residents had witnessed flash flooding after wildfire. The watersheds of the 2011 Las Conchas fire near Los Alamos experienced monsoon rains within weeks of the end of the fire, which sent rapidly downstream not only water but significant sediment and debris. That wildfire burned 245 square miles and held the record for the largest in

recorded New Mexico history, until eclipsed by the Whitewater-Baldy wildfire (almost twice as large!).

Figure CS4- 5. Gages in the vicinity of Whitewater Creek.

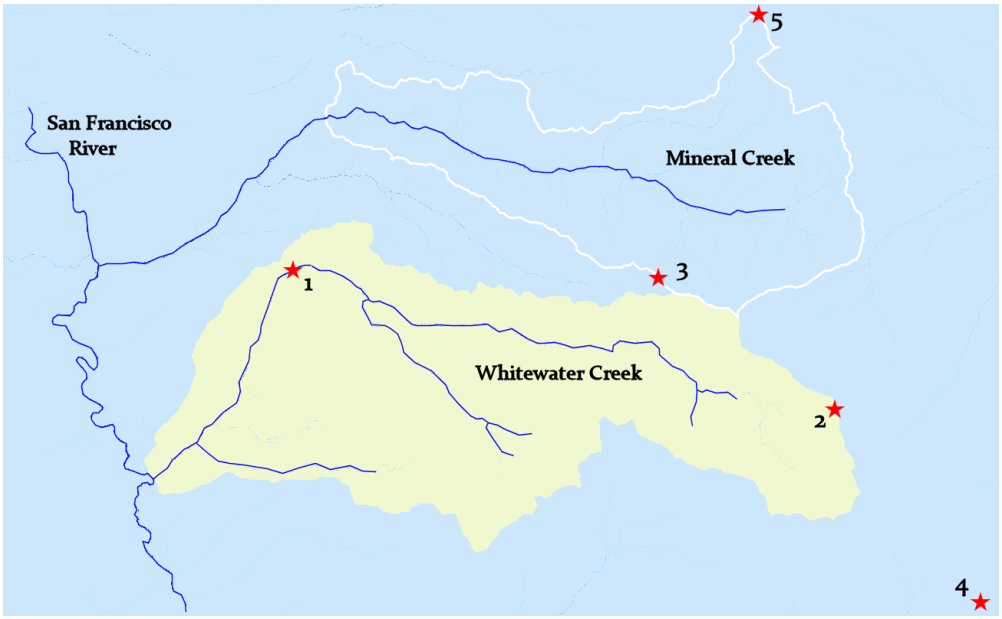

1 = Catwalk streamflow and precipitation (activated 4 July 2012 by USGS)
2 = Hummingbird Saddle precipitation (activated 29 June 2012 by USGS)
3 = Silver Creek Divide SNOTEL site (activated 1 Oct 1978 by NRCS)
4 = Mogollon Baldy Lookout precipitation (activated 28 June 2012 by USGS)
5 = Bear Wallow Lookout precipitation (activated 29 June 2012 by USGS)

The USDA Forest Service, through the BAER team process, also provided hydrologic assessments. In addition, the USGS held a workshop in early July 2012 for Glenwood residents to learn how to access the early warning data from the new gages. The data are on the web at: http://nm.water.usgs.gov/wildfire/.

The NRCS hydrologic modeling effort documented in this case study examined pre-fire floods, and post-fire floods both immediately after the fire and one year later. The latter modeling was able to make use of the precipitation and streamflow data from the new gages.

Figure CS4- 6. Burned trees along the trail to Hummingbird Saddle, Gila National Forest, where USGS scientists installed a rain gage.

Photo by Mike Sanders, USGS.

Methods and Application

As an alternative to the often used Curve Number (CN) runoff method, this case study modeled infiltration of rainfall by a process-based method called Green & Ampt, The CN method is not directly comparable to the Green & Ampt infiltration method, in that CN runoff equation comprises much more than infiltration.

A separate issue from infiltration loss is the method by which runoff is transformed into a hydrograph. The CN method employs a triangular unit hydrograph estimate, derived from subarea time of concentration and a peak rate factor. The alternative used in this case study was to derive an estimated unit hydrograph from a time-area histogram of each subarea using GIS. The complete documentation of modeling choices used in this case study is given in the sections below, following the summary of selected options:

- choice of hydrologic computer model: HEC-HMS
- unit hydrograph estimation: using time-area histograms and GIS analysis
- infiltration loss method: Green & Ampt equation

- initial abstraction, ponding: estimates of loss due to vegetation canopy, surface detention
- baseflow: pre-flood estimates based on subarea size, post-flood estimates based on non-linear recession curve.
- rainfall events examined: 2-year, 25-year, and 100-year, under three scenarios: pre-fire, post-fire immediately, and post-fire one year later.
- sediment bulking

Choice of Hydrologic Computer Model: HEC-HMS

The model HEC-HMS from the US Army Corps of Engineers Hydrologic Engineering Center (USCOE 2013) features many options for estimating flood hydrographs. One may use the NRCS curve number method to estimate losses, or one of a couple of process-based infiltration methods based on a simplification of the Richard's equation for unsteady water flow in soil. For transformation of excess rainfall into a hydrograph, one may use the SCS triangular unit hydrograph estimate, one of several other synthetic unit hydrograph options, or a user-derived unit hydrograph. The latter may be obtained by instrumentation of an actual watershed, or may be estimated using a time-area histogram. The HEC-HMS model also enables accounting for vegetation canopy and surface losses, as well as methods for estimating baseflow.

The main body of this technical note discusses a number of limitations of the curve number methodology for forested mountain watersheds. Curve numbers are difficult to estimate for post-fire conditions, especially when hydrophobic soil may allow more infiltration at higher rainfall rates than at lower ones. The SCS default peak rate factor is likely too low for steep mountain watersheds in the unburned condition and even further too low for a burned condition. Therefore, other options are worth exploring.

This case study used HEC-HMS. The hydrograph transform method was user-derived unit hydrographs from GIS. The loss method was Green & Ampt. The canopy and surface loss options and the baseflow options are discussed below.

Time-Area Histogram and Unit Hydrograph Estimation

As discussed in the main body of the technical note, a time-area histogram is a way to estimate a subarea unit hydrograph. The Whitewater Creek watershed was subdivided into several subareas, as shown in Figure CS4-7. The figure has an inset in red of the subarea "Baldy Fork". This subarea will be used in the discussion below to demonstrate the GIS operations applicable to any of the subareas.

Figure CS4- 7. Whitewater Creek hydrologic subareas.

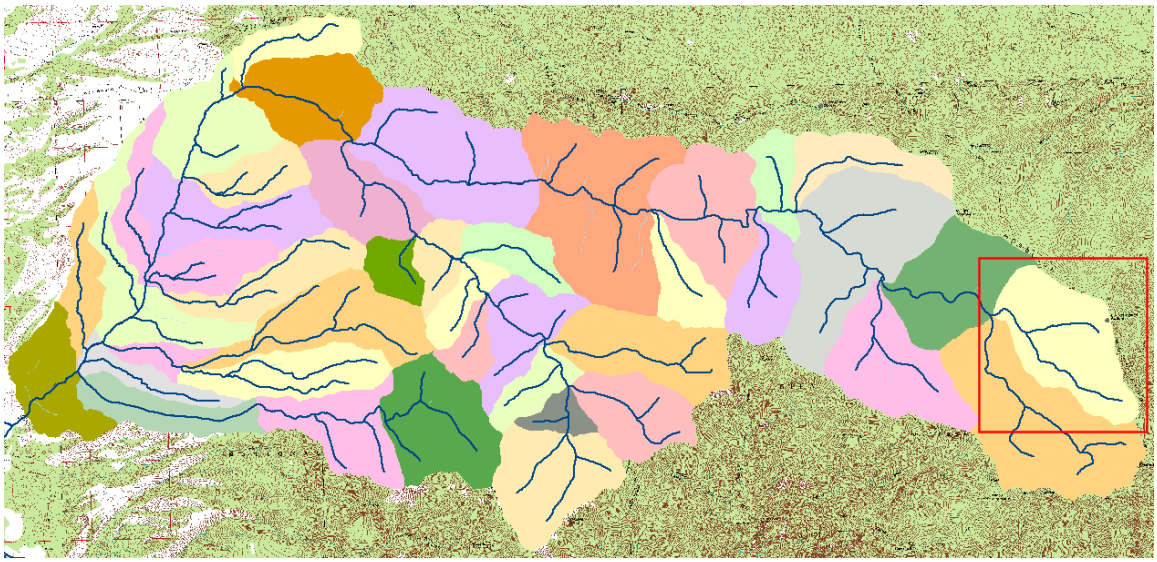

(Red inset shown in Figure CS4-8.)

Figure CS4- 8. Upper Whitewater subarea (called Baldy Fork)

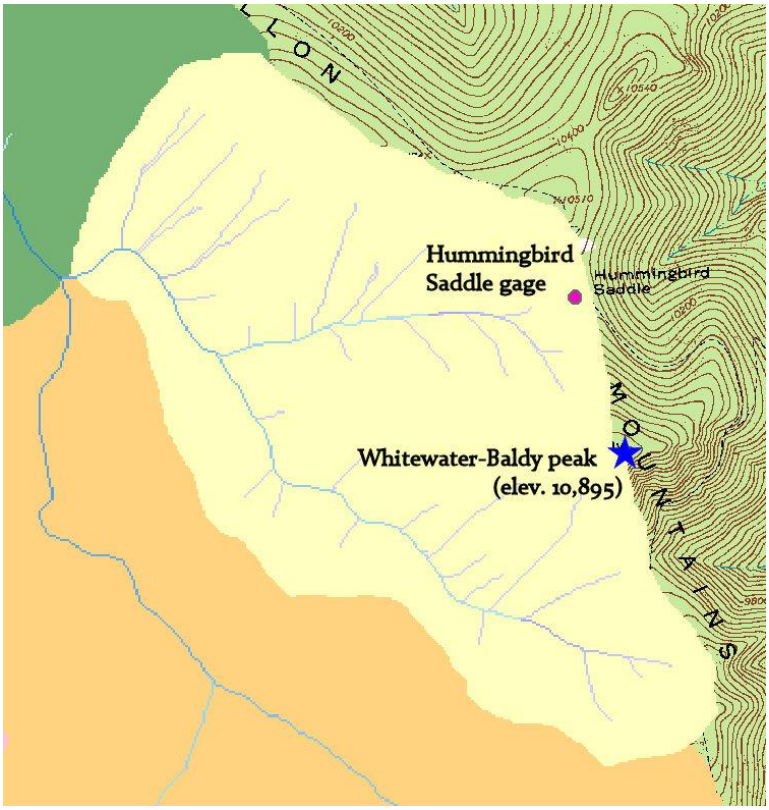

To determine a time-area histogram for Baldy Fork using GIS, the flow time from each GIS raster cell in the subarea to the outlet must be determined. Thus, flow velocity in each cell, given land roughness, slope, and flow cross-sectional area will be needed. Equation 7 from the main body of this technical note shows the velocity form of Manning's equation, and the variables for which a GIS raster layer will be needed to determine flow travel time.

roughness in GIS

The land roughness was determined, given pre-fire land cover and post-fire burn severity, as shown in Tables CS4-1 through CS4-3 below. (For typical overland and shallow-concentrated flow roughness values, see Tables 2 and 3 in the main body of this Technical Note.) Three roughness rasters were created, one for each fire condition. The raster grid sizes, based on the available digital elevation model (DEM) were ten meters square.

Table CS4- 1. Pre-fire roughness assumptions

flow segment	land assumptions	*n* value
overland	Grass, short-grass prairie	0.15
shallow-concentrated	steep, rocky, less depth flow	0.08
channel	steep, rocky, less debris	0.045

Table CS4- 2. Post-fire (immediately) roughness assumptions

flow segment	land assumptions	*n* value
overland	bare ground (severe, moderate burn)	0.011
	bare ground (low burn)	0.08
	bare ground (no burn)	0.15
shallow-concentrated	steep, rocky, more depth flow	0.06
channel	steep, rocky, more debris	0.05

Table CS4- 3. Post-fire (1-year) roughness assumptions.

flow segment	land assumptions	*n* value
overland	bare ground (severe, moderate burn)	0.03
	bare ground (low burn)	0.10
	bare ground (no burn)	0.15

Note that values for shallow concentrated flow and channel flow are the same as in Table 2.

In addition to the land surface assumptions shown in the tables, this method requires that one be able to determine whether a raster cell contains predominantly overland flow, shallow-

concentrated flow, or channel flow. Using typical hydrologic functionality in GIS, a flow accumulation raster is created. The value in each cell of that raster is the number of cells that drain to it. The type of flow segment for each cell was determined from the following assumptions. Overland flow was assumed to extend for about 100 feet (three cells). Thus, if the flow accumulation layer contains the number 3 or less, it is an overland flow cell. Shallow-concentrated flow was assumed to extend for another 1000 feet (thirty cells). Any cell with a flow accumulation value greater than 30 is considered a channel flow.

To assess the burn condition of each raster cell, the burn severity shape file provided by USDA Forest Service was transformed into a raster layer within GIS. In that layer, each cell with a high severity is assigned the number 4, medium 3, low 2, and unburned 1. For the pre-fire condition, using the data in Table CS4-1, the ArcMap Raster Calculator is given the command shown in Figure CS4-9. (Note that Con stands for Conditional, which is GIS language for an if-statement.)

Figure CS4- 9. ArcMap Raster Calculator expression creating a pre-fire roughness layer.

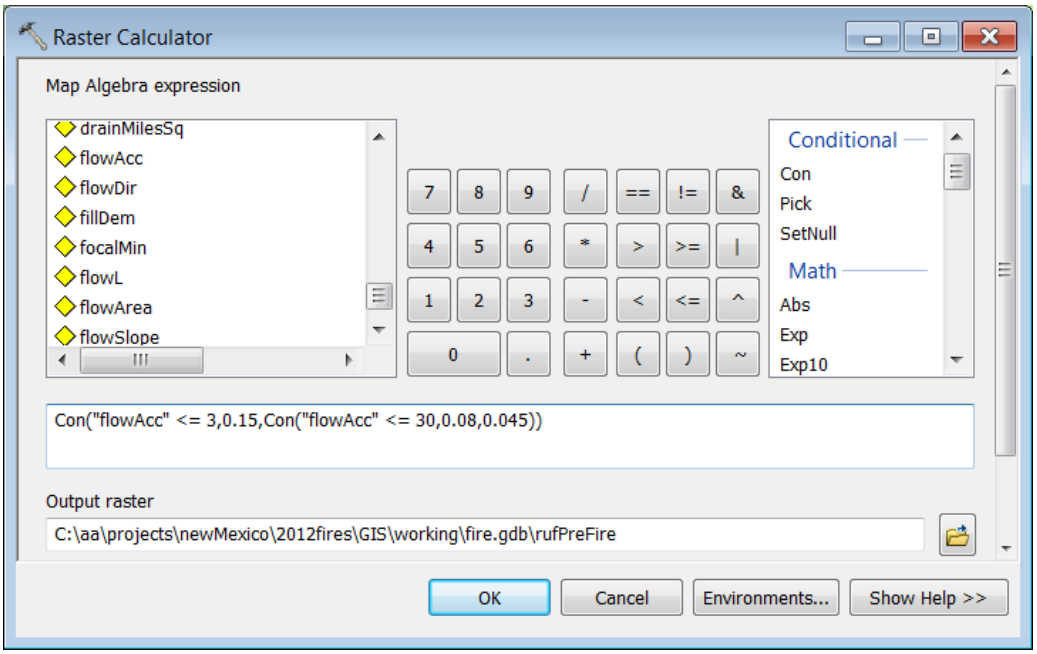

The output of the above command is a raster containing the pre-fire roughness and is named "rufPreFire." Note that the roughness layers are created for the entire watershed, not each subarea separately. The raster calculator expression for the "post-fire immediately" case, given Table 2, is slightly more complicated:

Con("rufPreFire" == 0.08,0.06,Con("rufPreFire" == 0.045,0.05,Con("burnRaster" >= 3,0.011,Con("burnRaster" == 2,0.08,"rufPreFire"))))

In English, this command says, "If cell in rufPreFire is 0.08 (i.e., a shallow-concentrated flow cell) then set the roughness to 0.06, otherwise, if the cell in rufPreFire is 0.045 (i.e., a channel cell) then set the roughness to 0.05. If neither of those conditions is true, then if the burn raster cell is greater than or equal to 3 (moderate or severe) then set the roughness to 0.011, otherwise if the burn raster cell is 2 then set the roughness to 0.08. Finally, if none of those conditions is true, then set the new raster value to the same as the old raster value (unburned overland flow cells).

flow slope in GIS

The direction of flow in any cell is provided by the typical hydrology GIS function "flow direction," which assigns a number to each cell which is a code for the direction of steepest descent. The flow length through a 10 m cell may be either 46.40 feet (diagonal) or 32.81 feet.

Figure CS4- 10. Flow direction codes

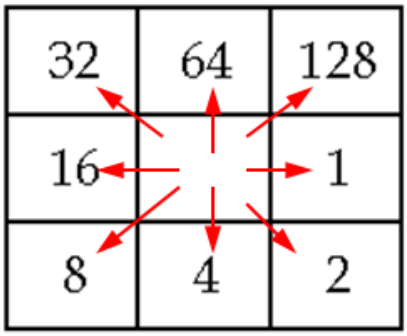

A flow length raster is created using the following command:

Con("flowDir" == 1,32.81,Con("flowDir" == 4,32.81,Con("flowDir" == 16,32.81,Con("flowDir" == 64,32.81,46.4))))

To obtain flow slope, not only is the flow length needed, but also the land surface drop between a given cell and its lowest neighbor. The ArcToolbox function "Focal Statistics" determines the DEM elevation of the lowest neighbor. Then flow slope is determined by dividing the elevation difference by the flow length. (Note that because zero slopes are possible, the minimum slope is set to some small positive value.)

velocity relationship derivations

These techniques for determining velocity in the three flow segment types are known generally as "kinematic wave routing" and are discussed in numerous references including USCOE (2013) and MacArthur and DeVries (1993). Those references transform Manning's equation into the general form shown in equation 1, where *y* is flow depth:

$$Q = ay^{5/3} \quad where \quad a = \frac{1.486S^{0.5}}{n} \qquad \text{(equation CS4-1)}$$

For overland flow, the flow width is considered to be so much greater than flow depth, that hydraulic radius can be assumed equal to depth. The equation can be expressed in the velocity form (equation 2), where *w* is assumed flow width.

$$V = ay^{2/3} \quad where \quad a = \frac{1.486S^{0.5}}{wn} \qquad \text{(equation CS4-2)}$$

To estimate overland flow velocity we can group terms as shown in equation CS4-3, and create a table to reference the effect of various assumptions of flow depth and width.

$$V_{overland} = \frac{\emptyset S^{0.5}}{n} \quad where \quad \emptyset = \frac{1.486y^{2/3}}{w} \qquad \text{(equation CS4-3)}$$

Table CS4-4. Values of φ, given assumptions of overland flow width and depth.

y (in)	*w* (ft)	φ
0.25	2.0	0.056
0.25	2.5	0.045
0.25	3.0	0.038
0.25	3.5	0.032
0.25	4.0	0.028
0.50	2.0	0.089
0.50	2.5	0.071
0.50	3.0	0.060
0.50	3.5	0.051
0.50	4.0	0.045

For shallow-concentrated flow (collector channels), assuming a triangular channel shape, MacArthur and DeVries (1993) develop the following equation (given here in the velocity form).

$$V_{collector} = \frac{\emptyset S^{0.5}}{n} \quad where \quad \emptyset = 0.94A^{1/3}\left(\frac{z}{1+z^2}\right)^{1/3} \qquad \text{(equation CS4-4)}$$

where *A* is the flow cross-sectional area in square feet and *z* is the side slope (length horizontal divided by length vertical). By assuming a flow depth and side slope, φ can be obtained from Table CS4-5.

Table CS4- 5. Shallow-concentrated flow parameters

y (ft)	*z*	*A* (ft^2)	φ
0.5	3	0.75	0.572
0.5	4	1.00	0.580
0.5	5	1.25	0.584
1.0	3	3.00	0.908
1.0	4	4.00	0.921
1.0	5	5.00	0.928

For channel flow segments, assuming a trapezoidal channel shape (figure CS4-11), MacArthur and DeVries (1993) develop the following equation (given here in the velocity form).

$$V_{channel} = \emptyset A^{2/3}\left[\frac{1}{w+2y(1+z^2)^{1/2}}\right]^{2/3} \quad where\ \emptyset = \frac{1.486S^{0.5}}{n} \qquad \text{(equation CS4-5)}$$

where *A* is the cross-sectional flow area in square feet and *w* is the bottom width in feet.

Figure CS-4- 11. Trapezoidal channel dimensions.

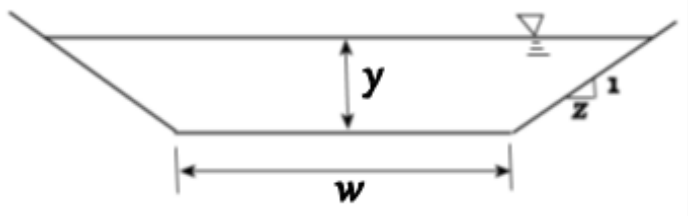

By assuming *w* to be a multiple (*m*) of *y* the equation can be re-written in terms of *A* only.

$$w = my \qquad \text{(equation CS4-6)}$$

$$A = w + zy^2 = y^2(m + z) \qquad \text{(equation CS4-7)}$$

Substituting equation CS4-6 into equation CS4-5 yields equation CS4-8:

$$V_{channel} = \emptyset \frac{A^{2/3}}{y^{2/3}} \left[\frac{1}{m+2(1+z^2)^{1/2}} \right]^{2/3} \quad \text{(equation CS4-8)}$$

Rewriting equation CS4-7 to solve for *y* and taking it to the one-third power yields equation CS4-9:

$$y^{2/3} = \frac{A^{1/3}}{(m+z)^{1/3}} \quad \text{(equation CS4-9)}$$

Substituting equation CS4-9 into equation CS4-8 yields equation CS4-10:

$$V_{channel} = \emptyset A^{1/3} (m+z)^{1/3} \left[m + 2(1+z^2)^{1/2} \right]^{-2/3} \quad \text{(equation CS4-10)}$$

This can be expressed in the form of equation CS4-11, where μ is a function of assumed channel parameters *z* and *m* from table CS4-6.

$$V_{channel} = \emptyset A^{1/3} \mu \quad where \quad \emptyset = \frac{1.486 S^{0.5}}{n} \quad \text{(equation CS4-11)}$$

Table CS4- 6. Trapezoidal channel parameters, assuming bottom width = *m* times depth.

Z	*m*	μ
2	2	0.457
2	3	0.447
2	4	0.437
3	2	0.416
3	3	0.410
3	4	0.403
4	2	0.385
4	3	0.381
4	4	0.376

The channel flow segment requires some estimate of cross-sectional flow area. A common approach for this is regional regression equations. Although such equations, which relate

bankfull flow area to watershed drainage area, are not universally available, for the Gila Wilderness region Moody, Wirtanen, and Yard (2003) derived the following:

$$A = 4.78B^{0.512} \quad (r^2 = 0.9163) \qquad \text{(equation CS4-12)}$$

where:

A = flow cross-sectional area (ft^2)

B = watershed area (mi^2)

Although the equation has a relatively high correlation, the authors included their data, which shows that they used many watersheds much larger than the subarea sizes within Whitewater Creek. To obtain a more applicable equation for such small subareas the authors' data was culled for only the small watershed sizes, 23 in total, and the following equation derived, for use in Whitewater Creek:

$$A = \exp(0.5036lnB + 1.595) \quad (r^2 = 0.88) \qquad \text{(equation CS4-13)}$$

velocity relationships used in Whitewater Creek

Note that the kinematic wave methods discussed above can be used in HEC-HMS without determining a unit hydrograph. The KINEROS model also uses the landscape flow routing option. For the subareas of Whitewater Creek, however, the unit hydrograph option was selected and the following assumptions made, yielding equations CS4-14 through CS4-17. For the overland flow segment, assumed depth was 0.25 inches and width 3 feet. From equation CS4-3 and Table CS4-4, equation CS4-14 results.

$$V_{overland} = \frac{0.038S^{0.5}}{n} \qquad \text{(equation CS4-14)}$$

For the shallow-concentrated flow segments, depth was assumed to be 0.5 feet and z was assumed to be 4, which yields (from equation 4 and Table 5) equation 15:

$$V_{overland} = \frac{0.58S^{0.5}}{n} \qquad \text{(equation CS4-15)}$$

For the channel flow segments, a separate raster layer for flow cross-sectional area was obtained using equation CS4-13. Then, assuming a trapezoidal channel, two different relationships were

derived depending on slope. For a flow slope greater than or equal to 0.05, bottom width was assumed 3 times the flow depth and z = 2. For flow slope less than 0.05, bottom width was assumed 5 times the flow depth and z = 3. Then, using equation CS4-11 and Table CS4-6, the following equations were derived:

For steeper channels:

$$V_{channel} = \frac{0.665 S^{0.5}}{n} A^{1/3} \qquad \text{(equation CS4-16)}$$

For less steep channels:

$$V_{channel} = \frac{0.589 S^{0.5}}{n} A^{1/3} \qquad \text{(equation CS4-17)}$$

When creating the velocity rasters, the possibility exists that velocity will come out unreasonably high due to very steep slopes, such as vertical drops, or zero due to flat slopes. A better travel time estimate was obtained for Whitewater Creek by restricting the maximum and minimum velocities to 15 and 0.10 feet per second, respectively.

travel time in GIS

In ArcGIS, the hydrology tool "Flow Length" is used to obtain the flow travel time of any cell to its outlet. The reason this is possible is that the tool can apply an optional "weight" raster, which can contain such parameters as unit conversions and channel sinuosity, as shown in equation CS4-18. The time in minutes is obtained using a weight raster that includes a sinuosity of 1.1, a conversion of meters to feet (since the tool is using the 10m DEM), and from seconds to minutes.

$$time = flowLength \times weight \quad where\ weight = \frac{1.1 \times 3.28083}{flow\ Velocity \times 60} \qquad \text{(equation CS4-18)}$$

The resulting time raster can then be reallocated to group the cells into time bands of, say, five minutes. The resulting raster for Baldy Fork subarea is shown in Figure 12.

Figure CS4- 12. Twenty-one five-minute travel time bands for Baldy Fork, with Attribute Table.

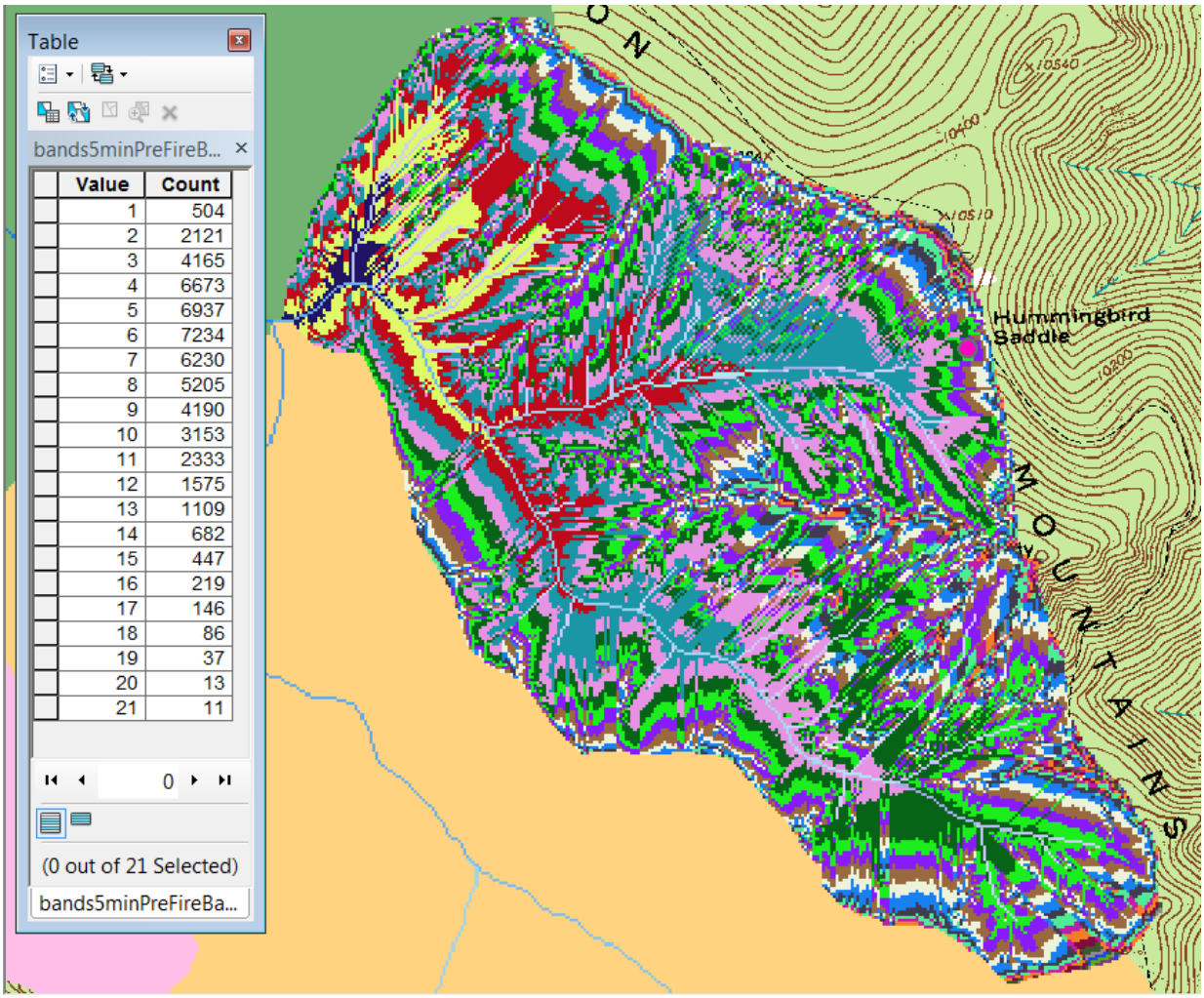

The Attribute Table shows the number of cells in each of 21 time bands in Baldy Fork. Since there are 21 five-minute bands the longest drainage time (or time of concentration) may be considered 1 hour and 45 minutes. However, the hydrologist can note the number of cells in those later time bands. Sometimes they become so few that a better estimate of time of concentration is taken to be earlier. For Baldy Fork, one might select timeband 18, or 90 minutes. Note that a separate travel time raster is produced for the three scenarios, pre-fire, post-fire immediately and post-fire after one year.

spreadsheet derivation of time-area histogram and unit hydrograph

To obtain a time-area histogram the five-minute time band attribute table is copied into a spreadsheet. This procedure is described in many hydology textbooks, such as Bedient, Huber, and Vieux (2012). Since the cells are 100 square meters each, the area drained by each time band can be converted to any convenient unit, such as acres, in the spreadsheet. The resulting time-area histogram for Baldy Fork pre-fire is shown in figure CS4-13. To obtain a unit hydrograph, a duration must be chosen and one inch of rainfall applied within that timeframe. The runoff from each time band is computed, lagged, and summed.

Figure CS4- 13. Pre-fire time-area histogram for Baldy Fork.

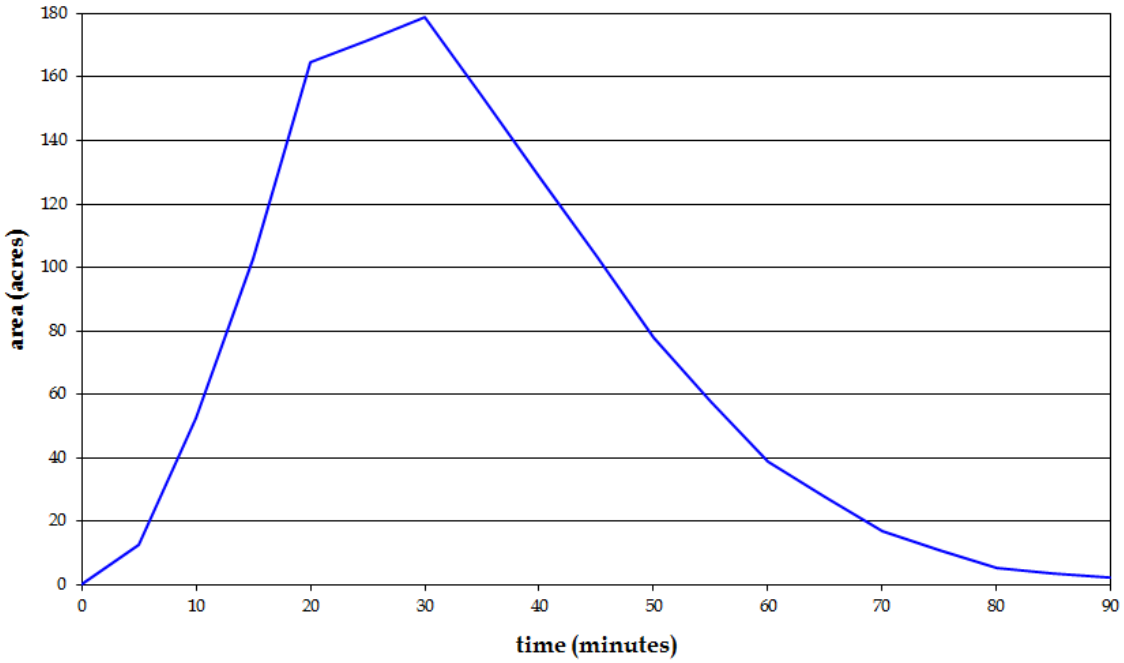

Figure CS4- 14. Pre-fire spreadsheet. (30-minute unit hydrograph in column H)

BaldyCkUH

	A	B	C	D	E	F	G	H	I	J	K	L	M
1	time	timeband	5	cellsize	100	UH	0.5						
2	to outlet	cells	area	area		time	flow	flow	rainfall	area	time --------->		
3	(min)	(#)	(ac)	(m^2)		(min)	(ac-in/timeband)	(cfs)	(in)	(ac)	5	10	15
4	**histogram**	preFire					**30-min UH:**		1.0000				
5	0	0	0	0		0	0.00	1.20	0.16667	0.00			
6	5	504	12.5	50400		5	2.08	2.00	0.16667	12.45	2.08		
7	10	2121	52.4	212100		10	10.81	130.81	0.16667	52.41	8.74	2.08	
8	15	4165	102.9	416500		15	27.96	338.37	0.16667	102.92	17.15	8.74	2.08
9	20	6673	164.9	667300		20	55.45	670.91	0.16667	164.89	27.48	17.15	8.74
10	25	6937	171.4	693700		25	84.02	1016.60	0.16667	171.42	28.57	27.48	17.15
11	30	7234	178.8	723400		30	113.81	1377.09	0.16667	178.76	29.79	28.57	27.48
12	35	6230	153.9	623000		35	137.39	1662.44		153.95	25.66	29.79	28.57
13	40	5205	128.6	520500		40	150.09	1816.12		128.62	21.44	25.66	29.79
14	45	4190	103.5	419000		45	150.20	**1817.37**		103.54	17.26	21.44	25.66
15	50	3153	77.9	315300		50	135.70	1641.96		77.91	12.99	17.26	21.44
16	55	2333	57.7	233300		55	116.74	1412.53		57.65	9.61	12.99	17.26
17	60	1575	38.9	157500		60	93.43	1130.52		38.92	6.49	9.61	12.99
18	65	1109	27.4	110900		65	72.34	875.32		27.40	4.57	6.49	9.61
19	70	682	16.9	68200		70	53.71	649.93		16.85	2.81	4.57	6.49

dataPreFire | histogramPreFire | 30min UH | S curve | dataPostFireImm

In figure CS4-14 the flow values in column G, in acre-inches, are obtained by summing the lagged flow values in columns K through P. Those flow values are obtained by multiplying the 5-minute increment of rainfall (0.167 inches) by the area in acres of each time band. Then, in column H, the flow is converted to cfs. The 30-minute unit hydrograph peak (cell H14) is 1,817 cfs, the peak that would be expected from Baldy Fork if one inch of rain was evenly distributed over the subarea in thirty minutes. Figure CS4-15 shows the 30- minute unit hydrographs for Baldy Fork under the three scenarios.

Figure CS4- 15. Unit Hydrographs, 30-minute duration for Baldy Fork.

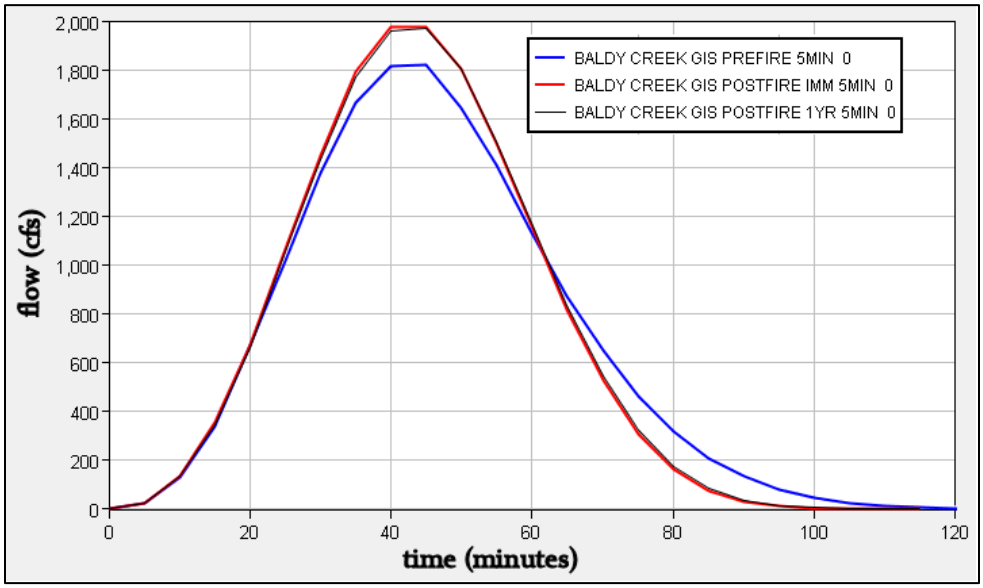

The 30-minute unit hydrograph is applicable when the duration of excess rainfall from a given event is thirty minutes long. To enable a unit hydrograph compilation to apply for any duration of excess rainfall, a so-called "S-curve" is derived by lagging the 30-minute unit hydrographs in successive 30-minute periods, as shown in figure CS4-16.

Figure CS4- 16. S-curve from lagged and summed 30-minute unit hydrographs

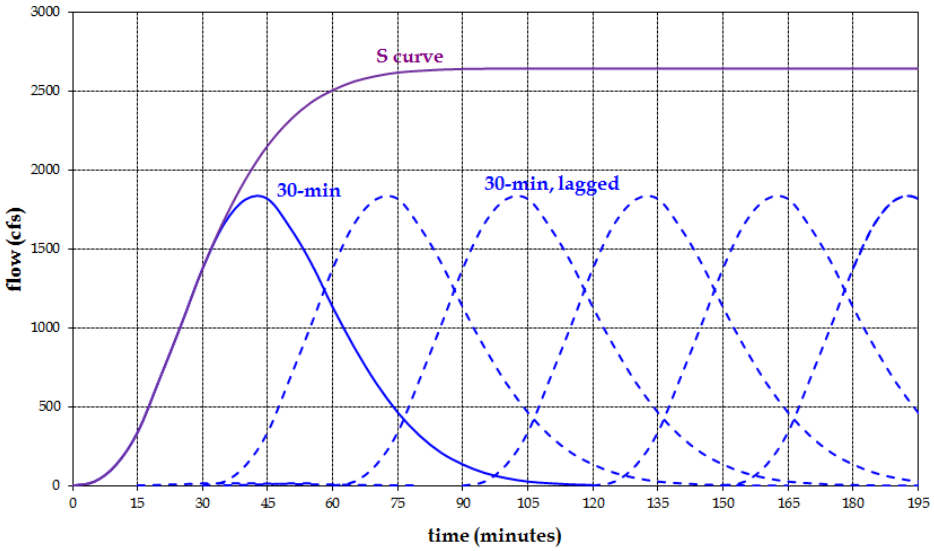

The maximum of the S-curve is the "unit flow" for the subarea—the amount of runoff if a full inch of rain runs off the entire watershed area in thirty minutes. In the case of Baldy Fork, since the total area is 57,124,070 square feet the computation is shown in equation CS4-19.

$$\frac{57{,}124{,}070\ ft^2 \times 1\ in}{30\ min} \times \frac{1\ ft}{12\ in} \times \frac{1\ min}{60\ sec} = 2{,}644\ cfs \qquad \text{(equationCS4-19)}$$

The hydrology model HEC-HMS requires the S-curve to be given as a percent of lag versus percent of unit flow. Watershed lag is the time from the center of the rainfall duration to the runoff peak. The lag for Baldy Fork can be seen from the 30-minute unit hydrograph, figure CS4-15, to go from 15 minutes (center of rainfall) to 45 minutes (peak) or 30 minutes.

Figure CS4- 17. Baldy Fork S-curves for HEC-HMS, three scenarios

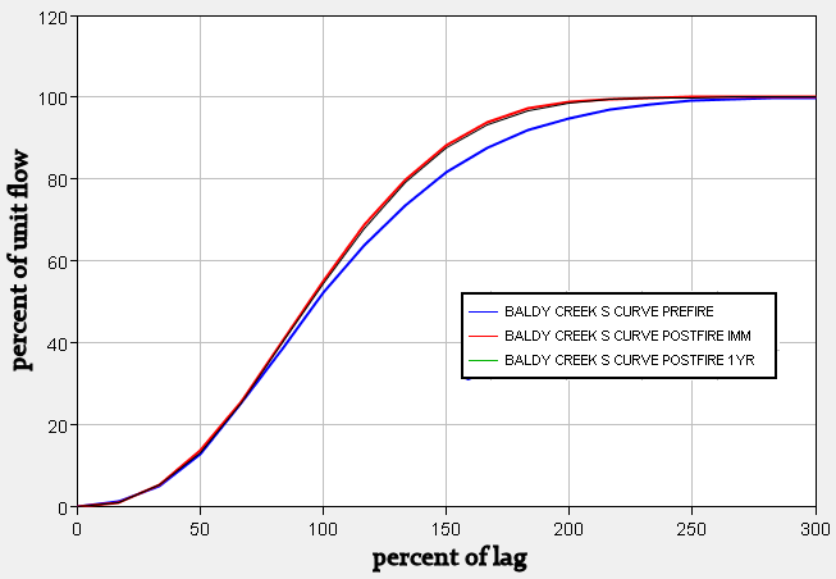

This section has shown the development of the hydrograph transform S-curve input to HEC-HMS for one subarea in the Whitewater Creek watershed. The same procedures were followed to produce S-curves for every subarea in the model for the three scenarios.

Infiltration Loss Method: Green & Ampt Equation

The process-based Green & Ampt method of infiltration uses soil properties to model progressive loss of surface water into the soil and the change in soil moisture capacity. Although it is a point-model, the more spatially homogeneous the soil in a given subarea the more applicable this method. HEC-HMS does have the ability to do a grid-based Green & Ampt infiltration, modeling from cell to cell within a subarea, but this requires more data than is available for the Whitewater Creek basin. Being within the Gila Wilderness, spatially distributed soil data is not available. For the entire watershed, the Green & Ampt parameters were estimated based on soil type and using Table 12, from the main body of the technical note. The assumed soil texture was loamy sand with porosity of 0.42 cubic inches of pore space per cubic inch of soil. The initial moisture content was assumed to be near field capacity or 15 percent of the porosity. Converting from the metric units of Table 12, the wetting front suction was estimated at 2.4 inches and the hydraulic conductivity 1.6 inches per hour.

A final specification for this method is the percent impervious surface of the subarea. This was set at zero for the pre-fire condition. For post-wildfire conditions, the percent imperviousness was used as a way to take into account soil hydrophobicity. However, water-repellent soil is not the same as a parking lot pavement. It is not spatially consistent, nor consistent in depth or thickness. In addition, higher rainfall rates can sometimes penetrate hydrophobic soils and infiltrate more than lower rainfall rates. (The hydrophobicity will then generally return upon drying.) Finally, high soil burn severity is not a fool-proof predictor of the location of hydrophobic soil.

For modeling soil hydrophobicity in the Whitewater Creek watershed, the percent imperviousness for the immediately post-fire condition for each subarea was set to 65% of the high soil burn severity area for the 25-year and more frequent rainfall events. For the 100-year rainfall event, the imperviousness was set to 30% of the high burn severity area. For the post-fire 1-year later condition, the imperviousness was set to 45% of the high burn severity for the 25-year rainfall and more frequent events. For the 100-year rainfall event, the imperviousness was set to 15% of the high burn severity.

Initial Abstraction, Surface Ponding, Canopy Loss

The CN method includes an "initial abstraction" which is considered to represent interception by vegetation, surface storage, and infiltration prior to runoff. This initial abstraction is not changeable by the user and is a function of the potential maximum loss to infiltration, ultimately a fraction of the user choice of curve number. While the CN method is provided as an option by HEC-HMS, the program also provides explicit canopy loss and surface loss methods. Since the Green & Ampt loss method was chosen for the Whitewater Creek analysis, further losses due to vegetation and surface depressions needed to be selected.

The options for these losses are not highly sophisticated in HEC-HMS. A maximum retention is specified by the user and an initial condition. The HEC-HMS user manual states that use of a canopy method is generally not necessary for storm events, whereas continuous simulation modeling would take into account the evaporation of intercepted moisture between storms. However, forest canopy is not an insignificant moisture interceptor. The flashiness of Southwestern US storm events contributes to raising the significance of canopy. In addition, for wildfire events in forests the near total loss of canopy represents a widespread landscape change. For Whitewater Creek, pre-fire conditions the canopy initial storage was set to zero and the maximum storage set to 0.05 inches. For post-wildfire conditions, the canopy interception was set to none.

Surface storage is a separate option in HEC-HMS, represents loss of incoming rainfall to surface depressions, and may be used to represent the retention of moisture in the forest litter or duff layer. For Whitewater Creek pre-fire condition the initial storage was set to zero and maximum loss set to 0.03 inches. For post-fire conditions, the maximum loss was set to 0.01 inches.

Baseflow

While the NRCS hydrology programs WinTR-20 and WinTR-55 produce hydrographs of direct runoff they do not give the user the ability to include some form of baseflow, which would somewhat increase the peak of an actual flood hydrograph. In the arid Southwest US, however, baseflow is generally less significant when the concern is storm-event flood peaks. However, the Whitewater Creek analysis included a simple baseflow option (termed "recession baseflow" in

HEC-HMS). The method allows initial baseflow to be a user-selected flow value per unit subarea drainage size. For Whitewater Creek, this was set to a relatively small 0.25 cfs per square mile. The recession proceeds to a value set by the user as a ratio to the peak flow. For Whitewater Creek, this was set at 10 percent.

Rainfall events examined

The NOAA National Weather Service Precipitation Frequency Data Server (on the web at: http://dipper.nws.noaa.gov/hdsc/pfds/) has recently been updated for New Mexico. The website allows the user to select a given precise location on a map and provides the total storm values for various recurrence intervals and durations. Often the 24-hour duration values are used. In the flashy thunderstorm prone Southwestern US, a shorter duration may be more applicable. Since the BAER hydrologic analysis for the Gila Wilderness used a 6-hour duration, this was selected for the current analysis.

The total rainfall values shown in Table CS4-7 show that there is some reduction within the watershed, lowering with descending elevation toward the outlet. The analysis first assumed that these rainfall amounts would fall on all subareas at the same time. This is unrealistic but provides conservatively high peaks and larger hydrographs.

Table CS4- 7. Whitewater Creek watershed 6-hour duration storm totals.

watershed area	2-year (in)	25-year (in)	100-year (in)
Upper Whitewater	1.54	2.73	3.49
SF Whitewater	1.42	2.49	3.19
Lower Whitewater	1.20	2.12	2.73

A second and third set of analyses ran the three recurrence interval 6-hour rainfalls from Table 7 with an areal reduction factor obtained from Figure 18. The second set of analyses centered the storms over the upper Whitewater Creek portion of the watershed and the third set centered the storms over the SF Whitewater sub-watershed. For these areally reduced analyses, each basin received a rainfall rate reduces in proportion to their distance from the center of the storm.

Figure CS4- 18. Areal reduction factors developed for 6-hour duration storms at Walnut Gulch AZ Experimental Watershed (modified, from Osborn, Lane, and Myers (1980).

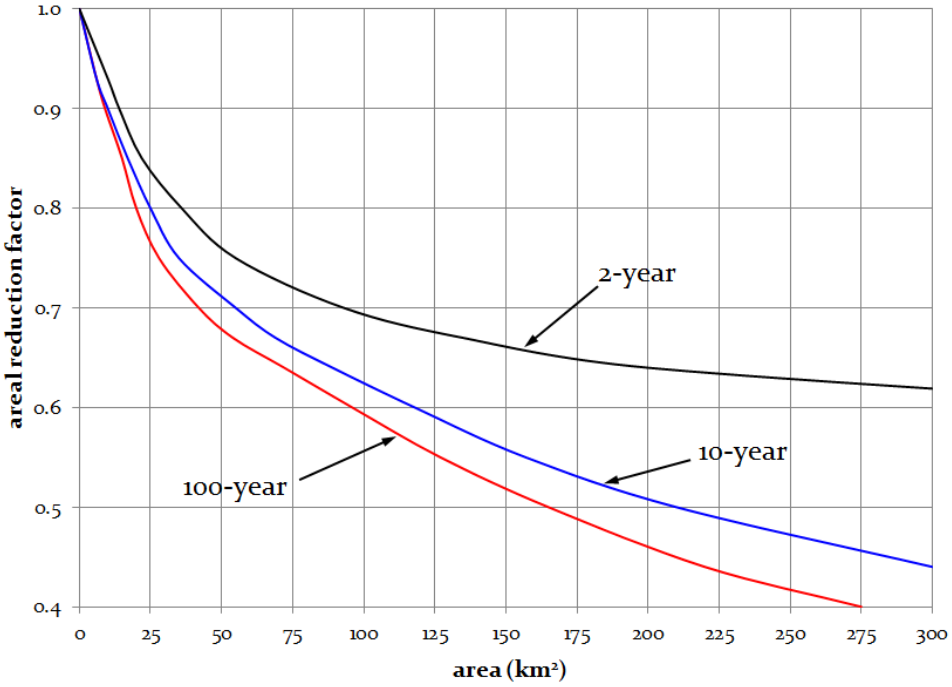

Figure CS4-18, developed for Walnut Gulch AZ, is assumed applicable to Whitewater Creek, in the same geographic region, about 180 miles away. As Whitewater Creek is about 23 km wide, east to west, the areal reduction from figure CS4-18 is significant. The largest area on the graph is 300 square kilometers, which corresponds to a radius of about 10 kilometers. Therefore, many of the sub-basins of Whitewater Creek will be farther away from the storm center than can be analyzed with figure CS4-18. Rather than reduce the rainfall of more remote subareas to zero, the analyses applied minimum values from figure CS4-18. Figure CS4-19 shows the selected storm centerings for the areally reduced analyses. The red star marks the upper Whitewater centering and the red circular line shows the 10km radius for that storm. The blue star marks the storm centering in the SF Whitewater sub-basin, with blue circular line showing the 10km radius from that point.

To distribute the rainfall totals over time, the standard SCS Type II rainfall distribution, considered applicable in New Mexico, was used. Although the standard distribution pertains to a 24-hour duration, it is easily modified for shorter durations, including the 6-hour.

Figure CS4- 19. Two storm centerings for Whitewater Creek and 10km radii.

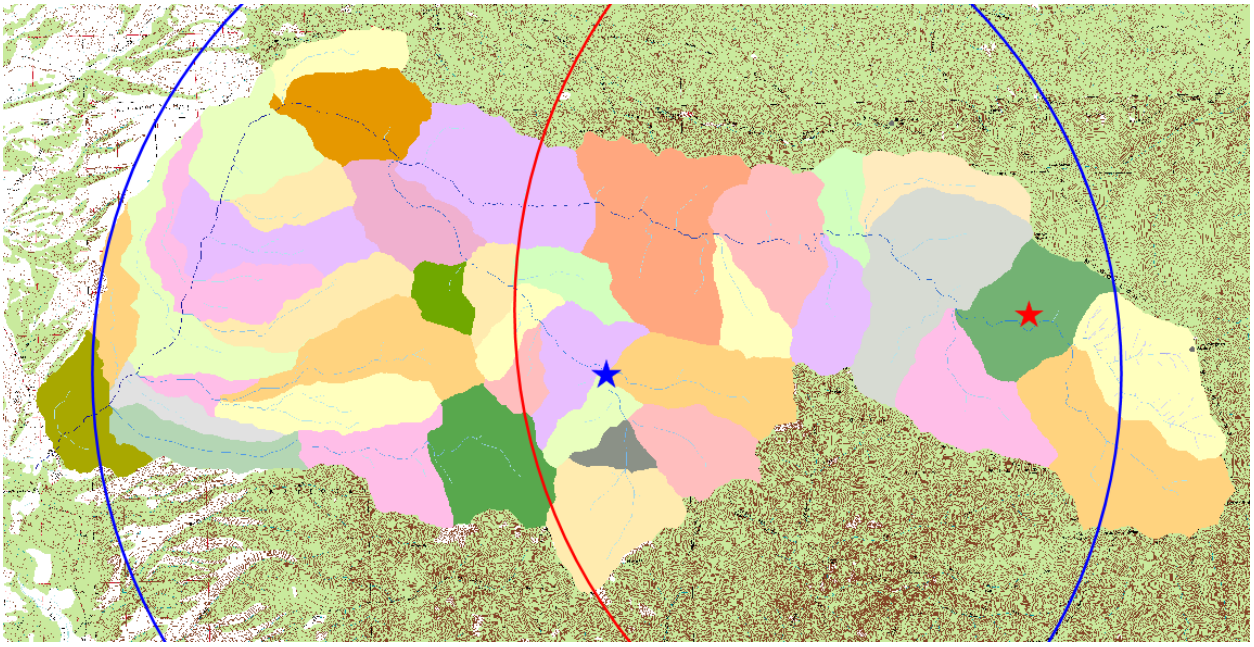

Sediment Bulking

This analysis did not attempt to model sedimentation. As discussed in the main body of the technical note, the maximum sediment concentration short of debris flow is considered twenty percent. A USGS report specifically concerning the Whitewater Baldy Complex wildfire (Tillery, Matherne, and Verdin, 2012) estimated high probabilities in Whitewater Creek of debris flows from 30-minute duration rainfall events for recurrence intervals of 2-year, 10-year, and 25-year. A shorter duration storm of higher intensity is generally required to generate debris flow.

Figure CS4-20 is a screenshot from Plate 3 of Tillery, Matherne, and Verdin (2012) which shows their overall debris flow hazard findings in Whitewater Creek. Notice the main channel of Whitewater Creek in blue and the community of Glenwood at the downstream end circled in red. Sub-basins labeled 92 and 93 are the upper Whitewater, sub-basin 91 is the SF Whitewater, and sub-basin 90 is the upper Little Whitewater. These of brown color are the highest hazard for debris flow in response to a 25-year 30-minute rainfall event (a total storm rainfall of about 1.54 inches).

Figure CS4- 20. Whitewater debris flow hazard (Tillery, Matherne, and Verdin (2012)

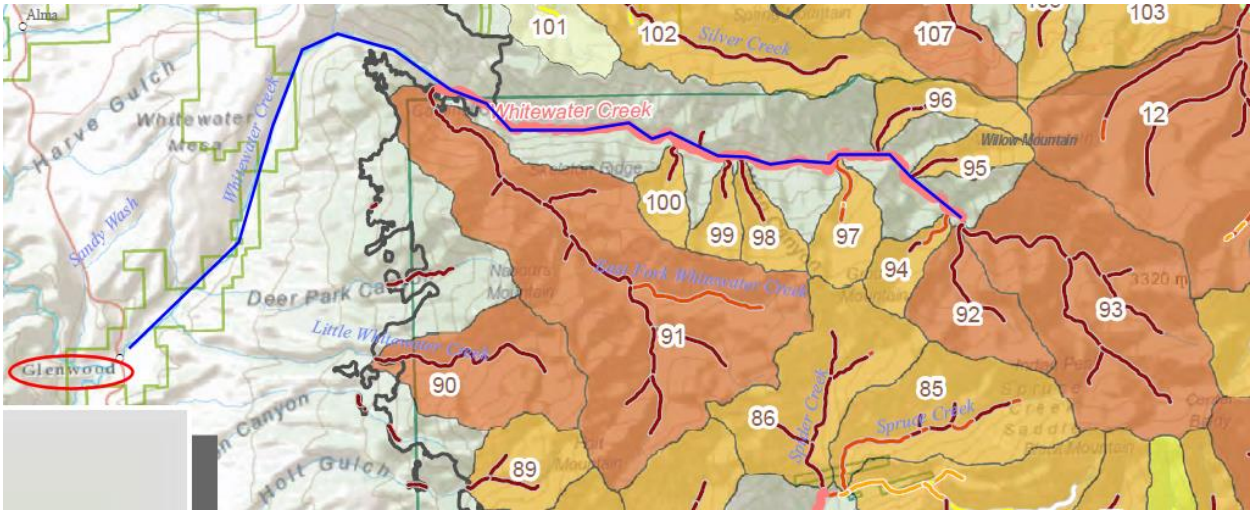

As a conservative estimate of possible sediment bulking for the events examined in this analysis, with six-hour duration, the sub-basins in brown from figure CS4-19 will be considered 20 percent bulked and the sub-basins in yellow, 10 percent bulked.

Results and Discussion

Figure CS4-21 shows the four locations for which modeling data is reported herein. The model user can receive results for the outlet of any sub-basin (shown in the figure by different pastel colors). The output will be reported for three recurrence intervals, 2-year, 25-year, and 100-year, for the three scenarios, pre-fire, post-fire immediately, and post-fire 1 year later. In addition, three types of storm centerings were considered. One for which no areal reduction is applied and the rainfall values of Table CS4-7 are applied at the same time over the entire watershed. The second and third centerings as shown in figure CS4-19, over the upper Whitewater subarea or over the SF Whitewater, with areal reductions determined from the curves of figure CS4-18.

Figure CS4- 21. Locations of reported HEC-HMS modeling output.

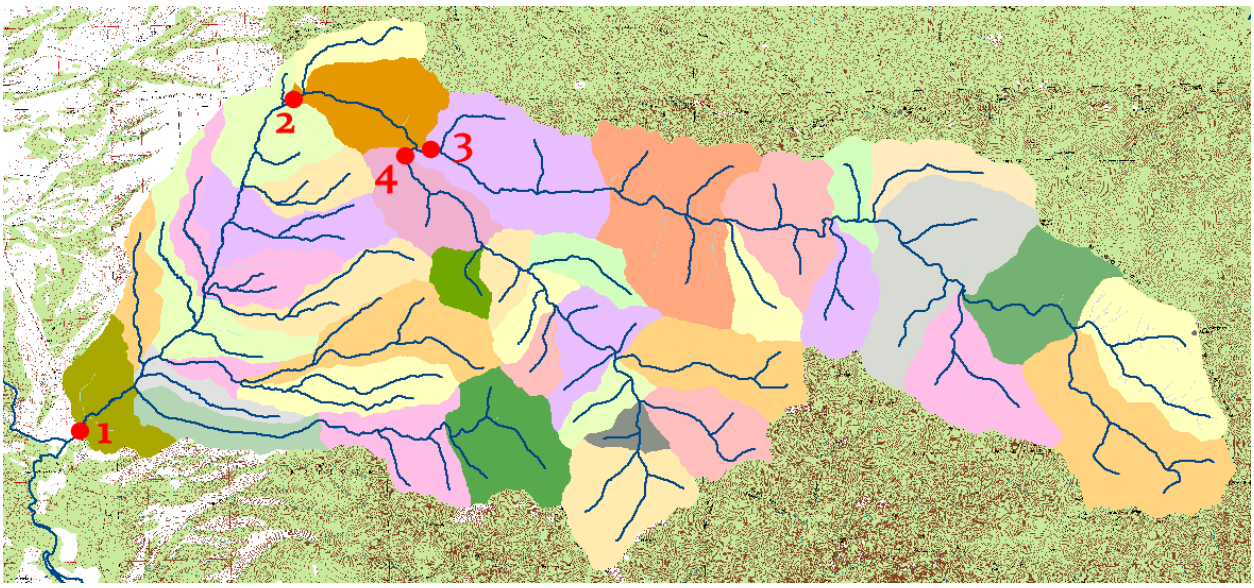

1 = Whitewater Creek outlet at Glenwood NM

2 = USGS gage "Whitewater Creek at Catwalk" (installed 2012)

3 = upper Whitewater Creek just above the confluence of SF Whitewater

4 = SF Whitewater just above the confluence of the Whitewater.

Table CS4-8 shows HEC-HMS modeling results for the rainfall events with no areal reduction. (A very slight reduction, shown in Table CS4-7, is provided by NOAA for three general areas of

the watershed, due to the change in specific location for which data was requested from the NOAA precipitation-frequency data server.)

Table CS4- 8. HEC-HMS output: hydrograph peaks at four locations (no areal reduction)

storm	location	pre-fire	post-fire (immediately)	post-fire (one year)
100-yr	abv SF	9839	14595	12492
100-yr	SF at mouth	3618	5492	4818
100-yr	gage	13119	18861	16160
100-yr	Glenwood	14304	20970	17768
25-yr	abv SF	3386	12324	9387
25-yr	SF at mouth	1087	3843	3064
25-yr	gage	4371	15285	11824
25-yr	Glenwood	4326	16229	12312
2-yr	abv SF	969	8611	6051
2-yr	SF at mouth	661	3125	2323
2-yr	gage	1712	10958	7932
2-yr	Glenwood	1781	12035	8613

These peaks are considered conservatively high, since no areal reduction was applied and the nature of storms in the Gila Wilderness area is more localized convective thunderstorms. In addition, although the unit hydrographs did change between the two post-fire scenarios, due to the consideration of some vegetation regrowth, the majority of the drop in the peak for the one year later condition came from assumptions about the reduction in hydrophobic soils. No field verification was completed for this analysis and the BAER report (USDA Forest Service, 2012) did not report the extent of hydrophobic soil. Estimates for this analysis were made using the

soil burn severity GIS shapefiles and from the findings of Tillery, Matherne, and Verdin (2012). Figure CS4-22 shows the full hydrographs for the 100-year no areal reduction scneario at the Whitewater Creek outlet, near Glenwood.

Figure CS4- 22. HEC-HMS results, 100-year storm peaks at Glenwood (no areal reduction)

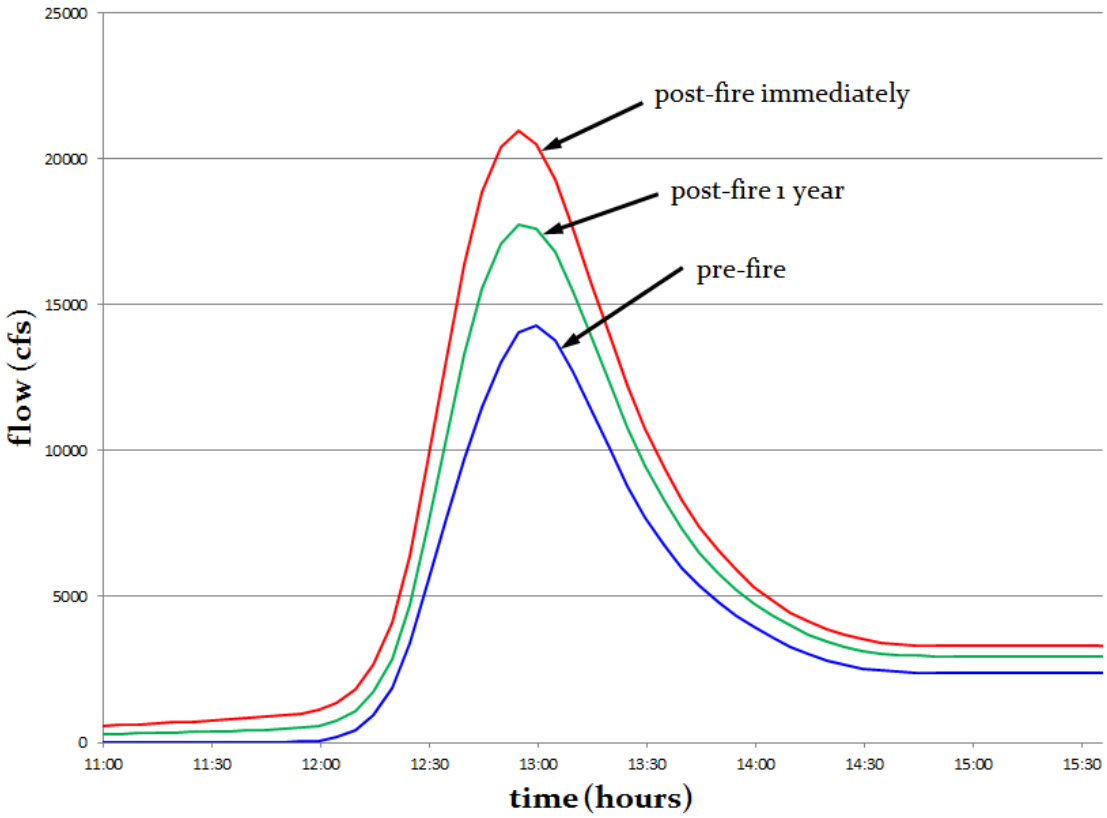

The areal reductions, as discussed above came from Osborn, Lane, and Myers, (1980), in particular their examination of Walnut Gulch AZ. That paper also examined a watershed near Alamogordo NM, which showed less areal reduction than Walnut Gulch. However, the Gila Wilderness area is considered closer geographically to Walnut Gulch than to Alamogordo. Nevertheless, the areal reductions may be less at Whitewater Creek than what were applied for the results reported in table CS4-9. Note that the 100-year pre-fire peak at Glenwood between tables CS4-8 and CS4-9 drops from 14304 cfs to 2904 cfs. The post-fire drops in peak are less dramatic; with the post-fire immediately peak at Glenwood dropping from 20970 cfs to 11826 cfs.

Table CS4- 9. HEC-HMS output: hydrograph peaks at four locations (areal reductions applied, with centerings as shown in Figure19).

storm	location	upper Whitewater centering			SF Whitewater centering		
		pre-fire	post-fire (immediately)	post-fire (one year)	pre-fire	post-fire (immediately)	post-fire (one year)
100-yr	abv SF	3126	10708	8140	943	7346	5162
100-yr	SF at mouth	3	1534	1052	1967	4741	3875
100-yr	gage	3118	11785	8886	2230	11010	8119
100-yr	Glenwood	2904	11826	8808	2259	11952	8672
25-yr	abv SF	763	7274	5010	12	5022	3218
25-yr	SF at mouth	3	1338	914	290	2582	1889
25-yr	gage	753	8247	5634	290	7103	4793
25-yr	Glenwood	682	8355	5645	282	7770	5177

Figure CS4- 23. HEC-HMS results, 100-year storm peaks at Glenwood (areal reduction with centering over the upper Whitewood sub-basin)

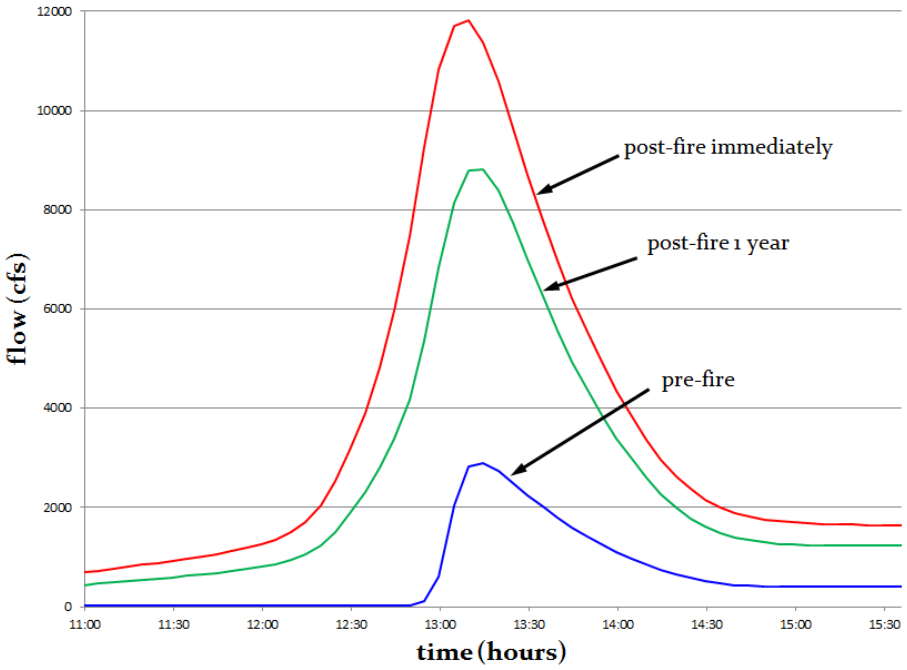

Comparing the results in table CS4-9 between the two storm centerings varies depending on recurrence interval. For the 100-year flood, the pre-fire peak at Glenwood is 22% less if the same storm is centered over the SF Whitewater rather than the upper Whitewater. However, the post-fire immediately results show a 1% greater peak at Glenwood if the storm is centered over the SF Whitewater. This is a direct result of the burn severity between the two sub-basins. As the sub-basins heal, the results show that the Glenwood 100-year peak moves toward being greater if the storm is centered over the upper Whitewater. Figure CS4-24 shows the post-fire results for the 100-year peaks at Glenwood under both centering conditions. Figure CS4-25 shows the same results for the 25-year recurrence interval. Note that storms centered over the SF Whitewater sub-basin peak at Glenwood about 15 minutes earlier than if they were centered over the upper Whitewater.

Figure CS4- 24. 100-year post-fire hydrographs at Glenwood between storm centerings in the upper Whitewater sub-basin and the SF Whitewater sub-basin.

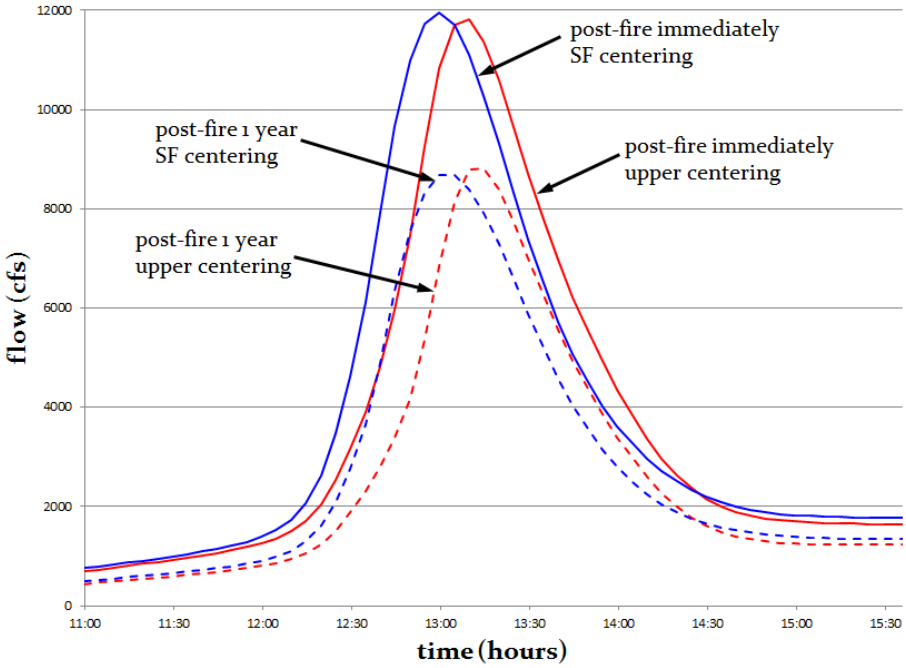

Figure CS4- 25. 25-year post-fire hydrographs at Glenwood between storm centerings in the upper Whitewater sub-basin and the SF Whitewater sub-basin.

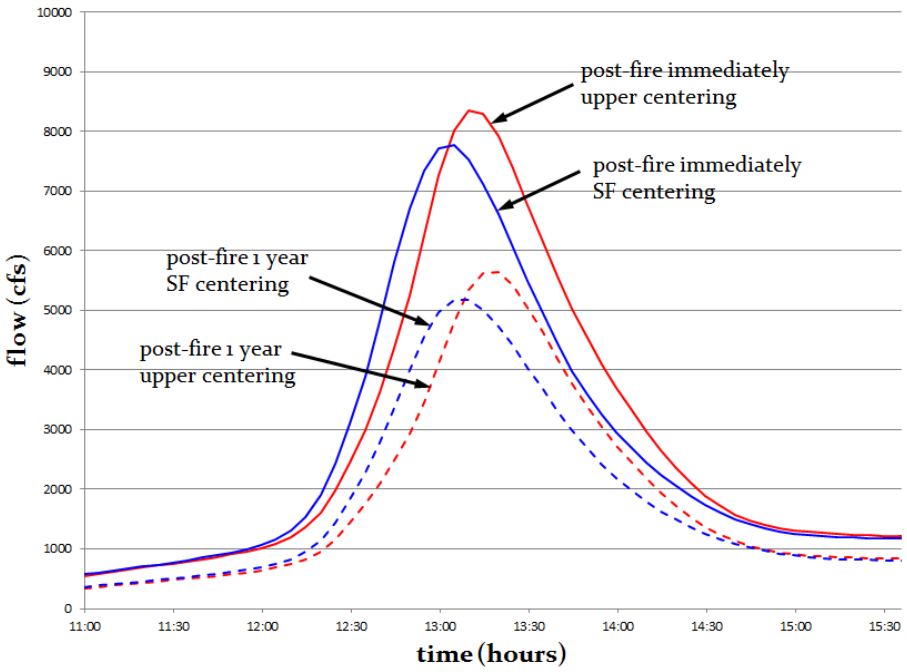

Sediment bulked peak flows have been computed, with the upstream end (about one third) of the Upper Whitewater sub-basin contributing a 20 percent sediment discharge, the lower end 10 percent, and the entire SF Whitewater sub-basin contributing 20 percent. These results are shown in Table CS4-10.

Table CS4- 10. Sediment bulked flows for Whitewater Creek.

storm	location	upper centering		SF centering	
		post-fire (immediately)	post-fire (one year)	post-fire (immediately)	post-fire (one year)
100-yr	abv SF	11848	8272	7478	6190
100-yr	SF at mouth	1534	1052	4741	3875
100-yr	gage	13591	10236	11536	10095
100-yr	Glenwood	13632	10158	12478	10648
25-yr	abv SF	7975	5011	5024	3921
25-yr	SF at mouth	1534	1052	4741	3875
25-yr	gage	9532	6518	7163	6012
25-yr	Glenwood	9641	6529	7829	6396

Conclusions

The post-fire hydrograph results are highly dependent on the amount of hydrophobic soil and the timing of its breakdown and return to pre-fire conditions. This is impossible to predict accurately without extensive field investigation. The burn severity mapping can be considered to at least rule out hydrophobicity in unburned and low burned areas. The extent to which hydrophobicity truly excludes infiltration in highly burned areas should be investigated. Although the findings of the research literature indicate that post-wildfire hydrophobic soils can persist for over five years, critical questions remain for hydrologic modeling. For example, does hydrophobicity immediately post-fire completely cover a landscape or only partially? And does the breakdown of hydrophobic effects on runoff occur more rapidly than the complete disappearance of the phenomenon because of the non-homogeneity on a landscape?

The second major issue for hydrologic modeling, particularly in the arid Southwestern US, is the extent of areal reduction in any given area. A literature search for this analysis turned up very little and studies by NOAA that were scheduled to be underway by 2006 apparently have not been completed.

References

Bedient, P.B., Huber, W.C., and Vieux, B.E. 2012. Hydrology and Floodplain Analysis, Prentice Hall, NJ, 5th Edition, 801 pages.

MacArthur, R., and DeVries, J.J. (1993) Introduction and application of kinematic wave routing techniques using HEC-1. U.S. Army Corps of Engineers Hydrologic Engineering Center, Davis CA, 68 pages.

Moody. T., Wirtanen, M., and Yard, S.N. (2003) Regional relationships for bankfull stage in natural channels of the arid Southwest. Report from Natural Channel Design, Inc., Flagstaff AZ, 38 pages.

Osborn, H.B., Lane, L.J., and Myers, V.A. (1980) Rainfall/watershed relationships for Southwestern Thunderstorms. Transactions ASAE 23(1), 82-91.

Tillery, A.C., Matherne, A.M., and Verdin, K.L. (2012) Estimated probability of postwildfire debris flows in the 2012 Whitewater-Baldy fire burn area, Southwestern New Mexico. USGS Open File Report 2012-1188, 11 pages.

USCOE-HEC (U.S. Army Corps of Engineers, Hydrologic Engineering Center), 2013. Hec-HMS Technical Reference Manual. Available at http://www.hec.usace.army.mil/software/hec-hms/. Accessed in April, 2013.

USDA Forest Service (2012) Glenwood, Reserve and Wilderness Ranger Districts, BAER Report Executive Summary for the Whitewater Baldy Complex fire, including hydrology appendices.